

12-31-1990

Analysis of field distribution of a dielectric resonator and its applications

Manohar R. Kamath
New Jersey Institute of Technology

Follow this and additional works at: <https://digitalcommons.njit.edu/theses>



Part of the [Electrical and Electronics Commons](#)

Recommended Citation

Kamath, Manohar R., "Analysis of field distribution of a dielectric resonator and its applications" (1990).
Theses. 2773.

<https://digitalcommons.njit.edu/theses/2773>

This Thesis is brought to you for free and open access by the Electronic Theses and Dissertations at Digital Commons @ NJIT. It has been accepted for inclusion in Theses by an authorized administrator of Digital Commons @ NJIT. For more information, please contact digitalcommons@njit.edu.

Copyright Warning & Restrictions

The copyright law of the United States (Title 17, United States Code) governs the making of photocopies or other reproductions of copyrighted material.

Under certain conditions specified in the law, libraries and archives are authorized to furnish a photocopy or other reproduction. One of these specified conditions is that the photocopy or reproduction is not to be “used for any purpose other than private study, scholarship, or research.” If a user makes a request for, or later uses, a photocopy or reproduction for purposes in excess of “fair use” that user may be liable for copyright infringement,

This institution reserves the right to refuse to accept a copying order if, in its judgment, fulfillment of the order would involve violation of copyright law.

Please Note: The author retains the copyright while the New Jersey Institute of Technology reserves the right to distribute this thesis or dissertation

Printing note: If you do not wish to print this page, then select “Pages from: first page # to: last page #” on the print dialog screen

The Van Houten library has removed some of the personal information and all signatures from the approval page and biographical sketches of theses and dissertations in order to protect the identity of NJIT graduates and faculty.

2) **Analysis of field distribution of a Dielectric
Resonator and its Applications**

by

1) **Manohar R. Kamath**

Thesis submitted to the Faculty of the Graduate School of the New Jersey
Institute of Technology in partial fulfillment of the requirements for the degree of
Master of Science in Electrical Engineering.

Dec 1990.

Approval Sheet

Title of Thesis:

Analysis of field distribution of a
Dielectric Resonator and its
Applications

Name of candidate:

Manohar R. Kamath

Thesis and abstract approved:

1st Nov, 1990

Date

Professor

Dept of Electrical Engineering

New Jersey Institute of Technology

11/1/1990

Date

Professor

Dept of Electrical Engineering

New Jersey Institute of Technology

11/1/90

Date

Professor

Dept of Physics

New Jersey Institute of Technology

VITA .

Name: Manohar R. Kamath

Permanent address:

Degree and date conferred: M.S.E.E., Dec 1990

Date of birth:

Place of birth:

Secondary education: S.I.E.S College of Arts and Science,
Sion, Bombay, India.

Collegiate institution attended	Date	Degree	Date of degree
---------------------------------	------	--------	-------------------

New Jersey Institue of Technology	09/88 to 12/90	M.S.	Dec 1990
-----------------------------------	----------------	------	----------

Manipal Institute of Techonology	08/81 to 07/85	B.S.	Aug 1985
----------------------------------	----------------	------	----------

University of Bombay	07/78 to 04/81	B.S.	May 1981
----------------------	----------------	------	----------

Major: Electrical Engineering.

Position held: Field Applications Engineer
Philips India Ltd
Bombay, India

Abstract

New Jersey Institute of Technology
Newark, New Jersey 07102

Dielectric resonators (DR) are suitably shaped objects made of high dielectric constant materials like TiO_2 , BaO , ZnO , and accessory ingredients, which can function as electrical resonators covering a very wide frequency range upto 40GHz. The physical dimensions of dielectric resonators are in mm range. High dielectric constant material resonators seem to be ideally suited for microwave applications because of their miniature size, low loss, insensitivity to magnetic dc biasing fields, and ability to concentrate large RF magnetic fields in small volumes. However temperature stabilization of dielectric resonators is an important consideration as the center frequency is a function of temperature. The present dissertation describes the theoretical analysis of such DR's based on two different mathematical and physical models. These models present a simplified approach to the solution of the electromagnetic field behaviour in the DR, and are capable of giving results which are near to the exact values.

One of the practical applications of such DR's is an oscillator. Here in this thesis report, the dynamic characteristics of a GaAsFET oscillator have also been investigated in details. Especially, studies have been made about the stabilized oscillator temperature coefficient, maximum frequency deviation and the pushing figure as a function of the coupling coefficient. These results would be useful for precise custom made design of such oscillators. Finally, the effects of the environmental conditions on the operation of a practical DR structure are studied by using a computer simulation technique. The study is based on approximate expression for the resonant frequency stability of dielectric resonators.

ACKNOWLEDGEMENT

Many people have assisted me in completing my thesis successfully. First, I would like to express my gratitude and appreciation to my advisor Dr. T. Bhattacharjee for his valuable guidance and encouragement during the entire course of the thesis work. I would also like to thank Dr. Edip Niver and Dr. N.M. Ravindra for being in my thesis committee.

I am greatly indebted to my parents and my wife for their moral and monetary support. Last but not the least, I would like to thank all my friends who had helped me in one way or the other during the entire course of this thesis.

Contents

1		1
1.1	Introduction	1
2		5
2.1	Introduction	5
2.1.1	The Cohn Model	6
2.1.2	Special cases	14
2.1.3	To calculate the resonant frequency of parallel-plate DR	14
2.1.4	Perturbational Method	16
2.1.5	Simplification of the model	19
2.1.6	Numerical solution of the pair of Transcendental equations	21
2.1.7	Variational improvement of the simplified model	25
2.1.8	Results and discussions	28
3		35
3.1	Introduction	35
3.1.1	Analysis	37
3.1.2	Theoretical aspects of the oscillator stabilization	39
3.1.3	Mechanical tuning of a DR mounted on microstrip	43
4		47
4.1	Introduction	47
4.1.1	The resonant frequency stability	49
4.1.2	Computation	53
5		54
5.1	Conclusion	54
6		56

List of Figures

1.1	Magnetic intensity profile	2
1.2	Dielectric resonator in a microwave network	3
2.1	First order Cohn's model	6
2.2	Second order Cohn's model	7
2.3	Modified Cohn's model	8
2.4	Expanded DR model	16
2.5	Perturbed DR (before and after)	18
2.6	Variational model	26
3.1	Typical GaAsFET oscillator	36
3.2	Typical oscillator circuit	37
3.3	Dielectric Resonator coupled to the microstrip	38
3.4	Stabilized oscillator	38
3.5	Tuning mechanism of a DR mounted on microstrip	44
3.6	Experimental set-up for measuring the oscillation frequency	45
4.1	DR on a substrate	48

Chapter 1

1.1 Introduction

Dielectric resonators are important components in microwave communication circuits. They are used as filters, oscillators, amplifiers, and tuners among other applications. Due to recent advances in miniaturization of microwave circuits, the cost has gone down. The consequences of the above mentioned facts were that the bulky waveguides and rigid coaxial lines have been replaced with microstrip and striplines within the majority of microwave systems. Further, carefully designed microwave oscillators which utilize dielectric resonators yield better temperature stability over conventional microwave resonant cavities. Materials having a dielectric constant between 30 and 100 with good temperature stability and low dielectric losses have been chosen for the present study. Dielectric resonator of a small size as compared to conventional empty resonant cavity can operate at the same frequency provided the dielectric constant is higher than unity.

The usual shape of a dielectric is solid cylindrical type, but one can find tubular, spherical and parallelepiped shapes too. There are many possible modes which can be excited in dielectric resonators. These modes can be divided as, transverse electric (TE), transverse magnetic (TM), and hybrid electromagnetic (HEM) modes. Selecting the lowest order modes is the approach in choosing the proper mode for a

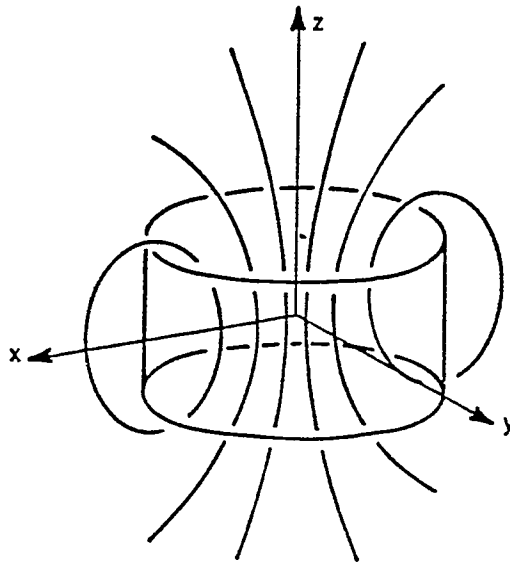


Figure 1.1: Magnetic intensity profile

particular application [17]. A commonly used resonant mode in cylindrical dielectric resonators is denoted by $TE_{01\delta}$, as introduced by Cohn. In this mode, when the relative dielectric constant is around 40 more than 95% of the electric energy stored and about 60% of the magnetic energy stored is found within the cylinder. The remaining energy is distributed in the air around the resonator, where they decay rapidly with distance away from the resonator surface. A typical magnetic field intensity profile is shown in Fig. 1.1. The electric field lines are simple circles concentric with the axis of the cylinder. In order to analyze and get the exact solution of the field equations by using Maxwell's theory for an isolated dielectric resonator it becomes very much involved. Specially with other configuration such as when the dielectric resonator is mounted on a microstrip or placed within a shielding metal cavity. For this reason, the exact resonant frequency of certain resonant mode, such as $TE_{01\delta}$, are generally computed by numerical procedures. A simple formula for estimating the resonant frequency of the isolated dielectric resonator is given by:

$$f(\text{inGHz}) = \frac{34}{a_{mn} \cdot \epsilon_r} [a/L + 3.45]$$

where 'a' is the radius of the resonator and 'L' is its length. Also 'm' and 'n' are used to designate the eigenvalues. A combination of 'm' and 'n' designate a given mode. The above formula has an accuracy of 2% in the range $0.5 < a/L < 2$ and

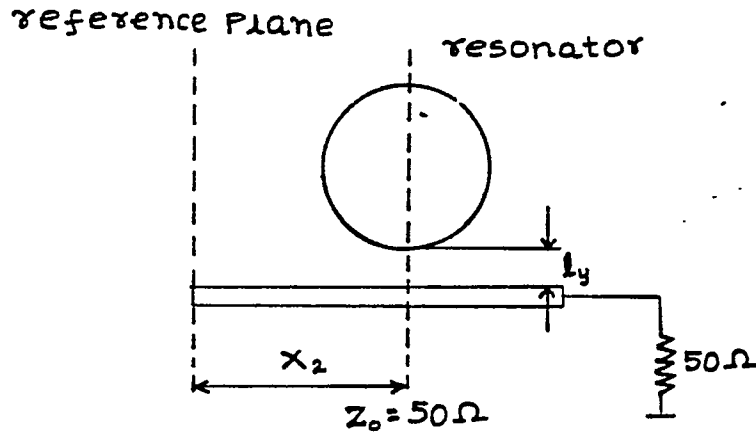


Figure 1.2: Dielectric resonator in a microwave network

$30 < \epsilon_r > 50$. A typical dielectric resonator as used in a microwave network is shown in Fig. 1.2. The lateral distance between the resonator and the microstrip determines the amount of coupling between them. The entire assembly is enclosed within a shielded structure to prevent radiation losses. Two simple mathematical models to represent a shielded dielectric resonator are, the Cohn model and the simplified Perturbational model. These two models facilitate the analysis of the field distribution. We have considered both the models and have programmed them in a personal computer, and the listings are given in appendix 1 and 2. Particularly comparison of the two different modes namely $TE_{01\delta}$ and $TE_{01,1+\delta}$ have been made and discussed in details.

Finally the effects of environmental conditions on the operation of a practical DR structure has been discussed. The effects of the variation of different physical parameters in a simple, shielded dielectric resonator is important especially when the dielectric resonator is subjected to varying environmental conditions. Dielectric resonators are widely used in microwave circuits due to its high Q-value, its low loss characteristics and good temperature stability. It is being used in MMIC's (Monolithic Microwave Integrated Circuits) due to its small size and its above mentioned characteristics. Also the small size of the DR has an advan-

tage over the empty resonant cavity at the same frequency, provided the dielectric constant of the DR is much larger than unity. Generally the DR's are placed in conductor shields to reduce radiation losses and it operates like a reaction cavity which reflects the RF energy at the resonant frequency. One of limitations of the dielectric resonators is the environmental dependence of the mechanical and electrical properties of the dielectric as the resonant frequency of the system becomes a function of the environmental parameters such as temperature and humidity. However one needs to know the type and extent of variation of these parameters in order to reduce their effects. Finally a stable resonant frequency is necessary for practical applications especially when they are used as stabilized oscillators.

Chapter 2

2.1 Introduction

This chapter deals with the field analysis of the dielectric resonator, based on two mathematical models. These models have been explained in details which can be used to analyze dielectric resonators. The computer programs have been written based on the above two models, with some corrections to improve accuracy of the results. The computer program gives us the energy distribution and also the plot of the field distribution within the DR structure. The results for two particular modes, namely TE_{01} , and $TE_{01,1+\delta}$ have been discussed in details.

A "mode" is a particular field configuration. For a given electromagnetic boundary value problem, many field configurations may satisfy the wave equations, Maxwell's equations and the boundary that usually exists. All these different field configurations (or solutions) are usually referred to as modes. Also we have restricted ourselves to a circular cylindrical geometry as the dielectric resonator considered here has that geometry. Considering TE_{mnp} mode, where subscript $p=l+\delta$ and $l=0,1,2,3,\dots$. When $l=0$ it is referred to as $MODE=0$ and when $l=1$ it is referred to as $MODE=1$. ' δ ' is a non-integer whose value is less than 1. As per the theory of perfectly electrical conducting (PEC) and perfectly magnetic conducting (PMC) walls applied to the DR, the third subscript of TE_{mnp} represents the number of half

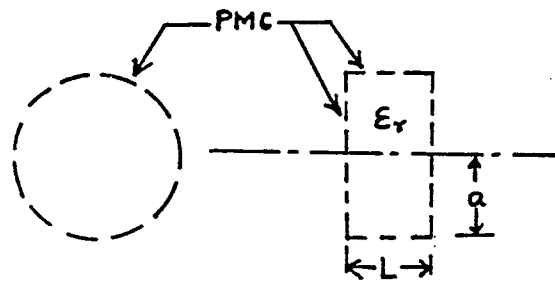


Figure 2.1: First order Cohn's model

wavelength variations the field undergoes in the z direction. An accurate mathematical description of the electromagnetic field in a dielectric resonator (DR) may be a little complicated. So it is of great practical interest to approach the solution of the electromagnetic field in the DR in a simplified manner that can give us sufficiently accurate results.

2.1.1 The Cohn Model

The first order Cohn's model which is based on the fact that electromagnetic field inside a DR with high dielectric constant, is considered to be covered by PMC. This represents a circular cavity resonator, the walls of which are made of PMC (Fig. 2.1). An improvement over this was the second order model as described by Cohn [1] is shown in Fig. 2.2. This cylindrical PMC shell is retained, but the PMC end caps are removed and replaced by the air filled hollow waveguides. The hollow waveguides operate below the cut off because they are filled with low dielectric constant. Thus the modes in these air filled PMC waveguides are evanescent so the fields decay exponentially in the z -direction away from each end resonator.

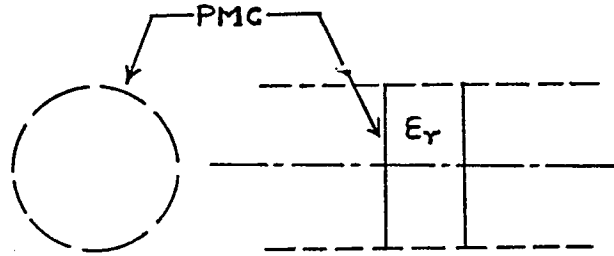


Figure 2.2: Second order Cohn's model

The Fig. 2.2 is also a case of isolated DR. This isolated DR acts as miniature antenna, and the energy lost on radiation is manifested in low Q values. The measured Q factor of an isolated $TE_{01\delta}$ resonator is about 50 [2]. In order to keep the unloaded Q factor of a DR resonator high (typically 5000), it is necessary to prevent radiation by enclosing the DR with a metal shield. The entire substrate with DR placed on it is placed in a metal box. The box acts as a shield which prevents the external fields from penetrating the system and, at the same time reduces the loss of energy due to radiation.

The modification of the Cohn model which incorporates the parallel plate metal enclosure is shown in Fig. 2.3. The radius of the dielectric resonator is 'a', its relative dielectric constant is ϵ_r , and its length is 'L'. The region with dielectric constant ϵ_{r1} represents the substrate on which resonator is attached. The thickness of the substrate is L_1 , and outside face of the substrate is covered with the perfect electric conductor. The region of length L_2 represents the air filled space above the resonator, and the PEC cap on the right most side.

We would like to look into the electromagnetic field of the TE_{01} mode which

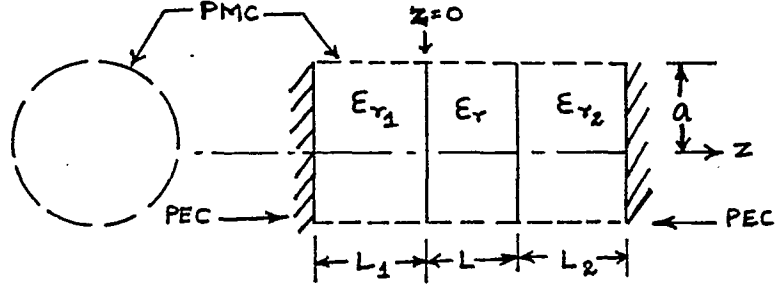


Figure 2.3: Modified Cohn's model

satisfies the boundaries of Fig. 2.3. Since $\epsilon_r \gg 1$, the mode within the PMC waveguide of length L is above cut-off so that propagation constant γ becomes equal to $j\beta$. The field within the region $0 < Z < L$ is then,

$$H_z = (Ae^{j\beta z} + Be^{-j\beta z})J_0(K_\rho \rho) \quad (2.1)$$

The azimuthal variation $\frac{\delta}{\delta\phi} = 0$ due to circular symmetry. The other field components can be calculated as follows:

To obtain the vector components of the electric and magnetic field, we take the z component of the magnetic field for convenience. The scalar Helmholtz equation is then given as:

$$\nabla^2 H_z = -K_o^2 \epsilon_r H_z \quad (2.2)$$

By using the method of separation of variables which is based on the assumption that solution of the above differential equation is a product of three functions, as :

$$H_z = P(\rho)F(\phi)Z(z) \quad (2.3)$$

Then by using the Maxwell's equation $\nabla \times E = -j\omega\mu_o H$ we get three scalar equations:

$$-\frac{\delta E_\phi}{\delta z} = -j\omega\mu_o H_\rho \quad (2.4)$$

$$\frac{\delta E_\rho}{\delta z} = -j\omega\mu_o H_\phi \quad (2.5)$$

$$\frac{1}{\rho} \frac{\delta}{\delta \rho}(\rho E_\phi) - \frac{1}{\rho} \frac{\delta E_\rho}{\delta \phi} = -j\omega\mu_o H_z \quad (2.6)$$

Also the other Maxwell equation, $\nabla \times H = j\omega\epsilon E$ is split into the following equations:

$$\frac{1}{\rho} \frac{\delta H_z}{\delta \phi} - \frac{\delta H_\phi}{\delta z} = j\omega\epsilon E_\rho \quad (2.7)$$

$$\frac{\delta H_\rho}{\delta z} - \frac{\delta H_\phi}{\delta z} = j\omega\epsilon E_\phi \quad (2.8)$$

$$\frac{1}{\rho} \frac{\delta}{\delta \rho}(\rho H_\phi) - \frac{1}{\rho} \frac{\delta H_\rho}{\delta \phi} = 0 \quad (2.9)$$

The right hand side of the last equation is zero because, for the TE modes, E_z is zero by definition. Eliminating E_ϕ by using (2.4) and (2.8) we get :

$$H_\rho = \frac{1}{K_\rho^2} \frac{\delta^2 H_z}{\delta \rho \delta z}$$

From circular waveguide theory as seen above we have, $H_\rho = \frac{1}{K_\rho^2} \frac{\delta^2 H_z}{\delta \rho \delta z}$.

$$H_\rho = \frac{1}{K_\rho^2} \frac{\delta^2}{\delta \rho \delta z} [Ae^{j\beta z} + Be^{-j\beta z}] J_o(K_\rho \rho) \quad (2.11)$$

$$= \frac{1}{K_\rho} [j\beta A e^{j\beta z} - j\beta B e^{-j\beta z}] J_o'(K_\rho \rho) \quad (2.12)$$

From Bessel function theory, we know that $J_o'(x) = -J_1(x)$, therefore

$$H_\rho = -\frac{1}{K_\rho} j\beta (Ae^{j\beta z} - Be^{-j\beta z}) J_1(K_\rho \rho) \quad (2.13)$$

Using Maxwell's equation, we get

$$E_\phi = \frac{j\omega\mu_o}{K_\rho^2} \frac{\delta H_z}{\delta \rho} \quad (2.14)$$

Therefore,

$$E_\phi = -\frac{j\omega\mu_o}{K_\rho}(Ae^{j\beta z} + Be^{-j\beta z})J_1(K_\rho\rho) \quad (2.15)$$

The radial propagation constant of the TE_{01} mode is fixed by the requirement given below:

$$J_m(x_{mn}) = 0, n = 1, 2, 3, \dots \quad (2.16)$$

And H_z must be zero at $\rho = a$.

Therefore,

$$K_\rho a = x_{m1} = x_{01} = 2.4048 \quad (2.17)$$

In the regions 1 and 2 the dielectric constant is much lower than ϵ_r and hence the mode is evanescent. The propagation constant γ is now given by α_1 or α_2 (attenuation constant) depending on the region being considered. The radial variation in these regions is specified by the same K_ρ as in (2.17) so that the fields are continuous at the interface $z=0$ and $z=L$.

For region 1, the H_z field is thus,

$$H_{z1} = (C_1e^{\alpha_1 z} + D_1e^{-\alpha_1 z})J_0(K_\rho\rho) \quad (2.18)$$

E_ϕ is obtained from circular waveguide theory as,

$$E_{\phi 1} = -\frac{j\omega\mu_o}{K_\rho}(C_1e^{\alpha_1 z} + D_1e^{-\alpha_1 z})J_1(K_\rho\rho) \quad (2.19)$$

At $z = -L_1$, E_ϕ must vanish because of the conducting wall. This results in,

$$0 = C_1e^{\alpha_1 L_1} + D_1e^{-\alpha_1 L_1} \quad (2.20)$$

Therefore,

$$D_1 = -C_1e^{2\alpha_1 L_1} \quad (2.21)$$

Substituting (2.21) in (2.19) we get,

$$E_{\phi 1} = -\frac{j\omega\mu_o}{K_\rho} 2C_1 e^{-\alpha_1 L_1} \sinh\alpha_1(z + L_1) J_1(K_\rho \rho) \quad (2.22)$$

The components of the magnetic field in region 1 are then given by,

$$H_{z1} = 2C_1 e^{-\alpha_1 L_1} \sinh(z + L_1) \alpha_1 J_o(K_\rho \rho) \quad (2.23)$$

$$H_{\rho 1} = -\frac{\alpha_1}{K_\rho} 2C_1 e^{-\alpha_1 L_1} \cosh(z + L_1) \alpha_1 J_1(K_\rho \rho) \quad (2.24)$$

In an analogous manner, the fields in region 2 are given as,

$$H_{z2} = 2C_2 e^{\alpha_2(L_2+L)} \sinh\alpha_2(z - L_2 - L) J_o(K_\rho \rho) \quad (2.25)$$

$$E_{\phi 2} = -\frac{j\omega\mu_o}{K_\rho} 2C_2 e^{\alpha_2(L_2+L)} \sinh\alpha_2(z - L_2 - L) J_1(K_\rho \rho) \quad (2.26)$$

$$H_{\rho 2} = -\frac{\alpha_2}{K_\rho} 2C_2 e^{\alpha_2(L_2+L)} \cosh\alpha_2(z - L_2 - L) J_1(K_\rho \rho) \quad (2.27)$$

In region 2 the field vanishes at $z = L_2 + L$. The separation constants are given as follows:

The radial wave number is $K_\rho^2 = \gamma^2 + K_o^2 \epsilon_r$. Also for mode propagating in the z -direction $\gamma^2 = -\beta^2$ and for evanescent mode $\gamma^2 = \alpha^2$. Also we have seen that in region of the DR it has a propagating mode and in regions 1 and 2 the mode is evanescent. Therefore separation constant in the dielectric region is given by,

$$K_\rho^2 = -\beta^2 + K_o^2 \epsilon_r \quad (2.28)$$

For TE_{01} mode $K_\rho a = x_{01} = 2.4048$, hence

$$K_\rho^2 = \left(\frac{x_{01}}{a}\right)^2 \quad (2.29)$$

Substituting (2.29) in (2.28) we get,

$$\left(\frac{x_{01}}{a}\right)^2 = -\beta^2 + K_o^2 \epsilon_r \quad (2.30)$$

Therefore,

$$\beta^2 = K_o^2 \epsilon_r - \left(\frac{x_{01}}{a}\right)^2 \quad (2.31)$$

Similarly for region 1, we have $K_p^2 = \alpha_1^2 + K_o^2 \epsilon_r$, and substituting (2.29) we get,

$$\alpha_1^2 = \left(\frac{x_{01}}{a}\right)^2 - K_o^2 \epsilon_{r1} \quad (2.32)$$

similarly,

$$\alpha_2^2 = \left(\frac{x_{01}}{a}\right)^2 - K_o^2 \epsilon_{r2} \quad (2.33)$$

The next step is to ensure that the tangential components of the electric as well as the magnetic field, are continuous at the interface. At $z=0$ we require $\vec{E}_{\phi 1} = E_{\phi}$ and $H_{\rho 1} = H_{\rho}$.

Equating (2.22) and (2.15) we get:

$$2C_1 e^{-\alpha_1 L_1} \sinh \alpha_1 L_1 = A + B \quad (2.34)$$

Similarly equating (2.24) and (2.13) we get,

$$\alpha_1 2C_1 e^{-\alpha_1 L_1} \cosh \alpha_1 L_1 = j\beta(A - B) \quad (2.35)$$

Dividing (2.34) by (2.35) C_1 is eliminated giving,

$$\tanh(\alpha_1 L_1) = \frac{\alpha_1 A + B}{j\beta A - B} \quad (2.36)$$

Similarly by equating $E_{\phi} = E_{\phi 2}$ and $H_{\rho} = H_{\rho 2}$ at $z=L$ we get,

$$\tanh(-\alpha_2 L_2) = \frac{\alpha_2 A e^{j\beta L} + B e^{-j\beta L}}{j\beta A e^{j\beta L} - B e^{-j\beta L}} \quad (2.37)$$

The constants A and B are the amplitude of the forward and reverse travelling waves inside the resonator. For a complete standing wave pattern the amplitudes

of A and B must be same. The ratio of the two constants is a complex number of unity magnitude and of undetermined phase given by,

$$\frac{B}{A} = e^{j\phi} \quad (2.38)$$

The right hand side fraction of (2.36) becomes,

$$\frac{A+B}{A-B} = j \cot \frac{\phi}{2} \quad (2.39)$$

And the right hand side of (2.37) becomes,

$$\frac{Ae^{j\beta L} + Be^{-j\beta L}}{Ae^{j\beta L} - Be^{-j\beta L}} = -j \cot(\beta L - \frac{\phi}{2}) \quad (2.40)$$

When (2.39) is substituted in (2.36) we get the result,

$$\tanh(\alpha_1 L_1) = \frac{\alpha_1}{j\beta} j \cot \frac{\phi}{2} \quad (2.41)$$

$$\tan \frac{\phi}{2} = \frac{\alpha_1}{\beta} \coth \alpha_1 L_1 \quad (2.42)$$

Therefore,

$$\frac{\phi}{2} = \frac{\phi_1}{2} = \tan^{-1} \left[\frac{\alpha_1}{\beta} \coth \alpha_1 L_1 \right] \quad (2.43)$$

Here (2.43) is the value of the phase angle ϕ_1 , expressed in terms of parameters of region 1 only. Similarly substituting (2.40) in (2.37) we get,

$$\frac{\phi_2}{2} = (\beta L - \frac{\phi_1}{2}) = \tan^{-1} \left[\frac{\alpha_2}{\beta} \coth \alpha_2 L_2 \right] \quad (2.44)$$

The resonance condition can be written as,

$$\beta L - \frac{\phi_1}{2} = \frac{\phi_2}{2} + l\pi \quad (2.45)$$

$$i.e. \beta L = \frac{\phi_1}{2} + \frac{\phi_2}{2} + l\pi, l = 0, 1, 2, \dots \quad (2.46)$$

The added angle $l\pi$ gives all possible resonance conditions. When $l=0$, the mode is called $TE_{01\delta}$, where δ signifies a non-integer number smaller than unity,

$$\delta = \frac{1}{\pi} \left[\frac{\phi_1}{2} + \frac{\phi_2}{2} \right] \quad (2.47)$$

In general the modes may be denoted by TE_{01p} , where

$$p = (l + \delta), l = 0, 1, 2, \dots \quad (2.48)$$

Also when $l=1$ we have $TE_{01,1+\delta}$ referred to as MODE=1.

2.1.2 Special cases

1. When $L_1 = 0$ and $L_2 = 0$, we get $\frac{\phi_1}{2} = \frac{\pi}{2}$ and $\frac{\phi_2}{2} = \frac{\pi}{2}$. Also the lowest order resonance ($l=0$) is given by $\beta L = \pi$. This is the case is when the two metal plates are touching each resonator ends.

2. When the two metal plates are removed to infinity (i.e. $L_1 = \infty$ and $L_2 = \infty$) we get $\frac{\phi_1}{2} = \tan^{-1} \left[\frac{\alpha_1}{\beta} \right]$ and $\frac{\phi_2}{2} = \tan^{-1} \left[\frac{\alpha_2}{\beta} \right]$. In this case $\epsilon_{r1} = \epsilon_{r2} = 1$, and the resonance condition becomes $\beta L = 2 \tan^{-1} \left[\frac{\alpha}{\beta} \right]$ with α and β given by equation (2.31) and (2.33).

The Cohn's first order model gives an accuracy of +32%, while the second order model gives an error of about -4.8%.

2.1.3 To calculate the resonant frequency of parallel-plate DR

$$\beta L = \frac{2\pi}{\lambda_{DR}} L = p\pi \quad (2.49)$$

λ_{DR} is the DR wavelength, and 'p' is an integer. Thus, the length L is an integral multiple of the half wavelength's

$$L = p \frac{\lambda_{DR}}{2}, p = 1, 2, \dots \quad (2.50)$$

There is only one discrete set of frequencies that satisfies (2.31) and (2.49)

$$x = K_p a \quad (2.51)$$

$$K_p^2 = K_o^2 \epsilon_r - \beta^2 \quad (2.52)$$

$$\beta^2 = K_o^2 \epsilon_r - \left(\frac{x}{a}\right)^2 \quad (2.53)$$

$$x^2 = -(\beta a)^2 + K_o a^2 \epsilon_r \quad (2.54)$$

$$x^2 = (K_o a)^2 \epsilon_r - \left(\frac{a}{L} p \pi\right)^2 \quad (2.55)$$

Rearranging and dividing throughout by $\left(\frac{a}{L} p \pi\right)^2$ in (2.55) we get,

$$\frac{K_o a^2 \epsilon_r}{\left(\frac{a}{L} p \pi\right)^2} - \frac{x^2}{\left(\frac{a}{L} p \pi\right)^2} = 1 \quad (2.56)$$

$$\frac{K_o a^2}{U_p^2} - \frac{x^2}{V_p^2} = 1 \quad (2.57)$$

where $U_p = p \frac{a\pi}{L\sqrt{\epsilon_r}}$ and $V_p = \sqrt{\epsilon_r} U_p$.

Equation (2.57) represents the equation of a family of hyperbolas. Given the values of 'a' and 'L', the family of hyperbolas can be plotted for different values of p's. The family of curves intersect at a point $(x_{mnp}, (K_o a)_{mnp})$. The resonance frequencies are then given by,

$$f_{mnp} = \frac{150}{\pi a} (K_o a)_{mnp} \text{ GHz} \quad (2.58)$$

where 'a' is measured in millimeters.

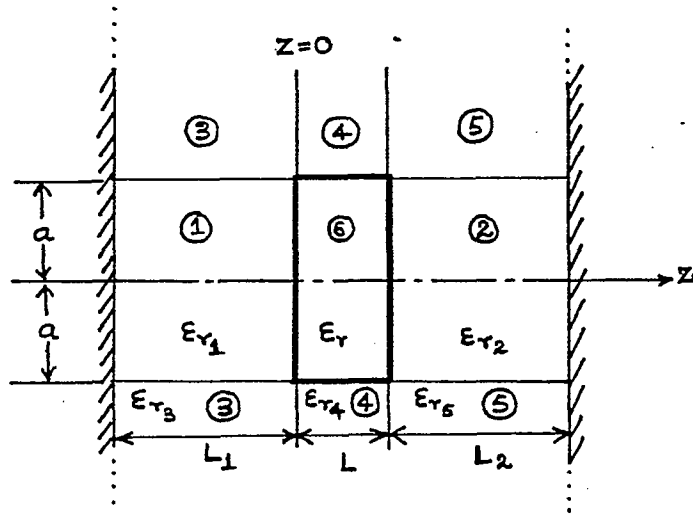


Figure 2.4: Expanded DR model

2.1.4 Perturbational Method

The electromagnetic field in the Cohn model of the DR, shown in the Fig. 2.1 and Fig. 2.2, is zero everywhere outside the PMC wall (i.e. for $\rho > a$). But in reality the tangential field outside cylindrical surface of the resonator is the same as the tangential field inside that surface, and gradually decreases, as we move away radially from the surface. Thus a part of the stored electric and the magnetic field exists in the region $\rho > a$, and this part of the energy was neglected by the Cohn's second order model.

To improve the model, we retain the same electric and magnetic fields inside $\rho < a$ as for the PMC model of the Fig. 2.1. However, the PMC wall is removed and is postulated that outside tangential electric field is continuous at $\rho = a$ with the inside tangential field. The expanded DR model consists of six regions, as shown in Fig. 2.4. The electric field in this region is the same as in the Cohn model:

$$E_{\phi 6} = E_o J_1(K_\rho \rho) \cos[\beta z - \frac{\phi_1}{2}] \quad (2.59)$$

The electric fields in the region 1 and 2 are,

$$E_{\phi 1} = E_o \frac{\cos \phi_1 / 2}{\sinh \alpha_1 L_1} J_1(K_\rho \rho) \sinh \alpha_1 (z + L_1) \quad (2.60)$$

$$E_{\phi 2} = E_o \frac{\cos \phi_2 / 2}{\sinh \alpha_2 L_2} J_1(K_\rho \rho) \sinh \alpha_2 (z - L_2 - L) \quad (2.61)$$

The multiplicative factors are selected in such a way that E_ϕ is continuous over the interfaces between regions 1 and 6, and between regions 2 and 6. The field in the outer regions 3, 4, and 5 are now selected in such a way that the radial dependence will be determined by the modified Bessel functions, which are monotonically decaying with increasing radius. The axial dependence should be the same as in the inner regions 1, 6 and 2. Thus, the electric fields are:

$$E_{\phi 4} = E_o \frac{J_1(K_\rho a)}{K_1(K_{\rho 2} a)} \cos(\beta z - \phi_1 / 2) \quad (2.62)$$

$$E_{\phi 3} = E_o \frac{J_1(K_\rho a) \cos \phi_1 / 2}{K_1(K_{\rho 2} a) \sinh \alpha_1 L_1} K_1(K_{\rho 2} r) \sinh \alpha_1 (z + L_1) \quad (2.63)$$

$$E_{\phi 5} = E_o \frac{J_1(K_\rho a) \cos \phi_2 / 2}{K_1(K_{\rho 2} a) \sinh \alpha_2 L_2} K_1(K_{\rho 2} \rho) \sinh \alpha_2 (z - L_2 - L) \quad (2.64)$$

The separation constant $K_{\rho 2} = \sqrt{\beta^2 - K_o^2}$. A convenient formula for computing ' $K_o a$ ' from known values of frequency 'f' and radius 'a' is the following [3]:

$$K_o a = \frac{\pi}{150} a_{mm} f_{GHz} \quad (2.65)$$

Similarly the magnetic field in each region can be computed by using the Maxwell equation. Also it was seen that $H_{z6}(\rho = a) = 0$, whereas H_{z4} has no zero and hence H_z is not continuous [4]. Thus it shows that this model is far from perfect. A crude approximation is made here to make the magnetic field continuous by assuming that $H_{z3} = 0$, $H_{z4} = 0$, and $H_{z5} = 0$ for $\rho > a$.

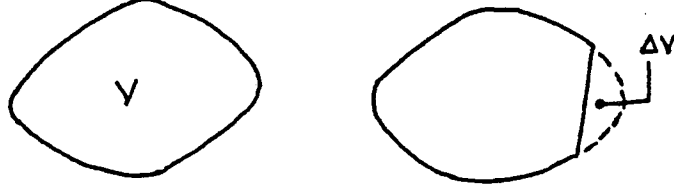


Figure 2.5: Perturbed DR (before and after)

The resonant frequency of a perturbed DR is found as follows. Before the perturbation the resonant frequency of the cavity is denoted as " w_o " and the fields by E_o and H_o . If now the cavity is disturbed or pushed inward by an amount δv , the resonant frequency change is given by (refer Fig. 2.5),

$$\frac{w - w_o}{w_o} = \frac{\int \int \int_{\Delta v} (\mu |H_o|^2 - \epsilon |E_o|^2) dv}{\int \int \int_v (\mu |H_o|^2 + \epsilon |E_o|^2) dv} \quad (2.66)$$

In Fig. 2.5, the Δv volume of the regions 3, 4, and 5 have been moved outward instead of inward. The resonant frequency w_r of the perturbed resonator is given as (W_m and W_e are the magnetic and electric energies),

$$w_r = w_o \left[1 + \frac{W_{m3} + W_{m4} + W_{m5} - W_{e3} - W_{e4} - W_{e5}}{W_{m1} + W_{m2} + W_{m6} + W_{e1} + W_{e2} + W_{e6}} \right] \quad (2.67)$$

The computer program 1 listed at the end, written in BASIC language computes the resonant frequency, for the Cohn model and the Perturbational method. It also plots the fields distribution as a function of the z-coordinates and also it gives the energy distribution table in the various regions.

2.1.5 Simplification of the model

From the perturbational correction to the Cohn's model it was seen that H_{z4} and H_{z6} were not continuous at $\rho = a$, and also a crude approximation was made that $H_{z4}=0$ for $\rho > a$. The analysis of the model can be simplified by ensuring the continuity of both electric and magnetic field, tangential to the surface between regions 4 and 6 [5], [6].

When we try to equate the fields tangential to the surface at the interface at $\rho = a$ we can come across a matrix "F" which is a 4 x 4 matrix [4], which is further split into the following.

$$F_1(x)F_2(x) - F_3^2(x) = 0 \quad (2.68)$$

$$F_1 = \frac{J_m'(x)}{x} + \frac{K_m'(y)J_m(x)}{\epsilon_r y K_m(y)} \quad (2.69)$$

$$F_2(x) = \frac{J_m'(x)}{x} + \frac{K_m'(y)J_m(x)}{y K_m(y)} \quad (2.70)$$

$$F_3(x) = \frac{\beta a m}{K_o a \sqrt{\epsilon_r}} J_m(x) \left[\frac{1}{x^2} + \frac{1}{y^2} \right] \quad (2.71)$$

Where J_m is the Bessel's function of the first kind and K_m is the modified Bessel's function. ϵ_r is the dielectric constant of the dielectric rod. " K_o " is the free space propagation constant, and 'a' is the radius of the rod.

$x = K_{\rho 1} a =$ eigenvalue of the dielectric rod waveguide.

$$y = K_{\rho 2} a = \sqrt{(K_o a^2)(\epsilon_r - 1) - x^2} \quad (2.72)$$

$$\beta a = \sqrt{(K_o a^2)\epsilon_r - x^2}$$

There are only finite number of eigenvalues for any specified 'm'. Another subscript 'n' is therefore chosen to enumerate the eigenvalues. Hence x_{mn} denote

the eigenvalues. If $m=0$, F_3 vanishes and hence (2.68) splits into two equations, as follows:

$$\frac{J_1(x)}{x} + \frac{K_1(y)J_0(x)}{\epsilon_r y K_0(y)} = 0 \quad (2.73)$$

$$\frac{J_1(x)}{x} + \frac{K_1(y)J_0(x)}{y K_0(y)} = 0 \quad (2.74)$$

corresponding to the TE and TM fields.

The requirement for continuity of the fields in the dielectric rod waveguide leads to the following eigenvalue equation for the TE_{on} modes [3]:

$$\frac{J_0(K_{\rho 1} a)}{J_1(K_{\rho 1} a)} = -\frac{K_{\rho 2} a K_0(K_{\rho 2} a)}{K_{\rho 1} a K_1(K_{\rho 2} a)} \quad (2.75)$$

where the argument $K_{\rho 2} a$ is given by,

$$K_{\rho 2} a = \sqrt{(K_0 a)^2 (\epsilon_{r6} - \epsilon_{r4}) - (K_{\rho 1} a)^2} \quad (2.76)$$

when eigenvalue $K_{\rho 1} a$ is known, the propagation constant of the dielectric rod waveguide is computed from,

$$\beta a = \sqrt{(K_0 a)^2 \epsilon_{r6} - (K_{\rho 1} a)^2} \quad (2.77)$$

Furthermore, it is postulated that fields in the regions 3 and 5 is zero everywhere. The fields regions in the 1 and 2 should be selected so that the Maxwell's equations, the boundary conditions, and the continuity between these regions are maintained.

$$E_{\phi 1} = E_o \frac{\cos \phi_1 / 2}{\sinh \alpha_1 L_1} J_1(K_{\rho 1} \rho) \sinh \alpha_1 (z + L_1) \quad (2.78)$$

$$E_{\phi 2} = E_o \frac{\cos \phi_1 / 2}{\sinh \alpha_2 L_2} J_1(K_{\rho 1} \rho) \sinh \alpha_2 (z - L - L_2) \quad (2.79)$$

$$E_{\phi 4} = E_o \frac{J_1(K_{\rho 1} a)}{K_1(K_{\rho 2} a)} K_1(K_{\rho 2} \rho) \cos(\beta z - \phi_1 / 2) \quad (2.80)$$

$$E_{\phi 6} = E_o J_1(K_{\rho 1} \rho) \cos(\beta z - \phi_1/2) \quad (2.81)$$

$\alpha_1, \alpha_2, \phi_1, \phi_2$ are the same as described in Cohn model. The continuity of the electric and magnetic field leads to the same equation (2.46). The difference here is that β is now determined by equation (2.77) in terms of the eigenvalue $K_{\rho 1} a$, which must satisfy the transcendental equation (2.75), whereas in the Cohn model, β was given by the equation (2.31) and the eigenvalue was a constant $x_{01}=2.4048$. In the Cohn model, the H_z field, which is given by the Bessel function $J_o(K_{\rho} r)$ vanishes at $\rho = a$, but for the simplified model $K_{\rho 1} a$ is larger, so H_z turns out to be negative at the resonator surface. Outside the dielectric, the radial dependence of H_z is specified by the monotonically decaying function $K_o(K_{\rho 2} \rho)$. For shielded DR this model had errors smaller than 2%. However, for an isolated DR the error is much larger.

2.1.6 Numerical solution of the pair of Transcendental equations

The two transcendental equations we wish to solve simultaneously are,

$$\beta L = \frac{\phi_1}{2} + \frac{\phi_2}{2} + l\pi, l = 0, 1, 2, \dots \quad (2.82)$$

$$\frac{J_o(K_{\rho 1} a)}{J_1(K_{\rho 1} a)} = -\frac{K_{\rho 2} a K_o(K_{\rho 2} a)}{K_{\rho 1} a K_1(K_{\rho 2} a)} \quad (2.83)$$

For an assumed value of frequency, an auxiliary constant " y_o " is computed using equation (2.72). Then the approximated eigenvalue is obtained as follows:

$$K_{\rho 1} a = 2.405 + \frac{y_o}{2.405[1 + 2.43/y_o + 0.291y_o]} \quad (2.84)$$

The attenuation constants for the regions 1 and 2 given by equations (2.32) and (2.33) respectively. The common propagation constant for region 4 and 6 is

calculated using equation (2.77). Then finally the length L is calculated using equation (2.82).

For simplicity we denote the implicit functions by $f(x,y)$ and $g(x,y)$ where x and y are two independent variables. We are looking for a point (x,y) at which both,

$$f(x,y) = 0, g(x,y) = 0 \quad (2.85)$$

In the vicinity of the solution f and g will be approximated by the linear equations:

$$f(x,y) = ax + by + c \quad (2.86)$$

$$g(x,y) = Ax + By + C \quad (2.87)$$

when $f=0$, (2.86) gives a straight line;

$$y = -\frac{ax}{b} - \frac{c}{b} \quad (2.88)$$

similarly when $g=0$, (2.87) gives:

$$y = -\frac{Ax}{B} - \frac{C}{B} \quad (2.89)$$

The intersection of the above straight lines got by subtracting (2.89) from (2.88) yielding,

$$\left(-\frac{a}{b} + \frac{A}{B}\right)x - \left(\frac{c}{b} - \frac{C}{B}\right) = 0 \quad (2.90)$$

Rearranging (2.90) gives,

$$x = \frac{Bc - bC}{Ab - aB} \quad (2.91)$$

Multiplying (2.88) by $\frac{A}{B}$ throughout,

$$\frac{Ay}{B} = -\frac{aAx}{bB} - \frac{Ac}{bB} \quad (2.92)$$

Multiplying (2.89) by $\frac{a}{b}$ throughout,

$$\frac{ay}{b} = -\frac{aAx}{bB} - \frac{aC}{bB} \quad (2.93)$$

subtracting (2.89) from (2.88) we get,

$$\frac{Ay}{B} - \frac{ay}{b} = -\frac{cA}{bB} + \frac{aC}{bB} \quad (2.94)$$

Rearranging above equation we get,

$$y = \frac{aC - cA}{Ab - aB} \quad (2.95)$$

Thus if the coefficients a, b, c, A, B, C are known, the zero of the equation (2.85) can be computed by (2.91) and (2.95). The function $f(x,y)$ is interpreted as a three dimensional surface over the x,y plane. If x and y are very small, the surface is approximated by a plane. The location of the plane is entirely specified by evaluating three points.

The starting point by $x = x_2$ and $y = y_2$ and corresponding value of f is denoted by f_2 . The next point is chosen as $x_1 = x_2 + \Delta x$, $y_1 = y_2$, with the corresponding f denoted by f_1 . The third point is selected as $x_3 = x_2$ and $y_3 = y_2 + \Delta y$, with corresponding function denoted by f_3 . Hence the linear coefficients from (2.86) are as follows;

$$f_2 = ax_2 + by_2 + c \quad (2.96)$$

$$f_1 = a(x_2 + \Delta x) + by_2 + c \quad (2.97)$$

$$f_3 = ax_2 + b(y_2 + \Delta y) + c \quad (2.98)$$

From (2.97), $f_1 = ax_2 + by_2 + c + a\Delta x = f_2 + a\Delta x$

$$a = \frac{f_1 - f_2}{\Delta x} \quad (2.99)$$

From (2.98), $f_3 = ax_2 + by_2 + c + b\Delta y = f_2 + b\Delta y$

$$b = \frac{f_3 - f_2}{\Delta y} \quad (2.100)$$

The value of 'c' is given by equation (2.96)

$$c = f_2 - ax_2 - by_2 \quad (2.101)$$

Using the same analogy for 'g' we get,

$$A = \frac{g_1 - g_2}{\Delta x} \quad (2.102)$$

$$B = \frac{g_3 - g_2}{\Delta y} \quad (2.103)$$

$$C = g_2 - Ax_2 - By_2 \quad (2.104)$$

The search consists of evaluating the functions 'f' and 'g' at three close points, computing the linear coefficients from (2.99) to (2.104) and then shifting the new points given by (2.91) and (2.95). The procedure is repeated again. The two variables x and y are selected as,

$$x = K_{\rho}a \text{ and } y = K_o a$$

The argument of the modified Bessel function as in (2.83) is denoted as $K_{\rho 2}a = z$. The two implicit functions are defined in accordance with (2.83) and (2.82) as:

$$f = \frac{J_o(x)}{J_1(x)} + \frac{z K_o(z)}{x K_1(z)} \quad (2.105)$$

$$g = \beta L - \frac{\phi_1}{2} - \frac{\phi_2}{2} - l\pi \quad (2.106)$$

The search is rapid and after three to four iterations we achieve an accuracy of 10^{-5} . If the starting point is far from correct solution, function 'f' and 'g' may depart from the linear model, the first computed by (2.91) and (2.95) may be too large, and the point may fall outside the feasible range. This situation may be seen as an attempt to evaluate the square root of a negative number as in (2.76). If this occurs the search algorithm (program 2) reduces the steps by half and the procedure is repeated.

2.1.7 Variational improvement of the simplified model

The variational formula is used to compute the resonant frequency of the resonant cavity. We have seen that the variational expressions contain some ratio of energies

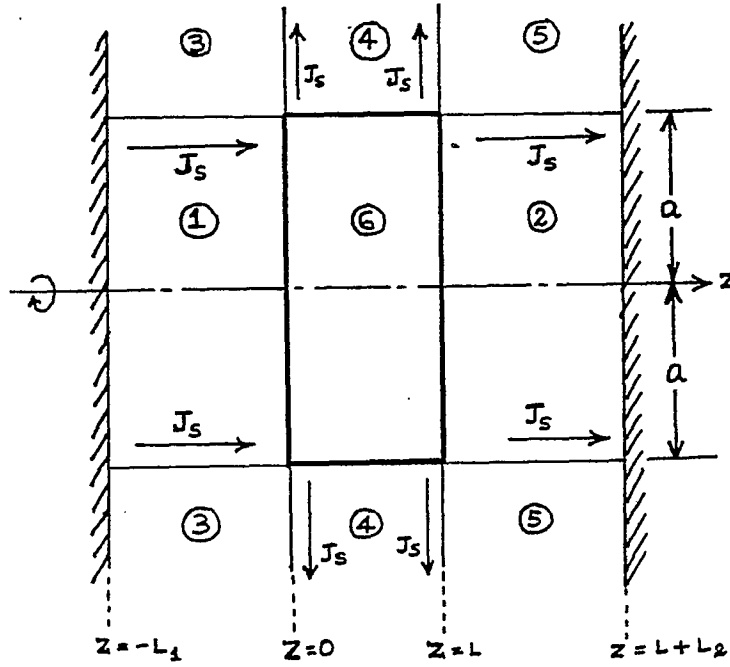


Figure 2.6: Variational model

stored inside the resonator volume. The advantage of the variational formula is that the small inaccuracies in the field distribution have a negligible effect on the resulting value of the frequency. The improvement of the simplified model was achieved by choosing the electric field in the corner regions according to (2.63) and (2.64). Then the electric field in regions 3 and 5 becomes continuous over the interfaces with the inner regions. Equations (2.63) and (2.64) do not satisfy the Helmholtz wave equation. Hence the magnetic field in the region 3 and 5 is left to be zero. However, to account for the sudden jump of the tangential magnetic field from zero to a finite value in the neighbouring regions, surface electric currents J_s are added on the interfaces, as shown in the Fig. 2.6. The variational formula for computing the resonant frequency of the model is derived by using the Rumsey's reaction concept [7]. The electric field is got from the self-reaction:

$$\iiint_V E \cdot J dV = 0 \quad (2.107)$$

The current density 'J' inside the resonant cavity is obtained from [7]:

$$J = -j\omega\epsilon E - \frac{1}{j\omega} \nabla X \mu^{-1} \nabla X E \quad (2.108)$$

The magnetic field in terms of electric field is given as:

$$J_s = -\frac{1}{j\omega\mu} \nabla X E X \hat{n} \quad (2.109)$$

Substituting (2.108) and (2.109) in (2.107), we get

$$-j\omega \iiint_V \epsilon E \cdot E dV - \frac{1}{j\omega} \iiint_V E \cdot (\nabla X \mu^{-1} \nabla X E) dV - \frac{1}{j\omega} \iint_S E \cdot \mu^{-1} (\nabla X E X \hat{n}) dS = 0 \quad (2.110)$$

\hat{n} is the unit vector, normal to the surface, pointing out of the inner region of the cavity. Using the vector identity,

$$A \cdot BXC = B \cdot CXA \quad (2.111)$$

for the above integral, we get the following variational formula:

$$\omega^2 = \frac{\iiint_V E \cdot (\nabla X \mu^{-1} \nabla X E) dV + \iint_S (\hat{n} X E) \cdot \mu^{-1} (\nabla X E) dS}{\iiint_V \epsilon E \cdot E dV} \quad (2.112)$$

The surface integral of the above equation is evaluated only on which J_s exists. For the isotropic dielectric materials, the Helmholtz wave equation is [7]

$$\nabla X \nabla X E = K^2 E \quad (2.113)$$

where the propagation constant of the medium is

$$K^2 = \omega_o^2 \mu_o \epsilon_o \epsilon_r \quad (2.114)$$

In the above equation ω_o is the frequency of the simplified model. From (2.112) the individual volume integrals in the denominator are denoted by D_i (subscript 'i' stands for the region $i=1$ to 6):

$$D_i = \iiint_{V_i} \epsilon_i |E_i|^2 dV \quad (2.115)$$

Similarly, the volume integrals in the numerator of the equation (2.112) are denoted by N_i :

$$N_i = \int \int \int_{V_i} E_i \cdot \nabla X \mu_i^{-1} \nabla X E_i dV \quad (2.116)$$

Using the analytical approach which includes integration of hyperbolic functions, integration of trigonometric functions and integration of Bessel functions [3], we get the resonant frequency ω_r as:

$$\omega_r^2 = \omega_o^2 \frac{D_1 + D_2 + N_3 + D_4 + N_5 + D_6 + N_H + N_V}{D_1 + D_2 + D_3 + D_4 + D_5 + D_6} \quad (2.117)$$

N_H and N_V are the surface integral terms (subscript H and V signifying the horizontal and vertical interfaces, respectively, as shown in Fig. 2.6). The computer program 2 listed at the end evaluates the approximate resonant frequency by the variational method. Also, besides the resonant frequency, the program also evaluates the Q factor due to resistive losses in the two shielding plates.

2.1.8 Results and discussions

The following results for $TE_{01\delta}$ and $TE_{01,1+\delta}$ modes have been discussed using program 1 (which is listed at the end) and Fig. 2.4.

Case 1)

$$\epsilon_{r6} = 38, a=5.25\text{mm}, L=4.6\text{mm}$$

$$\epsilon_{r1} = 1, L_1 = 15\text{mm}$$

$$\epsilon_{r2} = 1, L_2 = 15\text{mm}$$

Frequencies: For $TE_{01\delta}$ mode the frequency of Cohn as run by the program was found to be 4.6GHz. The perturbational frequency was found to be 4.855GHz. For the $TE_{01,1+\delta}$ mode, frequency of Cohn and Perturbational were found to be

7.685GHz and 8.194GHz respectively. Thus we could that change of modes greatly influenced the resonant frequency.

Energy distribution: For $TE_{01\delta}$ mode the percentage magnetic energy stored in the region 1, 2, 3 and 5 are greater than that for $TE_{01,1+\delta}$ mode. But in the region 4 the percentage stored magnetic energy is almost double in $TE_{01,1+\delta}$ mode. This gives us the idea that radial magnetic coupling for $TE_{01,1+\delta}$ mode would be more than that for $TE_{01\delta}$. In region 6, for both the modes, the percentage stored electric and magnetic energies are almost the same. The energy distribution for both the $TE_{01\delta}$ and $TE_{01,1+\delta}$ modes, it was seen that approximately 97% the electric energy and 63% of the magnetic energy is stored within the resonator. Also regions 1 and 2 have relatively large magnetic fields. So, one way to couple strongly to the resonator would be, to place some magnetic coupling mechanism in the regions 1 or 2.

Field distribution: The horizontal co-ordinate represents the distance in the z-direction, and the vertical co-ordinate represents the relative field amplitude. For $TE_{01\delta}$ mode the H_z, E_ϕ fields have the same sign everywhere in space, but this not true for $TE_{01,1+\delta}$ mode. For $TE_{01\delta}$ the H_z, E_ϕ component is an odd function of z, while H_ρ component is an even function of z. The greatest intensity for either field is concentrated within the resonator, and only rapidly decaying field exists outside the dielectric region. At $z=L/2$ distance, inside the DR the H_z, E_ϕ component has maximum amplitude, but H_ρ component is almost zero. But for $TE_{01,1+\delta}$ mode the case is almost the opposite. Also for $TE_{01,1+\delta}$ mode the H_z, E_ϕ component has a maximum at $z=0$ and a minimum at $z=L$.

Case 2)

$$\epsilon_r = 38, a=5.25\text{mm}, L=4.6\text{mm}$$

$$\epsilon_{r1} = 1, L_1 = 2.3$$

$$\epsilon_{r2} = 1, L_2 = 15$$

Here the left hand PEC wall is brought closer to the resonator by selecting $L_1 = L/2$.

Frequencies: Both the frequencies (Cohn model and Perturbational method) of $TE_{01\delta}$ and $TE_{01,1+\delta}$ have increased by a small amount, though not very significantly.

Energy distribution: We could observe that for $TE_{01\delta}$ mode the electric energy is approx. 98% and magnetic energy is approx. 61% within the dielectric resonator. For $TE_{01,1+\delta}$ mode the electric and magnetic energies are approx. 97.82% and 63% respectively within the DR.

Field distribution: Here the H_z, E_ϕ field components are even functions of z , and H_ρ component is an odd function of z for $TE_{01\delta}$ mode. For $TE_{01,1+\delta}$ the maximum amplitude of H_z, E_ϕ occurs at about $z=0.1L$, and drops as distance L increases. But H_ρ component has a maximum at about $z=0.6L$. The maximum of the H_z, E_ϕ field is no longer in the right for the $TE_{01\delta}$ mode. One most important fact that is observed in case of $TE_{01,1+\delta}$ mode is that the H_z, E_ϕ and H_ρ field components have crossovers, which looks as if they interact at some specific point. But this is not observed for $TE_{01\delta}$ mode except when two metal plates are touching the ends of the DR. In this case the crossover of H_z, E_ϕ and H_ρ is at approximately $z=0.3L$ within the DR.

Case 3)

$$\epsilon_{r6} = 38, a=5.25\text{mm}, L=4.6\text{mm}$$

$$\epsilon_{r1} = 1, L_1 = 0.0001\text{mm}$$

$$\epsilon_{r2} = 1, L_2 = 15\text{mm}$$

Here the DR is placed on the metal wall which is to the R.H.S.

Frequencies: The frequencies of the both $TE_{01\delta}$ and $TE_{01,1+\delta}$ modes have increased, for both the models.

Energy distribution: The stored electrical and magnetic energies for both $TE_{01\delta}$ and $TE_{01,1+\delta}$ modes in the regions 1, 2, 3 and 5 are zero. The region 2 has got a large amount of magnetic energy compared to the rest of the regions. The electrical and magnetic energies within the DR for both modes have increased, as compared to the previous cases.

Field distribution: The center of H_z, E_ϕ component for $TE_{01\delta}$ mode has shifted much to the right. The E_ϕ, H_z field component are zero on the left face of the resonator. The reason for this is that the tangential electric field on the surface of the PEC must vanish. This is true for $TE_{01\delta}$ and $TE_{01,1+\delta}$ modes. In case of $TE_{01,1+\delta}$ mode there is a crossover of H_z, E_ϕ and H_ρ component at $z=0.4L$. There is a kink or notch like structure observed in case of H_ρ field at $z=0.9L$.

Case 4)

$$\epsilon_{r6} = 38, a=5.25\text{mm}, L=4.6\text{mm}$$

$$\epsilon_{r1} = 1, L_1 = 0.0001\text{mm}$$

$$\epsilon_{r2} = 1, L_2 = 0.0001\text{mm}$$

In this case both the metal walls are touching the resonator.

Frequencies: The frequencies for both $TE_{01\delta}$ and $TE_{01,1+\delta}$ modes have been increased. This indicates that as the metal plates come closer to the resonator the frequency increases.

Energy distribution: The electrical and magnetic energies in the regions 1,

2, 3 and 5 were found to be zero.

Field distribution: The H_z, E_ϕ field components are zero on the left and right faces of the resonator. In case of $TE_{01\delta}$ mode the field variation consists of exactly one half wavelength. In case of $TE_{01,1+\delta}$ mode, it exhibits more than one half wavelength variation in the z-direction, within the resonator.

Case 5)

$$\epsilon_{r6} = 70, a=5.25\text{mm}, L=4.6\text{mm}$$

$$\epsilon_{r1} = 1, L_1 = 15\text{mm}$$

$$\epsilon_{r2} = 1, L_2 = 15\text{mm}$$

When L_1 and L_2 are greater than 3 times L , then the situation resembles as if the two metal plates are at infinity. The frequency for $TE_{01\delta}$ is observed to be less than that for $TE_{01,1+\delta}$ mode.

Field distribution: In $TE_{01\delta}$ mode the H_z, E_ϕ field component has the same sign everywhere, but in case of H_ρ field component it is not so. H_z is an even function of z , whereas H_ρ is an odd function of z . The fields fade away as we go away from the resonator on the either sides. In between $L/2 < z < L$ the H_ρ component increases and reaches its maximum, whereas H_z, E_ϕ slopes go down from its peak to approximately 60% of its maximum value. The peaks are broader in case of $TE_{01\delta}$ mode for H_ρ, E_ϕ, H_z field components, but in case of $TE_{01,1+\delta}$ mode the peaks are narrower for the same field components. There is a crossover of the H_ρ and H_z, E_ϕ field components at about $z=0.35L$. The H_z, E_ϕ field components undergo a maximum positive peak amplitude to a minimum negative peak amplitude within $0.1L < z < 0.9L$.

Case 6)

$$\epsilon_{r6} = 103, a=5.25\text{mm}, L=4.6\text{mm}$$

$$\epsilon_{r1} = 1, L_1 = 15\text{mm}$$

$$\epsilon_{r2} = 1, L_2 = 15\text{mm}$$

Frequency of $TE_{01\delta}$ mode is less than $TE_{01,1+\delta}$ mode.

The maximum amount of stored electrical and magnetic energies are concentrated within the DR region. Magnetic coupling would be advantageous as the magnetic energy is greater in the regions 1 and 2, hence fields would be stronger.

The field distribution is almost the same as in case of case 5.

Case 7)

$$\epsilon_{r6} = 70, a=5.25\text{mm}, L=4.6\text{mm}$$

$$\epsilon_{r1} = 1, L_1 = 2.3\text{mm}$$

$$\epsilon_{r2} = 1, L_2 = 15\text{mm}$$

Frequency of $TE_{01\delta}$ mode is greater than that of $TE_{01\delta}$ mode.

Stored electrical energy for region 6 is a little greater in case of $TE_{01\delta}$ mode. For region 1, $TE_{01\delta}$ mode has greater energy than that of $TE_{01,1+\delta}$ mode. But it is opposite in case of region 2. Magnetic energy stored in region 6 for $TE_{01\delta}$ mode is greater than that of $TE_{01,1+\delta}$ mode. Magnetic coupling is advantageous as for the reasons discussed earlier.

The fields H_z, E_ϕ peaks has slightly shifted to the right, also the crossover point of H_ρ from its negative to its positive peak has shifted to the right in case of $TE_{01\delta}$ mode. In case of $TE_{01,1+\delta}$ mode there is a small amount of flattening of the

positive peak in case of H_z, E_ϕ field components. Also after $L < z < L_2$ the curve of H_z, E_ϕ has a change of slope, as seen in the field distribution curve. In $TE_{01\delta}$ mode the relative amplitude of the H_ρ component is much smaller than the H_z, E_ϕ component.

Case 8)

$$\epsilon_{r6} = 103, a=5.25\text{mm}, L=4.6\text{mm}$$

$$\epsilon_{r1} = 1, L_1 = 2.3\text{mm}$$

$$\epsilon_{r2} = 1, L_2 = 15\text{mm}$$

Most of the observations were similar to that of case 7, which is discussed above.

&l6d0L

INPUT DATA

er= 38 a= 5.25 L= 4.6 LMODE= 0

er1= 1 L1= 15

er2= 1 L2= 15

ACCURCY OF SOLVING TRANSC. EQ. : 6 DIGITS

COUNTING.... 1

COUNTING.... 2

COUNTING.... 3

COUNTING.... 4

COUNTING.... 5

COHN'S MODEL

FREQ(COHN)= 4.600455 GHZ

PERTURBATIONAL RESULT

FREQ(PERT)= 4.855179 GHZ

WANT TO PLOT THE FIELD? (Y OR N)

?

WANT ENERGY TABLE DISTRI.? (Y OR N)

?

Ok

1LIST 2RUN← 3LOAD" 4SAVE" 5CONT← 6,"LPT1 7TRON← 8TROFF← 9KEY 0SCREEN

Case_1

16d0L

WANT ENERGY TABLE DISTRI.? (Y OR N)

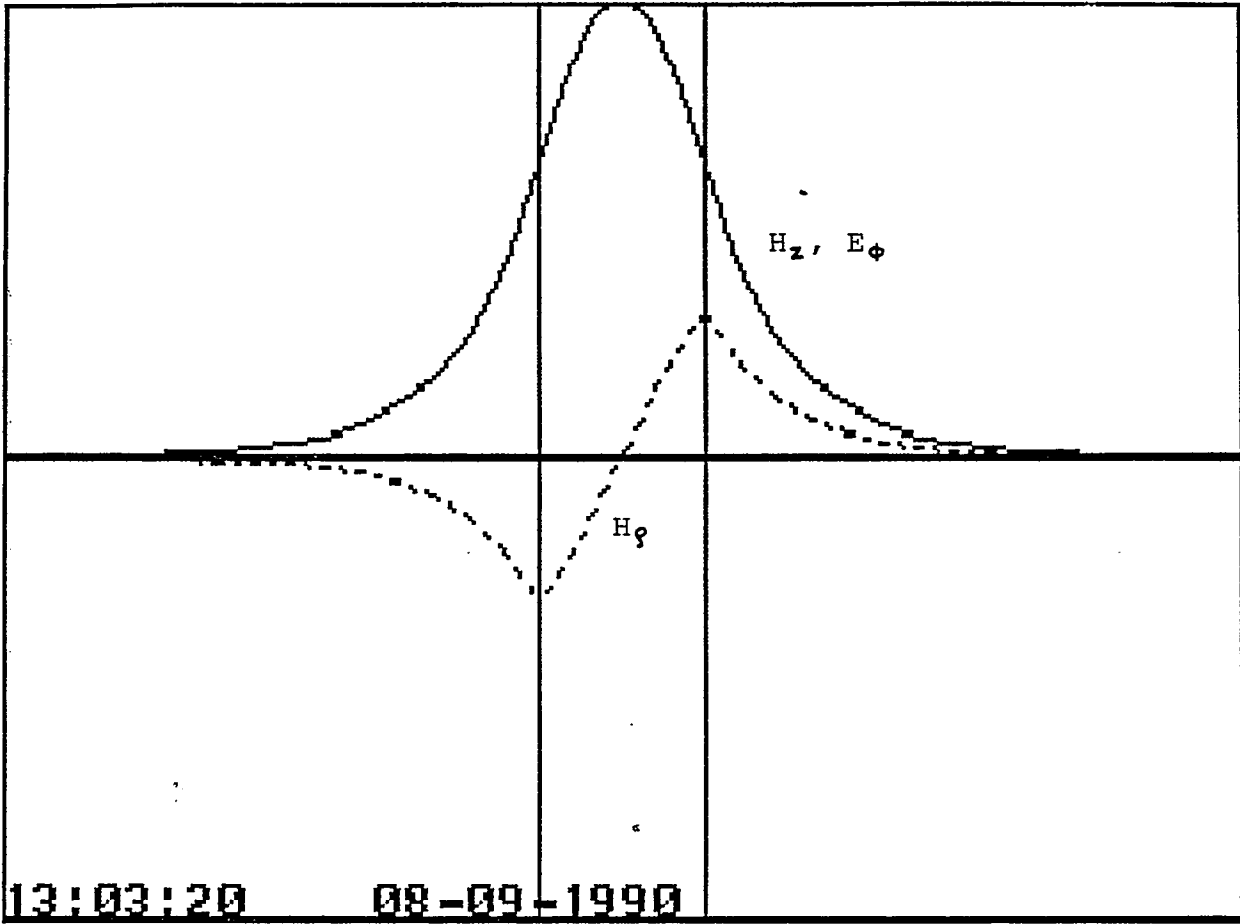
Y

	eps(j)	we(j)%	wm(j)%
1.00	1.00	0.33	13.22
2.00	1.00	0.33	13.22
3.00	1.00	0.16	3.19
4.00	1.00	1.27	4.88
5.00	1.00	0.16	3.19
6.00	38.00	97.74	62.29

k

LIST 2RUN← 3LOAD" 4SAVE" 5CONT← 6,"LPT1 7TRON← 8TROFF← 9KEY 0SCREEN

Case_1



Case 1) Field distribution

&l6d0L

INPUT DATA

er= 38 a= 5.25 L= 4.6 LMODE= 0

er1= 1 L1= 2.3

er2= 1 L2= 15

ACCURCY OF SOLVING TRANSC. EQ. : 6 DIGITS

COUNTING.... 1

COUNTING.... 2

COUNTING.... 3

COUNTING.... 4

COUNTING.... 5

COHN'S MODEL

FREQ(COHN)= 4.68649 GHz

PERTURBATIONAL RESULT

FREQ(PERT)= 5.002105 GHz

WANT TO PLOT THE FIELD? (Y OR N)

WANT ENERGY TABLE DISTRI.? (Y OR N)

ok

1LIST 2RUN← 3LOAD" 4SAVE" 5CONT← 6,"LPT1 7TRON← 8TROFF← 9KEY 0SCREEN

Case_2

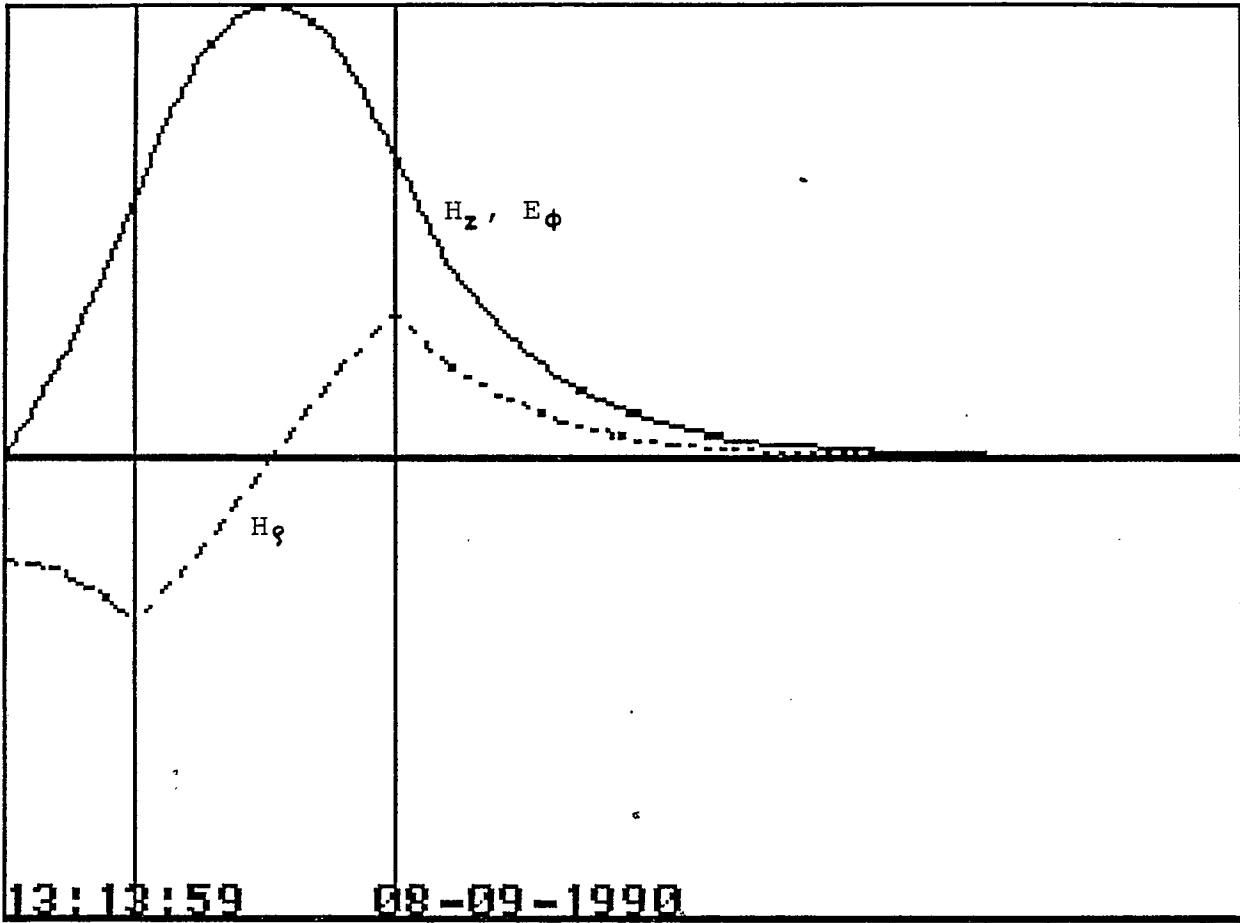
&l6d0L

WANT ENERGY TABLE DISTRI.? (Y OR N)

? Y
j eps(j) we(j)% wm(j)%
- 1.00 1.00 0.16 12.52
2.00 1.00 0.36 13.50
3.00 1.00 0.07 4.50
4.00 1.00 1.22 5.39
5.00 1.00 0.17 3.12
6.00 38.00 98.02 60.97

Dk

Case_2



Case 2) Field distribution

&l6d0L

INPUT DATA

er= 38 a= 5.25 l= 4.6 LMODE= 0

er1= 1 l1= .0001

er2= 1 l2= 15

ACCURCY OF SOLVING TRANSC. EQ. : 6 DIGITS

COUNTING.... 1

COUNTING.... 2

COUNTING.... 3

COUNTING.... 4

COUNTING.... 5

COHN'S MODEL

FREQ(COHN)= 5.249831 GHz

PERTURBATIONAL RESULT

FREQ(PERT)= 5.659552 GHz

WANT TO PLOT THE FIELD? (Y OR N)

WANT ENERGY TABLE DISTRI.? (Y OR N)

ok

Case_3

&l6d0L

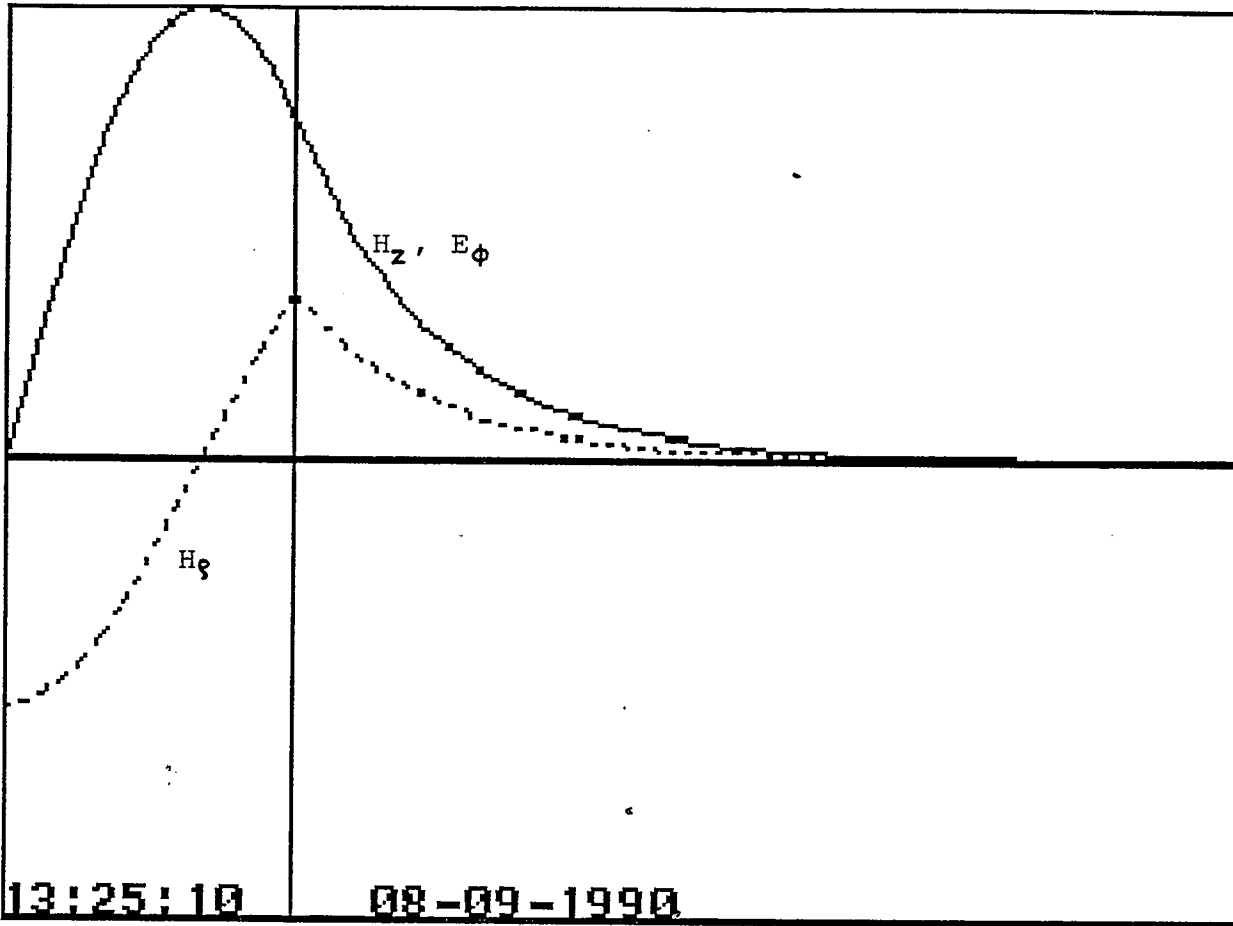
WANT ENERGY TABLE DISTRI.? (Y OR N)

Y

	eps(j)	we(j)%	wm(j)%
1.00	1.00	-0.00	0.00
2.00	1.00	0.58	16.93
3.00	1.00	-0.00	0.00
4.00	1.00	0.98	11.29
5.00	1.00	0.22	3.11
6.00	38.00	98.22	68.67

k

Case_3



Case 3) Field distribution

16d0L

INPUT DATA

nr= 38 a= 5.25 l= 4.6 LMODE= 0

nr1= 1 L1= .0001

nr2= 1 L2= .0001

ACCURACY OF SOLVING TRANSC. EQ. : 6 DIGITS

COUNTING.... 1

COUNTING.... 2

COUNTING.... 3

COUNTING.... 4

COUNTING.... 5

COHN'S MODEL

FREQ(COHN)= 6.369274 GHz

PERTURBATIONAL RESULT

FREQ(PERT)= 6.961879 GHz

WANT TO PLOT THE FIELD? (Y OR N)

WANT ENERGY TABLE DISTRI.? (Y OR N)

k

Case_4

&l6d0L

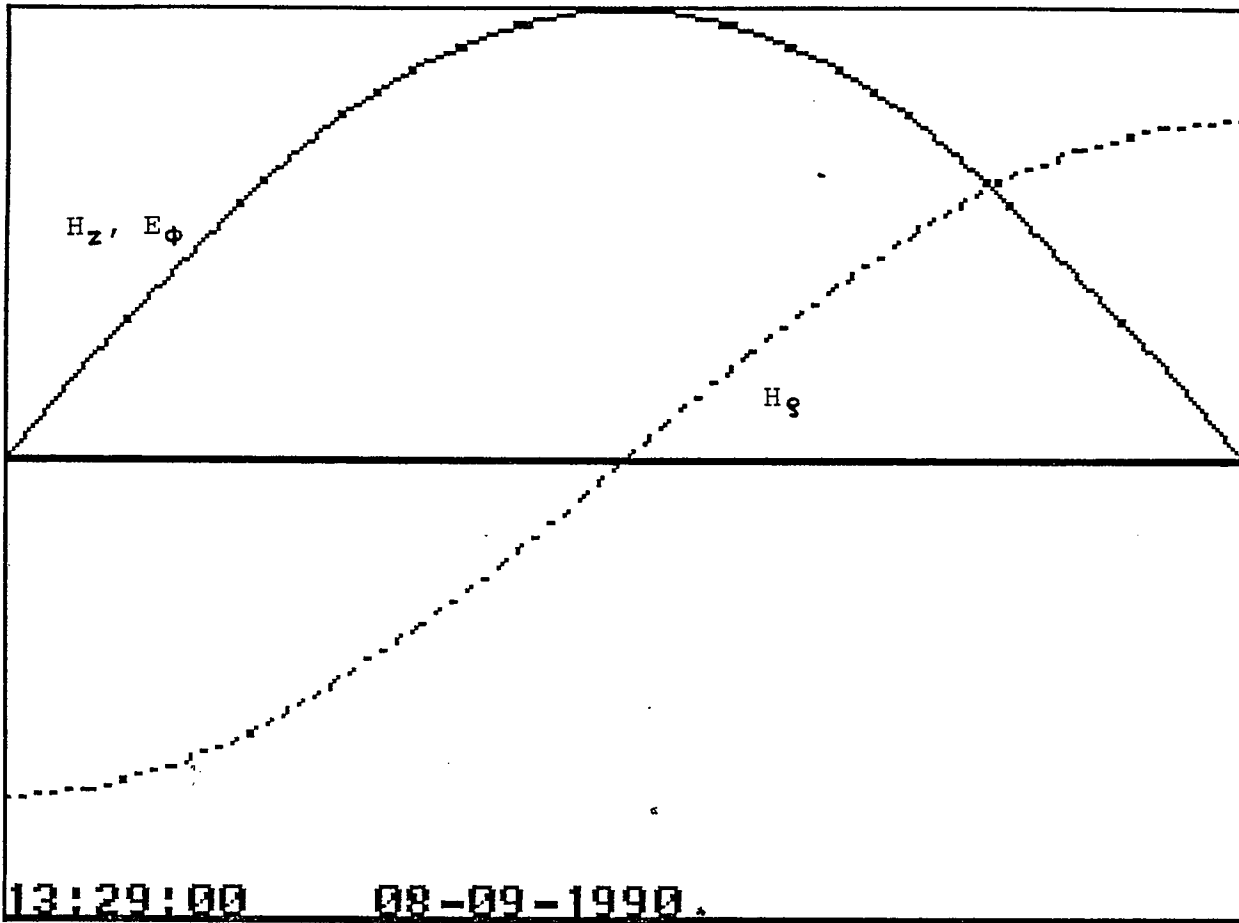
WANT ENERGY TABLE DISTRI.? (Y OR N)

Y

eps(j)	we(j)%	wm(j)%	
1.00	1.00	-0.00	0.00
2.00	1.00	-0.00	0.00
3.00	1.00	-0.00	0.00
4.00	1.00	0.73	16.21
5.00	1.00	-0.00	0.00
6.00	38.00	99.27	83.78

k

Case_4



Case 4) Field distribution

INPUT DATA

er= 70 a= 5.25 L= 4.6 LMODE= 0

er1= 1 L1= 15

er2= 1 L2= 15

ACCURACY OF SOLVING TRANSC. EQ. : 6 DIGITS

COUNTING.... 1

COUNTING.... 2

COUNTING.... 3

COUNTING.... 4

COUNTING.... 5

COHN'S MODEL

FREQ(COHN)= 3.394764 GHz

PERTURBATIONAL RESULT

FREQ(PERT)= 3.593789 GHz

WANT TO PLOT THE FIELD? (Y OR N)

?

WANT ENERGY TABLE DISTRI.? (Y OR N)

?

Ok

1LIST 2RUN; 3LOAD" 4SAVE" 5CONT; 6,"LPT1 7TRON; 8TROFF; 9KEY 0SCREEN

Case_5

WANT ENERGY TABLE DISTRI.? (Y OR N)

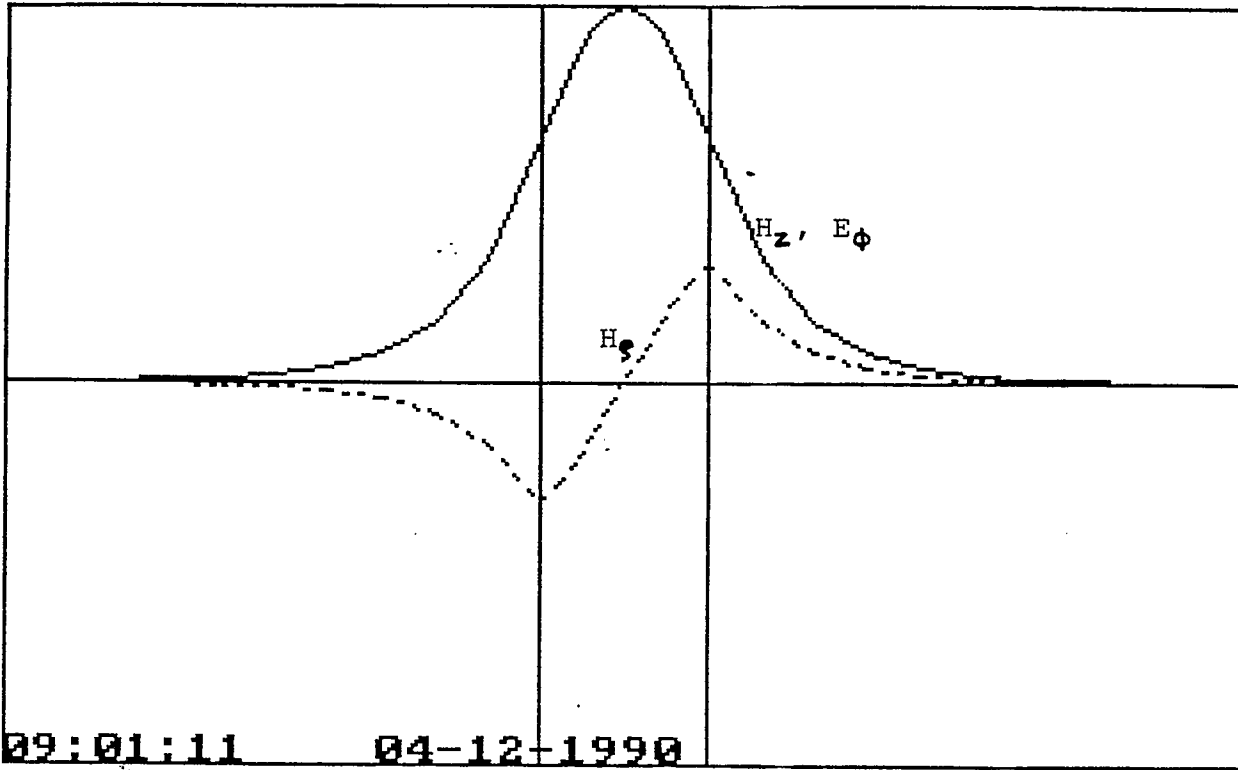
? Y

	eps(j)	we(j)%	wm(j)%
1.00	1.00	0.18	13.15
2.00	1.00	0.18	13.15
3.00	1.00	0.09	3.15
4.00	1.00	0.69	4.88
5.00	1.00	0.09	3.15
6.00	70.00	98.78	62.51

ok

LIST 2RUN; 3LOAD" 4SAVE" 5CONT; 6,"LPT1 7TRON; 8TROFF; 9KEY 0SCREEN

Case_5



Case 5) Field distribution

INPUT DATA

r= 103 a= 5.25 L= 4.6 LMODE= 0

r1= 1 L1= 15

r2= 1 L2= 15

CURCY OF SOLVING TRANSC. EQ. : 6 DIGITS

COUNTING.... 1

COUNTING.... 2

COUNTING.... 3

COUNTING.... 4

COUNTING.... 5

COHN'S MODEL

REQ(COHN)= 2.80021 GHz

PERTURBATIONAL RESULT

REQ(PERT)= 2.967771 GHz

WANT TO PLOT THE FIELD? (Y OR N)

WANT ENERGY TABLE DISTRI.? (Y OR N)

k

LIST 2RUN; 3LOAD" 4SAVE" 5CONT; 6,"LPT1 7TRON; 8TROFF; 9KEY 0SCREEN

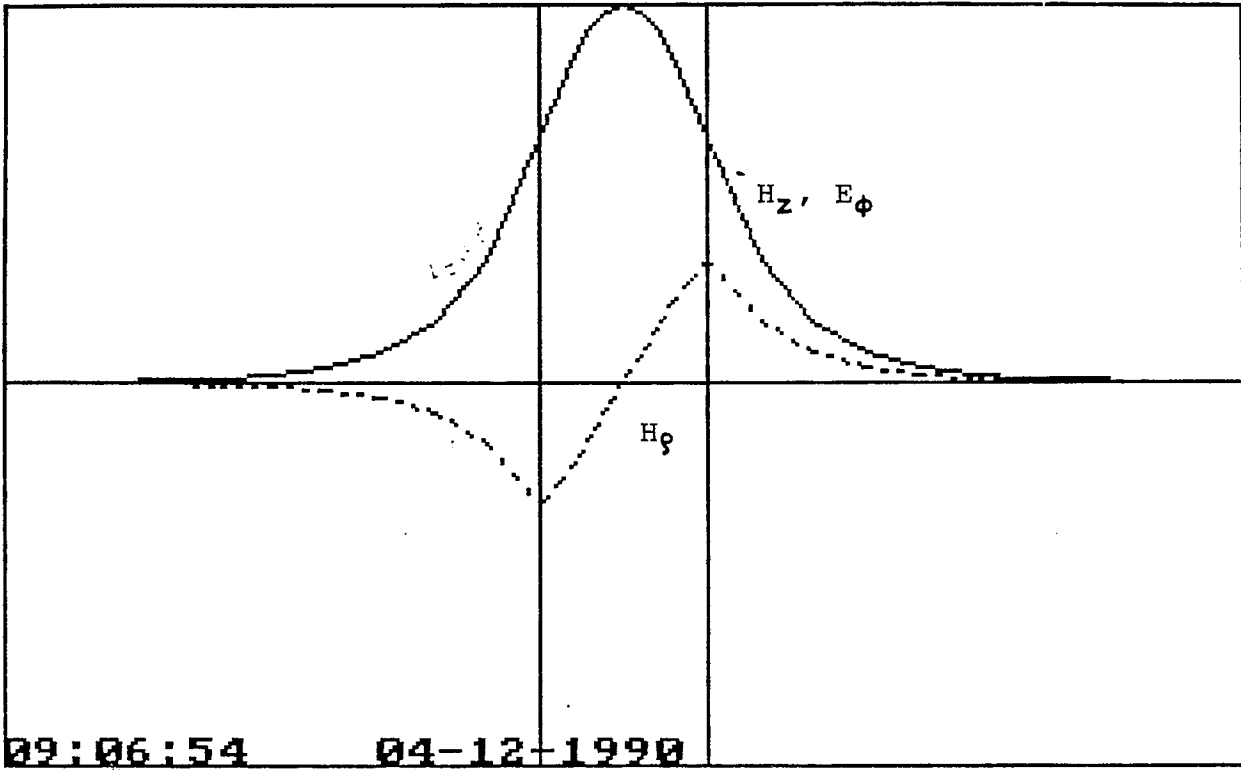
Case_6

WANT ENERGY TABLE DISTRI.? (Y OR N)

? Y
j eps(j) we(j)% wm(j)%
1.00 1.00 0.12 13.13
2.00 1.00 0.12 13.13
3.00 1.00 0.06 3.14
4.00 1.00 0.46 4.87
5.00 1.00 0.06 3.14
6.00 103.00 99.18 62.60

ok

Case_6



Case 6) Field distribution

INPUT DATA

er= 70 a= 5.25 L= 4.6 LMODE= 0

er1= 1 L1= 2.3

er2= 1 L2= 15

ACCURCY OF SOLVING TRANSC. EQ. : 6 DIGITS

COUNTING.... 1

COUNTING.... 2

COUNTING.... 3

COUNTING.... 4

COUNTING.... 5

COHN'S MODEL

FREQ(COHN)= 3.457059 GHz

PERTURBATIONAL RESULT

FREQ(PERT)= 3.698976 GHz

WANT TO PLOT THE FIELD? (Y OR N)

?

WANT ENERGY TABLE DISTRI.? (Y OR N)

?

ok

. Case__7

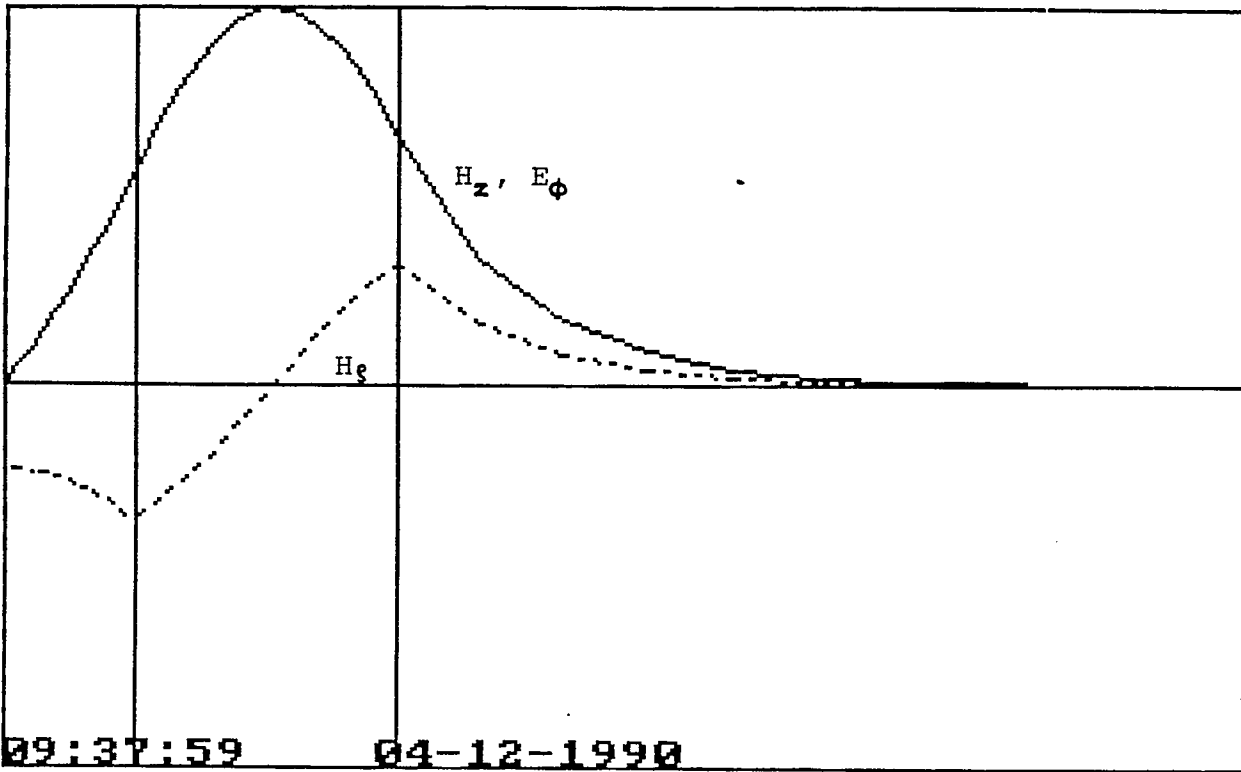
ANT ENERGY TABLE DISTRI.? (Y OR N)

Y

	eps(j)	we(j)%	wm(j)%
1.00	1.00	0.09	12.51
2.00	1.00	0.19	13.41
3.00	1.00	0.04	4.43
4.00	1.00	0.66	5.37
5.00	1.00	0.09	3.09
6.00	70.00	98.93	61.19

k

Case_7



Case 7) Field distribution

INPUT DATA

er= 103 a= 5.25 L= 4.6 LMODE= 0

er1= 1 L1= 2.3

er2= 1 L2= 15

ACCURACY OF SOLVING TRANSC. EQ. : 6 DIGITS

COUNTING.... 1

COUNTING.... 2

COUNTING.... 3

COUNTING.... 4

COUNTING.... 5

COHN'S MODEL

FREQ(COHN)= 2.851218 GHz

PERTURBATIONAL RESULT

FREQ(PERT)= 3.053543 GHz

WANT TO PLOT THE FIELD? (Y OR N)

WANT ENERGY TABLE DISTRI.? (Y OR N)

ok

Case_8

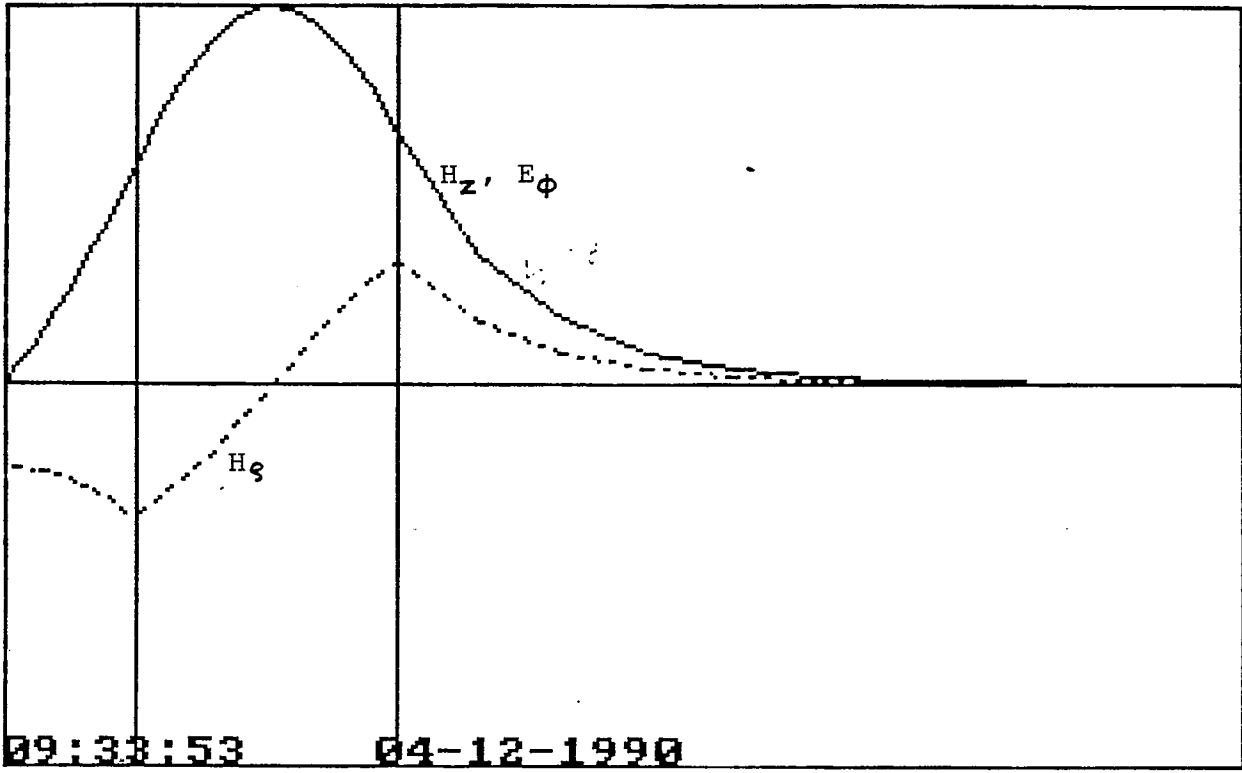
WANT ENERGY TABLE DISTRI.? (Y OR N)

Y

	eps(j)	we(j)%	wm(j)%
1.00	1.00	0.06	12.51
2.00	1.00	0.13	13.38
3.00	1.00	0.03	4.40
4.00	1.00	0.45	5.36
5.00	1.00	0.06	3.07
6.00	103.00	99.28	61.27

ok

Case_8



Case 8) Field distribution

16d0L

INPUT DATA

nr= 38 a= 5.25 L= 4.6 LMODE= 1

nr1= 1 L1= 15

nr2= 1 L2= 15

ACCURCY OF SOLVING TRANSC. EQ. : 6 DIGITS

COUNTING.... 1

COUNTING.... 2

COUNTING.... 3

COUNTING.... 4

COUNTING.... 5

COHN'S MODEL

REQ(COHN)= 7.684845 GHz

PERTURBATIONAL RESULT

REQ(PERT)= 8.19373 GHz

WANT TO PLOT THE FIELD? (Y OR N)

WANT ENERGY TABLE DISTRI.? (Y OR N)

k

Case 1

&l6d0L

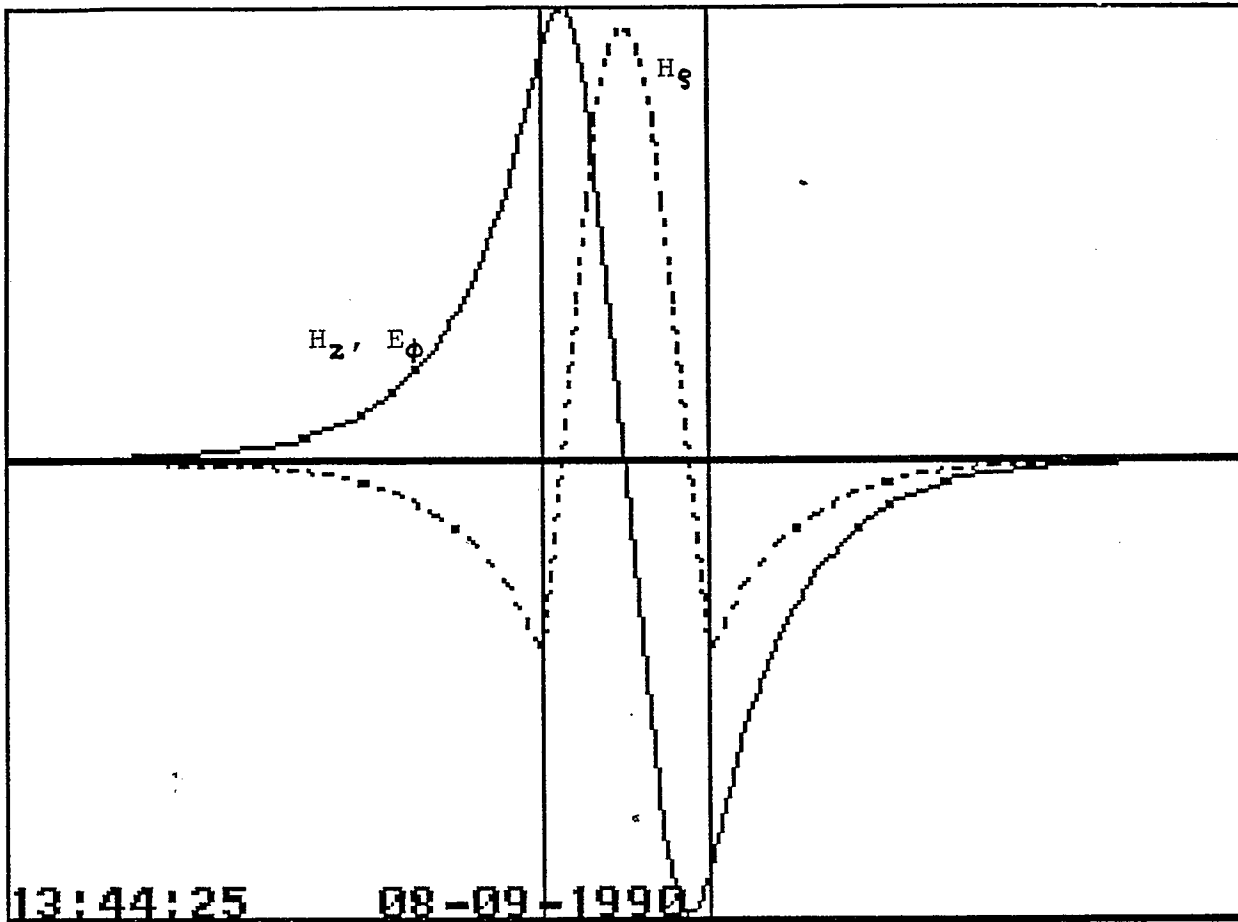
ANT ENERGY TABLE DISTRI.? (Y OR N)

Y

eps(j)	we(j)%	wm(j)%	
1.00	1.00	0.88	11.80
2.00	1.00	0.88	11.80
3.00	1.00	0.19	1.21
4.00	1.00	0.56	10.02
5.00	1.00	0.19	1.21
6.00	38.00	97.30	63.97

k

Case_1



Case 1) Field distribution

16d0L

INPUT DATA

nr= 38 a= 5.25 l= 4.6 LMODE= 1

nr1= 1 L1= 2.3

nr2= 1 L2= 15

PRECURCY OF SOLVING TRANSC. EQ. : 6 DIGITS

COUNTING.... 1

COUNTING.... 2

COUNTING.... 3

COUNTING.... 4

COUNTING.... 5

COHN'S MODEL

REQ(COHN)= 7.830875 GHz

PERTURBATIONAL RESULT

REQ(PERT)= 8.37872 GHz

WANT TO PLOT THE FIELD? (Y OR N)

WANT ENERGY TABLE DISTRI.? (Y OR N)

k

Case_2

&l6d0L

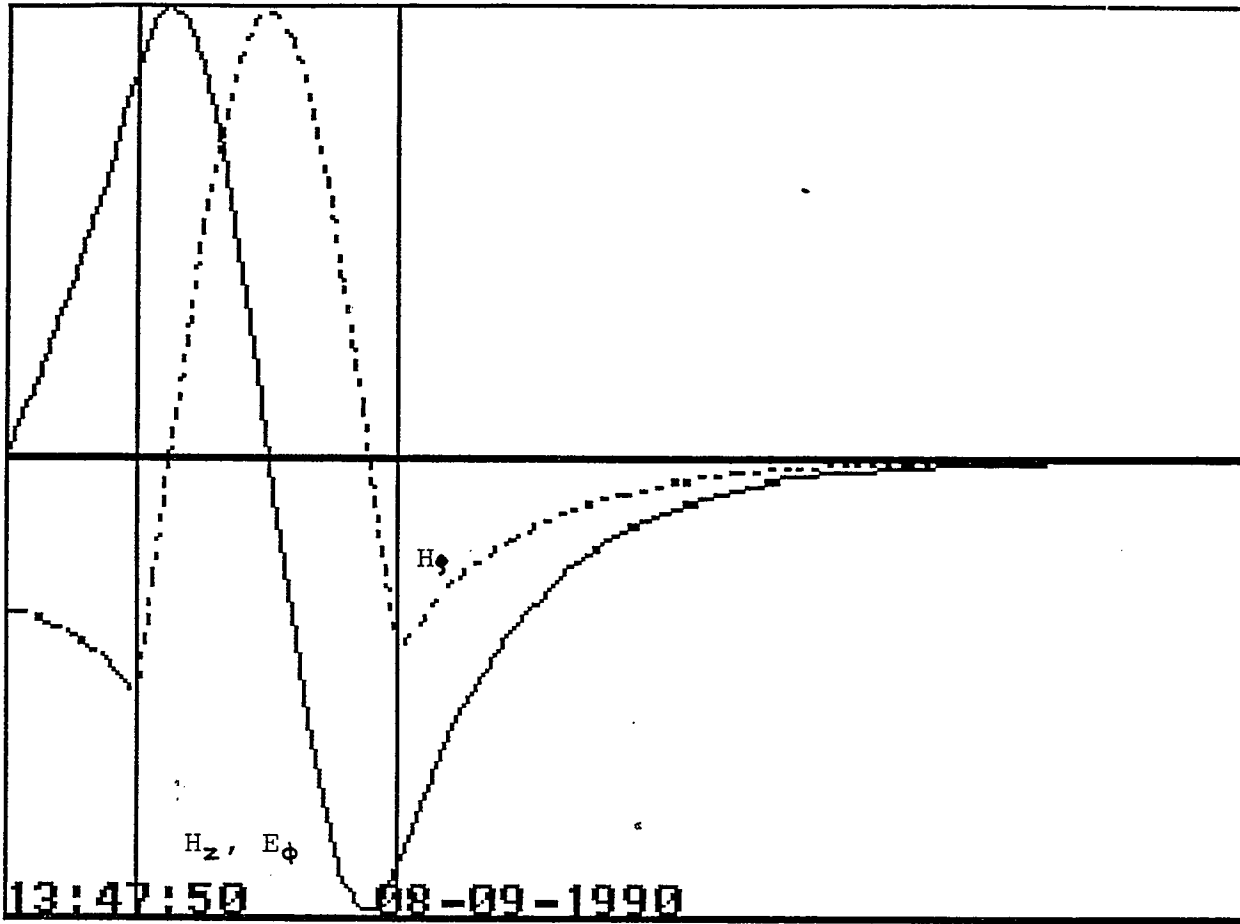
WANT ENERGY TABLE DISTRI.? (Y OR N)

Y

	eps(j)	we(j)%	wm(j)%
1.00	1.00	0.45	12.74
2.00	1.00	0.89	11.39
3.00	1.00	0.10	2.07
4.00	1.00	0.55	9.72
5.00	1.00	0.19	1.14
6.00	38.00	97.82	62.94

ok

Case_2



Case 2) Field distribution

&l6d0L

INPUT DATA

er= 38 a= 5.25 L= 4.6 LMODE= 1

er1= 1 L1= .0001

r2= 1 L2= 15

ACCURCY OF SOLVING TRANSC. EQ. : 6 DIGITS

COUNTING.... 1

COUNTING.... 2

COUNTING.... 3

COUNTING.... 4

COUNTING.... 5

COHN'S MODEL

FREQ(COHN)= 9.24841 GHz

PERTURBATIONAL RESULT

FREQ(PERT)= 9.863364 GHz

WANT TO PLOT THE FIELD? (Y OR N)

?

WANT ENERGY TABLE DISTRI.? (Y OR N)

?

ok

Case_3

&l6d0L

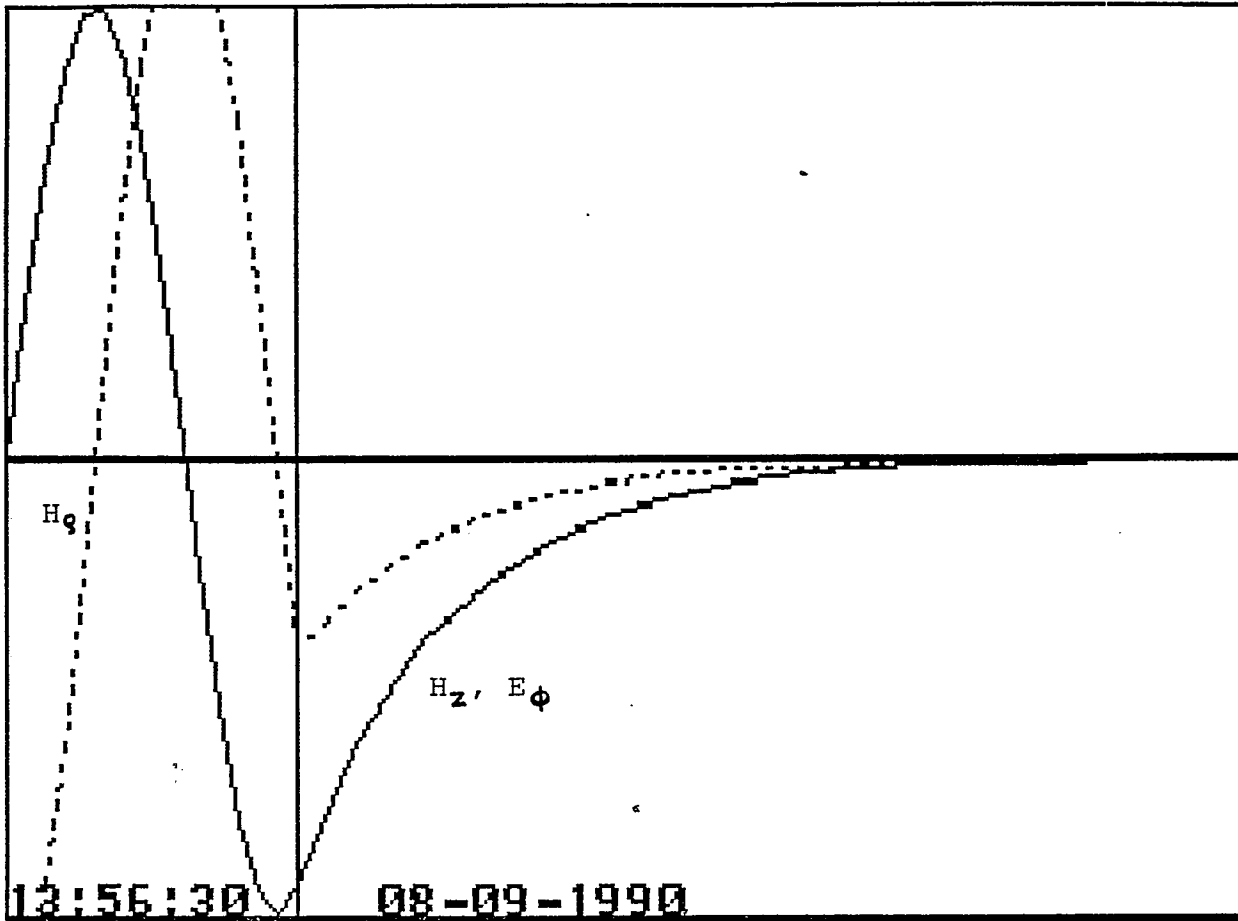
WANT ENERGY TABLE DISTRI.? (Y OR N)

? Y

j	eps(j)	we(j)%	wm(j)%
1.00	1.00	-0.00	0.00
2.00	1.00	1.11	10.02
3.00	1.00	-0.00	0.00
4.00	1.00	0.46	11.45
5.00	1.00	0.20	0.80
6.00	38.00	98.23	77.73

ok

Case_3



Case 3) Field distribution

16d0L

INPUT DATA

er= 38 a= 5.25 l= 4.6 LMODE= 1

er1= 1 L1= .0001

er2= 1 L2= .0001

ACCURACY OF SOLVING TRANSC. EQ. : 6 DIGITS

COUNTING.... 1

COUNTING.... 2

COUNTING.... 3

COUNTING.... 4

COUNTING.... 5

COHN'S MODEL

FREQ(COHN)= 11.1583 GHz

PERTURBATIONAL RESULT

FREQ(PERT)= 11.8543 GHz

WANT TO PLOT THE FIELD? (Y OR N)

WANT ENERGY TABLE DISTRI.? (Y OR N)

ok

Case_4

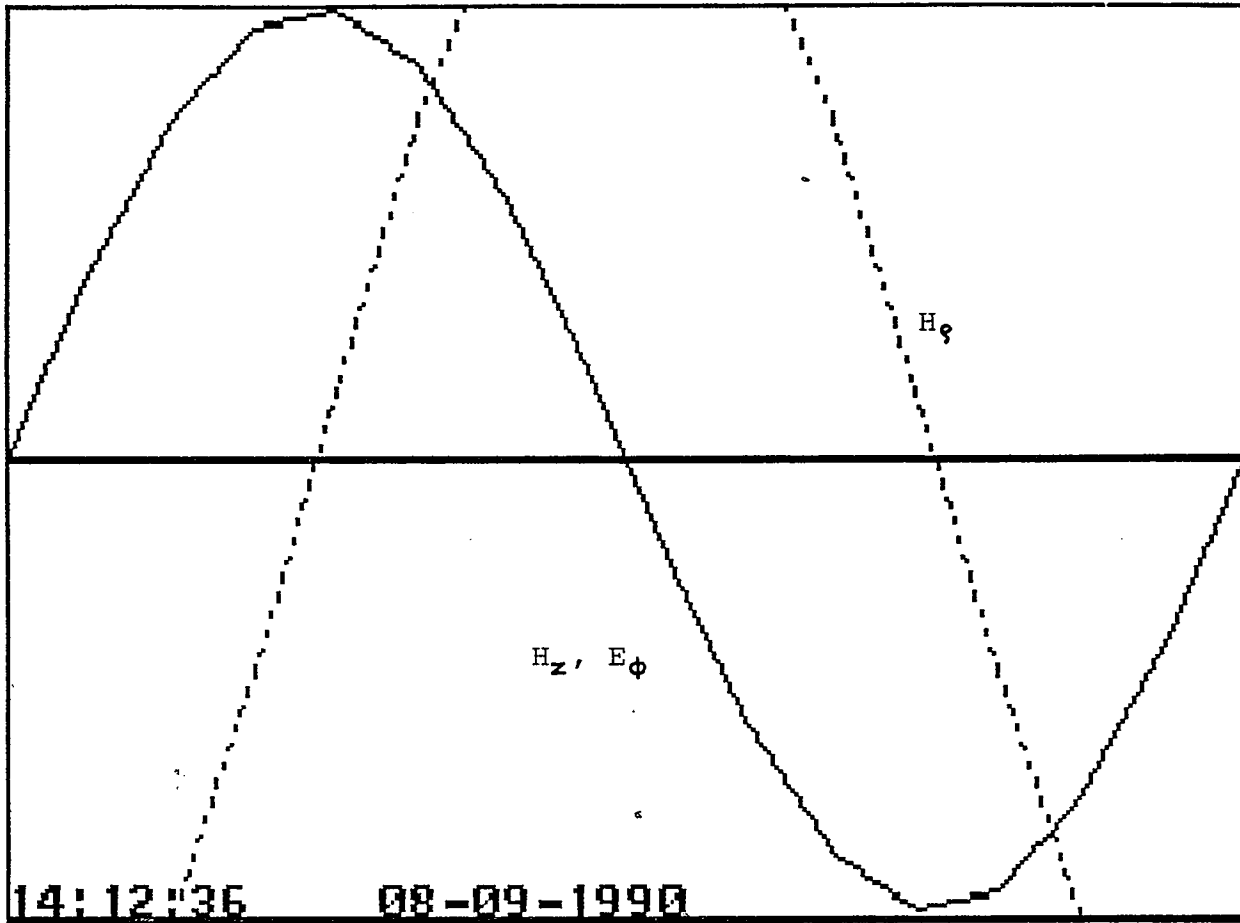
&16d0L

WANT ENERGY TABLE DISTRI.? (Y OR N)

? Y
j eps(j) we(j)% wm(j)%
- 1.00 1.00 0.00 0.00
 2.00 1.00 0.00 0.00
 3.00 1.00 0.00 0.00
 4.00 1.00 0.37 11.39
 5.00 1.00 0.00 0.00
 6.00 38.00 99.63 88.61

Ok

Case_4



Case 4) Field distribution

INPUT DATA

er= 70 a= 5.25 L= 4.6 LMODE= 1

er1= 1 L1= 15

er2= 1 L2= 15

ACCURCY OF SOLVING TRANSC. EQ. : 6 DIGITS

COUNTING.... 1

COUNTING.... 2

COUNTING.... 3

COUNTING.... 4

COUNTING.... 5

COHN'S MODEL

FREQ(COHN)= 5.68469 GHz

PERTURBATIONAL RESULT

FREQ(PERT)= 6.072447 GHz

WANT TO PLOT THE FIELD? (Y OR N)

?

WANT ENERGY TABLE DISTRI.? (Y OR N)

?

Ok

Case_5

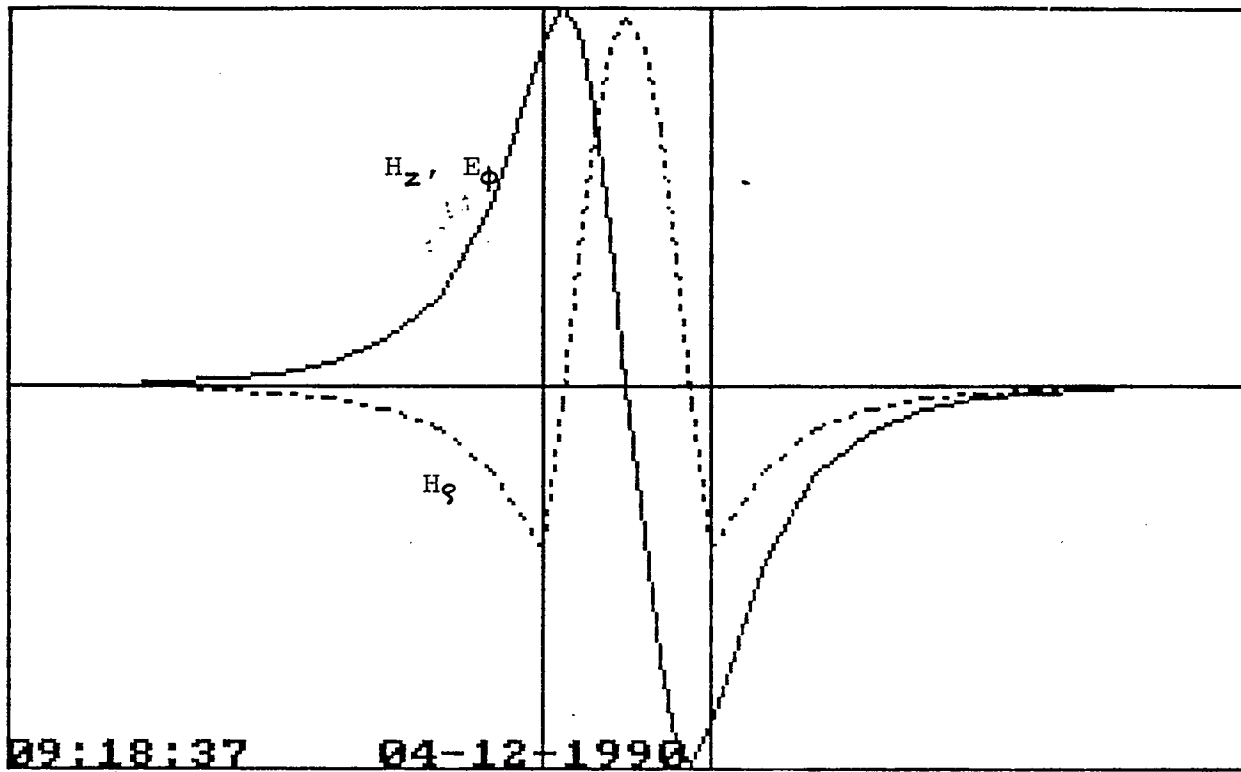
WANT ENERGY TABLE DISTRI.? (Y OR N)

Y

	eps(j)	we(j)%	wm(j)%
1.00	1.00	0.46	11.65
2.00	1.00	0.46	11.65
3.00	1.00	0.10	1.22
4.00	1.00	0.31	9.96
5.00	1.00	0.10	1.22
6.00	70.00	98.57	64.30

k

Case_5



Case 5) Field distribution

INPUT DATA

nr= 103 a= 5.25 L= 4.6 LMODE= 1

nr1= 1 L1= 15

nr2= 1 L2= 15

CURCY OF SOLVING TRANSC. EQ. : 6 DIGITS

COUNTING.... 1

COUNTING.... 2

COUNTING.... 3

COUNTING.... 4

COUNTING.... 5

COHN'S MODEL

REQ(COHN)= 4.693314 GHZ

PERTURBATIONAL RESULT

REQ(PERT)= 5.016868 GHZ

WANT TO PLOT THE FIELD? (Y OR N)

WANT ENERGY TABLE DISTRI.? (Y OR N)

k

Case_6

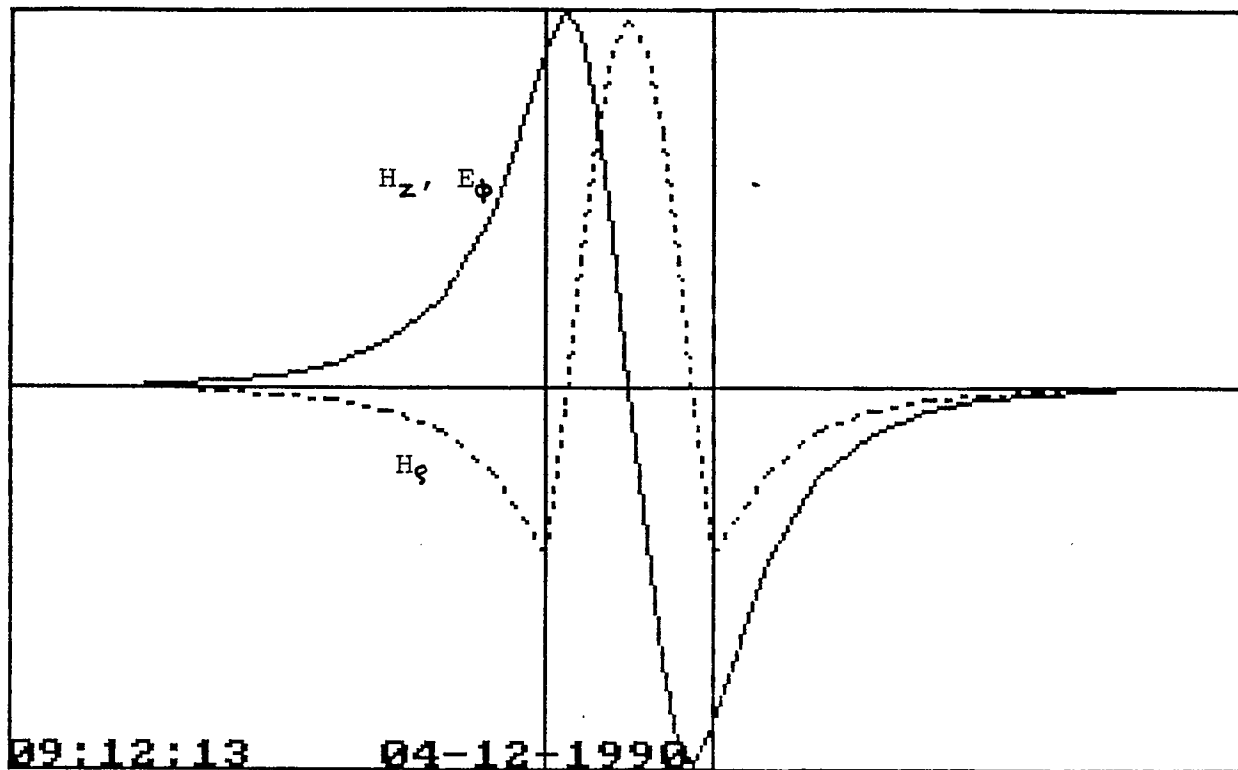
WANT ENERGY TABLE DISTRI.? (Y OR N)

? Y

j	eps(j)	we(j)%	wm(j)%
1.00	1.00	0.31	11.60
2.00	1.00	0.31	11.60
3.00	1.00	0.07	1.22
4.00	1.00	0.21	9.94
5.00	1.00	0.07	1.22
6.00	103.00	99.04	64.42

Ok

Case_6



Case 6) Field distribution

INPUT DATA

er= 70 a= 5.25 L= 4.6 LMODE= 1

er1= 1 L1= 2.3

er2= 1 L2= 15

!CURCY OF SOLVING TRANSC. EQ. : 6 DIGITS

COUNTING.... 1

COUNTING.... 2

COUNTING.... 3

COUNTING.... 4

COUNTING.... 5

COHN'S MODEL

FREQ(COHN)= 5.787344 GHz

PERTURBATIONAL RESULT

FREQ(PERT)= 6.200962 GHz

WANT TO PLOT THE FIELD? (Y OR N)

WANT ENERGY TABLE DISTRI.? (Y OR N)

ok

Case_7

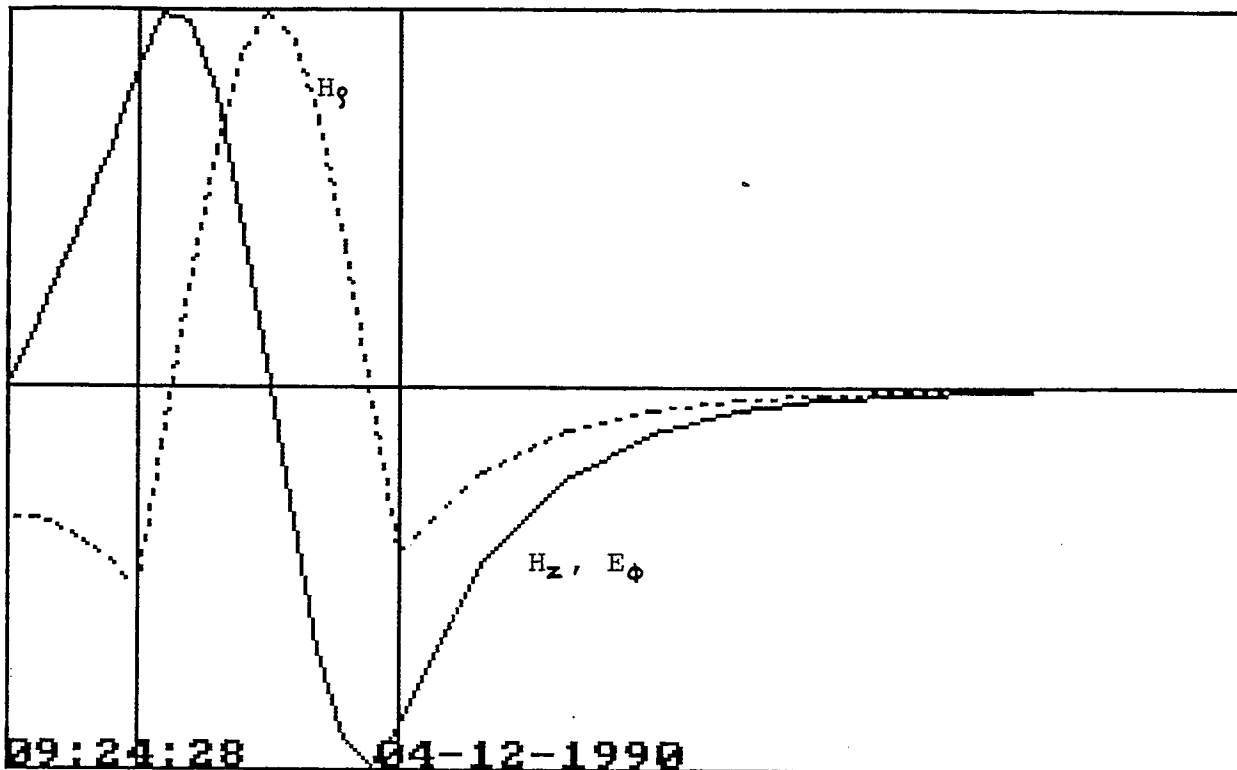
WANT ENERGY TABLE DISTRI.? (Y OR N)

? Y

j	eps(j)	we(j)%	wm(j)%
1.00	1.00	0.25	12.66
2.00	1.00	0.47	11.25
3.00	1.00	0.05	2.04
4.00	1.00	0.30	9.67
5.00	1.00	0.10	1.15
6.00	70.00	98.84	63.23

ok

Case_7



Case 7) Field distribution

INPUT DATA

r= 103 a= 5.25 L= 4.6 LMODE= 1

r1= 1 L1= 2.3

r2= 1 L2= 15

PRECISION OF SOLVING TRANSC. EQ. : 6 DIGITS

COUNTING.... 1

COUNTING.... 2

COUNTING.... 3

COUNTING.... 4

COUNTING.... 5

COHN'S MODEL

REQ(COHN)= 4.776432 GHz

PERTURBATIONAL RESULT

REQ(PERT)= 5.120466 GHz

WANT TO PLOT THE FIELD? (Y OR N)

WANT ENERGY TABLE DISTRI.? (Y OR N)

k

Case_8

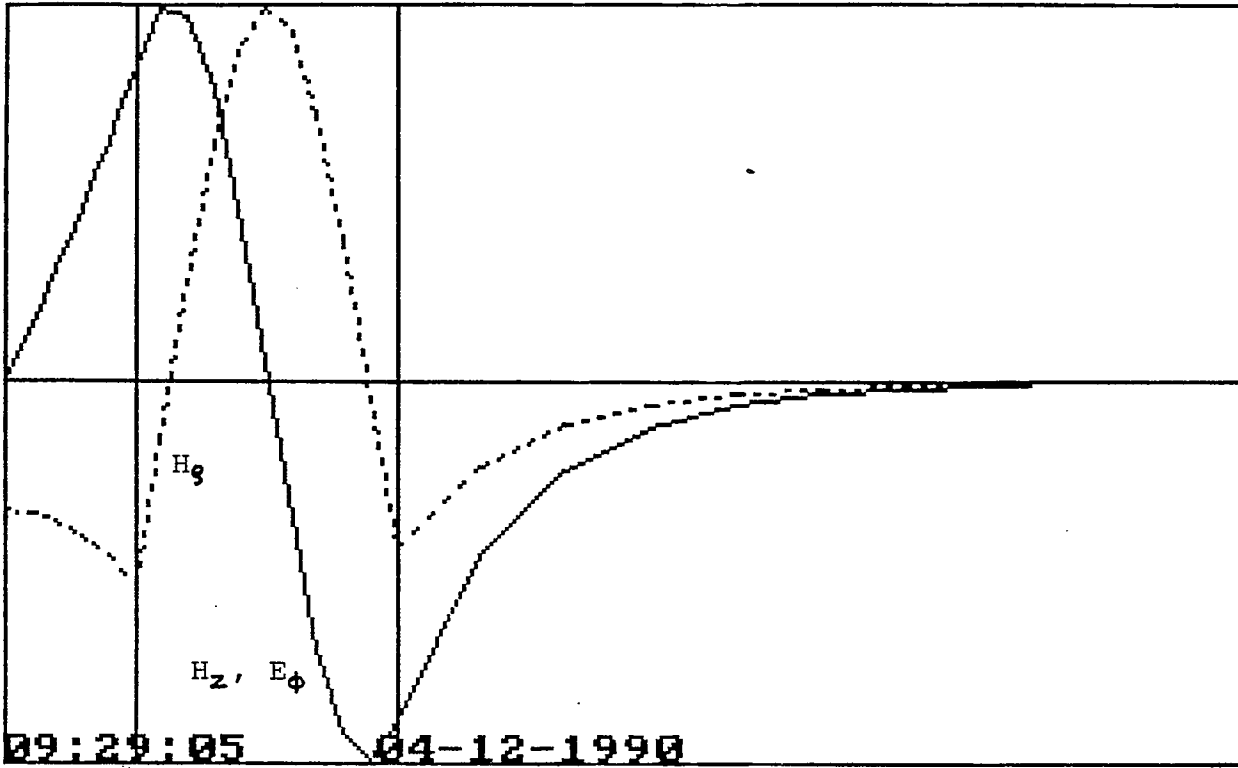
WANT ENERGY TABLE DISTRI.? (Y OR N)

? Y

j	eps(j)	we(j)%	wm(j)%
1.00	1.00	0.17	12.63
2.00	1.00	0.31	11.20
3.00	1.00	0.04	2.02
4.00	1.00	0.20	9.65
5.00	1.00	0.07	1.15
6.00	103.00	99.22	63.34

Ok

Case_8



Case 8) Field distribution

Chapter 3

3.1 Introduction

The recent advanced technology has produced GaAsFET oscillator to function as a high efficiency and low operational voltage solid state microwave oscillator [18] [19]. An oscillator is specifically a system which consists of a passive circuit (typically DR mounted near a microstrip transmission line), and of an active device, which produces the oscillation. The oscillations occur at the frequency where the susceptance of the active device is equal and opposite to the susceptance of the passive circuit. In order to ensure that the oscillation frequency does not depend on the temperature, the temperature coefficient of the passive circuit susceptance must be equal and opposite to the temperature coefficient of the active device susceptance.

The use of a dielectric resonator, made of Barium tetratitanate ceramic compound, coupled to the oscillator drain output terminal gives an enhanced temperature stability and very low loss characteristics of such oscillators. Also, the small size, easy coupling and tunability makes these very popular microwave device components. GaAsFET oscillators are expected to be less noisy, more efficient and more flexible to design than other solid-state oscillators. The dielectric material used for the resonator is a low-loss ceramic compound, mainly consisting of $BaTi_4O_9$. The microwave characteristics of this dielectric material can be determined by measuring

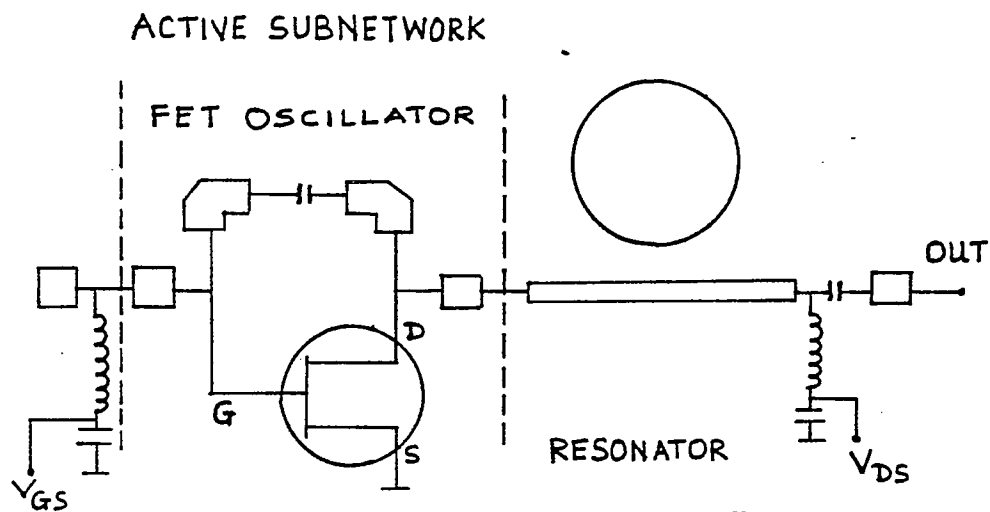


Figure 3.1: Typical GaAsFET oscillator

the resonant frequency for any TE_{mnp} for cylindrical resonator short circuited with metal plates on both sides. The above ceramic material has an expansion coefficient and dielectric constant temperature coefficient that offset each other and result in a small resonant frequency temperature coefficient.

Here in this, a typical GaAsFET oscillator integrated with a dielectric resonator is considered as shown in Fig. 3.1. For designing a stabilized FET oscillator, frequency temperature coefficient, pushing figure, pulling characteristics, stabilization range width etc. have to be taken into account. These performances depend strongly on the coupling constant between the resonant circuit and the transmission line. We have developed a computer aided design procedure for such stabilized oscillator circuits. The procedure also incorporates the numerical calculation of the resonant frequency of the dielectric resonator based on its physical dimensions such as the dimensions of the resonator itself, the air gap between the DR and the top wall and the substrate thickness. The dynamic characteristics of these oscillators are investigated. Especially the studies have been made about the stabilized oscillator temperature coefficient. The results of these investigations are presented and

ACTIVE SUBNETWORK

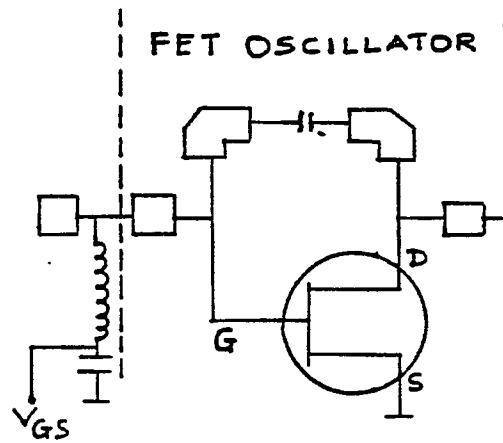


Figure 3.2: Typical oscillator circuit

compared with the experimental values. These results are important for precise custom made design of such oscillators [8].

3.1.1 Analysis

A typical oscillator circuit, considered here is shown in Fig. 3.2. The dielectric resonator is coupled to the 50Ω microstrip line which is connected to the output terminal. When a dielectric resonator is placed in the vicinity of a microstrip line on the alumina substrate, magnetic coupling between the resonator and the line is caused. Coupling constant increases if distance " l_y " between resonator edge and microstripline edge decreases, this is shown in Fig. 3.3. It can be shown that the dielectric resonant circuit is expressed as a high 'Q' parallel resonant circuit coupled to the transmission line of characteristic impedance $z_0 = 50\Omega$ (Fig. 3.3).

A block diagram of a stabilized oscillator is shown in Fig. 3.4. The dielectric resonator is placed in the vicinity of a 50Ω microstripline, is connected to the drain end of the active subnetwork.

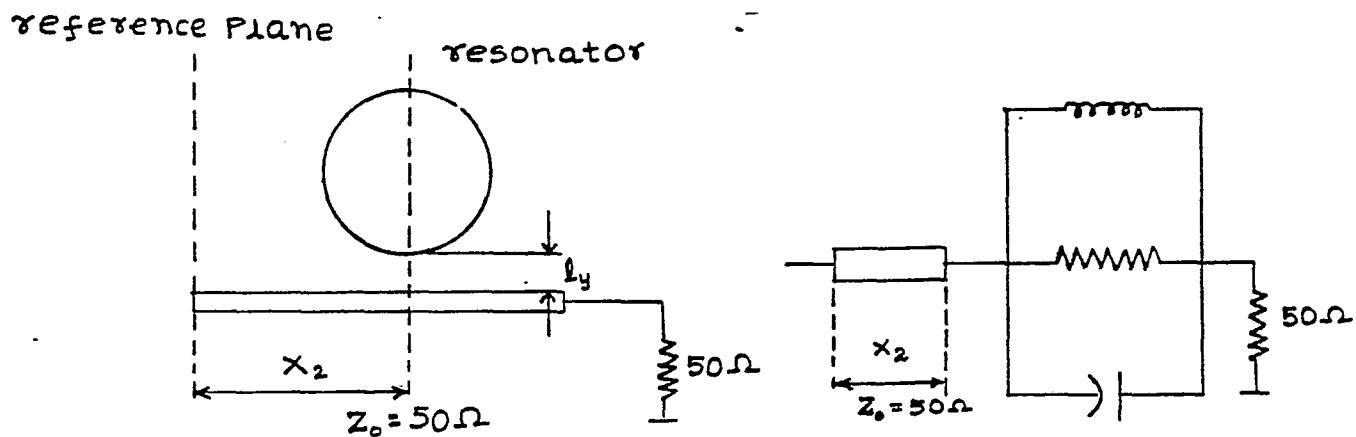


Figure 3.3: Dielectric Resonator coupled to the microstrip

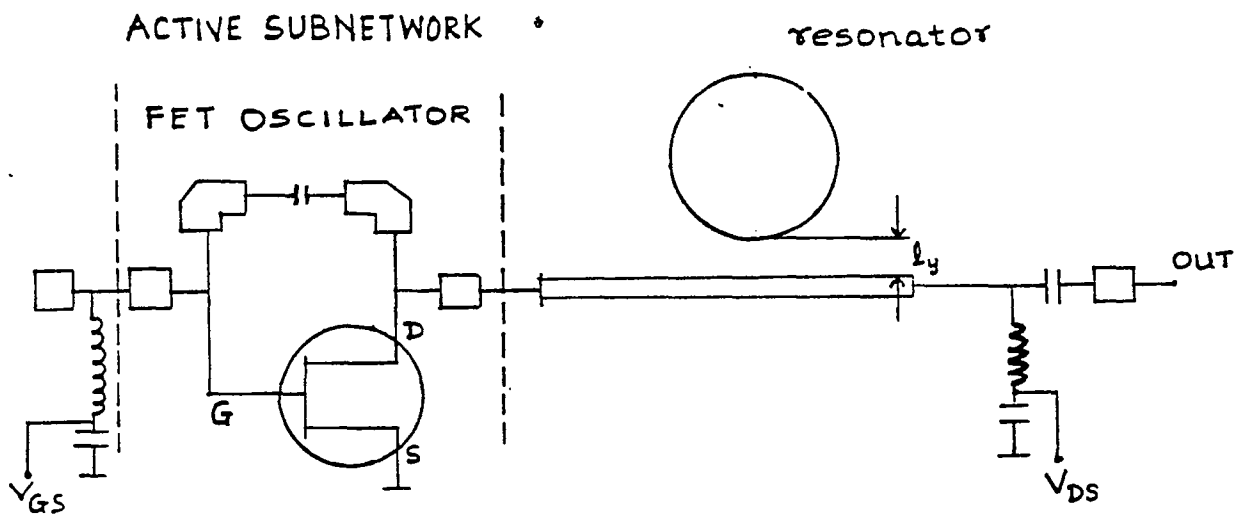


Figure 3.4: Stabilized oscillator

3.1.2 Theoretical aspects of the oscillator stabilization

Stabilization of a solid state microwave oscillator by loading a band rejection filter was theoretically investigated by K. Shirahata [9].

When a resonant circuit is coupled to a transmission line terminated by a load with reflection coefficient $\Gamma e^{j\phi}$, then the oscillation frequency can be obtained by equating the total susceptance 'B' to zero, under the condition that $\delta B/\delta f > 0$.

$$B = 2Q_o \left(\frac{f - f_r}{f_r} + \frac{f_r - f_o}{f_r} \right) \frac{f_r}{f_o} + \frac{2\beta Q_r \frac{f - f_r}{f_r} - b(1 + 4Q_r^2 (\frac{f - f_r}{f_r})^2)}{(1 + \beta + a - 2bQ_r \frac{f - f_r}{f_r})^2 + (b + 2Q_r(1 + a) \frac{f - f_r}{f_r})^2} = 0 \quad (3.1)$$

$$a + jb = \frac{1 + \Gamma e^{j\phi}}{1 - \Gamma e^{j\phi}} - 1 \simeq 2|\Gamma|e^{j\phi} \quad (3.2)$$

where,

f_o = unstabilized oscillator oscillation frequency.

Q_o = unstabilized oscillator external Q values.

f_r = resonant circuit resonant frequency.

Q_r = resonant circuit Q value.

β = coupling constant between resonant circuit and the transmission line.

In the equation (3.1), f_r/f_o is approximated as unity. When the terminating load is a non-reflecting load and subsequently the expression for unstabilized oscillator frequency (normalized to resonant circuit resonant frequency) as a function of the coupling constant can be obtained. Since it is a non-reflecting load, the reflecting load, the reflection coefficient $|\Gamma|=0$, hence $a+jb=0$ from (3.2) i.e. $a=b=0$.

Thus by substituting $a=b=0$ in (3.1) we get, .

$$0 = 2Q_o \left(\frac{f - f_r}{f_r} + \frac{f - f_o}{f_r} \right) + \frac{2\beta Q_r \left(\frac{f - f_r}{f_o} \right)}{(1 + \beta)^2 + (2Q_r \frac{f - f_r}{f_r})^2} \quad (3.3)$$

$$-2Q_o \left[\frac{f - f_r}{f_r} + \frac{f_r - f_o}{f_r} \right] = \frac{2\beta Q_r \left(\frac{f - f_r}{f_o} \right)}{(1 + \beta)^2 + (2Q_r \frac{f - f_r}{f_r})^2} \quad (3.4)$$

$$- \left[\frac{f - f_r}{f_r} - \frac{f_o - f_r}{f_r} \right] = \frac{\beta \frac{Q_r}{Q_o} \left(\frac{f - f_r}{f_r} \right)}{(1 + \beta)^2 + [2Q_r \frac{f - f_r}{f_r}]^2} \quad (3.5)$$

$$\frac{f_o - f_r}{f_r} = \frac{f - f_r}{f_r} + \frac{\beta \frac{Q_r}{Q_o} \left(\frac{f - f_r}{f_r} \right)}{(1 + \beta)^2 + [2Q_r \frac{f - f_r}{f_r}]^2} \quad (3.6)$$

$$\frac{f_o - f_r}{f_r} = \frac{f - f_r}{f_r} \left[1 + \frac{\beta \frac{Q_r}{Q_o}}{(1 + \beta)^2 + [2Q_r \frac{f - f_r}{f_r}]^2} \right] \quad (3.7)$$

$$\frac{f_o - f_r}{f_r} = F \left(\frac{f - f_r}{f_r} \right) \quad (3.8)$$

where,

$$F = 1 + \frac{Q_r}{Q_o} \frac{\beta}{(1 + \beta)^2} \frac{1}{1 + \left(\frac{2Q_r}{1 + \beta} \frac{f - f_r}{f_r} \right)^2} \quad (3.9)$$

The maximum deviation as a function of the coupling coefficient is estimated by the above expression. Further, such oscillator circuits also exhibits hysteresis effect [4], [10] (i.e. when $\delta f / \delta f_o$ and $\delta f / \delta f_r$ go to infinity). Differentiating both sides of (3.8), derivatives $\left(\frac{\delta f}{\delta f_o} \right)_{f_r}$ and $\left(\frac{\delta f}{\delta f_r} \right)_{f_o}$ are obtained as follows,

From (3.8) differentiating both sides w.r.t. f_o and keeping f_r constant,

$$\frac{1}{f_r} (1 - 0) = F' \left(\frac{f - f_r}{f_r} \right) \frac{\delta}{\delta f_o} \left(\frac{f - f_r}{f_r} \right) \quad (3.10)$$

$$\frac{1}{f_r} = F' \left(\frac{f - f_r}{f_r} \right) \frac{1}{f_r} \frac{\delta f}{\delta f_o} \quad (3.11)$$

$$\left(\frac{\delta f}{\delta f_o} \right)_{f_r} = \frac{1}{F' \left(\frac{f - f_r}{f_r} \right)} \quad (3.12)$$

Similarly taking derivatives w.r.t. f_r on both sides of (3.8) and keeping f_o constant we get,

$$\frac{f_r(0-1) - (f_o - f_r).1}{f_r^2} = F' \left(\frac{f - f_r}{f_r} \right) \left[\frac{f_r \left(\frac{\delta f}{\delta f_r} - 1 \right) - (f - f_r).1}{f_r^2} \right] \quad (3.13)$$

$$\frac{-f_r - f_o + f_r}{f_r^2} = F' \left(\frac{f - f_r}{f_r} \right) \left[\frac{f_r \frac{\delta f}{\delta f_r} - f_r - f + f_r}{f_r^2} \right] \quad (3.14)$$

$$-f_o = F' \left(\frac{f - f_r}{f_r} \right) \left[-f + f_r \frac{\delta f}{\delta f_r} \right] \quad (3.15)$$

$$-\frac{f_o}{F' \left(\frac{f - f_r}{f_r} \right)} = f_r \frac{\delta f}{\delta f_r} - f \quad (3.16)$$

Rearranging we get,

$$f - \frac{f_o}{F' \left(\frac{f - f_r}{f_r} \right)} = f_r \frac{\delta f}{\delta f_r} \quad (3.17)$$

$$\left(\frac{\delta f}{\delta f_r} \right)_{f_o} = (f - f_o / F' \left(\frac{f - f_r}{f_r} \right)) / f_r \quad (3.18)$$

Stabilization range with hysteresis effect can be expressed,

$$SR(\text{with}) \simeq \frac{1}{2Q_o} \frac{\beta}{1 + \beta} f_r \quad (3.19)$$

Whereas the stabilization range without hysteresis is given as,

$$SR(\text{without}) \simeq 2 \sqrt{\frac{\beta}{Q_o Q_r}} f_r \quad (3.20)$$

The above equations (3.19) and (3.20) is due to the inequality $Q_o \ll Q_r$. The stabilization range (with and without) are evaluated as a function of coupling constant and the results are presented. Further, the stabilized oscillator temperature coefficient (p) and the pushing figure (q) can be expressed as a function of the coupling coefficient, frequency 'f' and Q value and are given as follows:

Stabilized oscillator temperature coefficient 'p' is given by,

$$p = \frac{1}{f} \frac{\Delta f}{\Delta T} = \frac{1}{f} \left[\left(\frac{\delta f}{\delta f_r} \right)_{f_o} \frac{\Delta f_r}{\Delta T} + \left(\frac{\delta f}{\delta f_o} \right)_{f_r} \frac{\Delta f_o}{\Delta T} \right] \quad (3.21)$$

And pushing figure 'q' is given by,

$$q = \frac{\Delta f}{\Delta V_{GS}} = \left(\frac{\delta f}{\delta f_o} \right)_{f_r} \frac{\Delta f_o}{\Delta V_{GS}} \quad (3.22)$$

where $f = f_o = f_r$, p and q are expressed as functions of f_r , Q_o , Q_r and β .

Substituting values of (3.12) and (3.18) into (3.21) we get,

$$p = \frac{1}{f} \left[\frac{f - \frac{f_o}{F'(\frac{f-f_r}{f_r})}}{f_r} \frac{\Delta f_r}{\Delta T} + \frac{1}{F'(\frac{f-f_r}{f_r})} \frac{\Delta f_o}{\Delta T} \right] \quad (3.23)$$

After substituting $f = f_o = f_r$ in the above equation, it gets reduced to,

$$p = \frac{1}{f_r} \frac{\Delta f_r}{\Delta T} + \frac{1}{1 + \frac{\beta}{(1+\beta)^2} \frac{Q_r}{Q_o}} \frac{1}{f_o} \frac{\Delta f_o}{\Delta T} \quad (3.24)$$

Similarly substituting (3.18) into (3.22) and substituting $f = f_o = f_r$ we get,

$$q = \frac{1}{1 + \frac{\beta}{(1+\beta)^2} \frac{Q_r}{Q_o}} \frac{\Delta f_r}{\Delta V_{GS}} \quad (3.25)$$

Pulling characteristics, when $f_o = f_r$ are obtained by approximately solving equation (3.8), on the assumption that $|\Gamma| \ll \beta$, $|\Gamma| \ll 1$. This shows that when unstabilized oscillator oscillation frequency becomes equal to the resonator circuit resonant frequency the reflection coefficient is almost zero.

$$\frac{f - f_r}{f_r} \simeq \frac{b}{2Q_r \beta} \simeq \frac{|\Gamma|}{Q_r \beta} \sin \delta \quad (3.26)$$

Maximum frequency deviation can be thought as $(\Delta f)_{pull} = f - f_r$ and $\sin\delta = 1$ which is given by,

$$(\Delta f)_{pull} = f - f_r \simeq \frac{|\Gamma|}{Q_r\beta} f_r \quad (3.27)$$

The above expressions are evaluated and results are presented. The computer aided design procedure presented here incorporates the evaluation of all the above dynamic characteristics of such oscillator circuits. The microwave performances of these are evaluated in the frequency range 6 - 12GHz. For designing a stabilized FET oscillator, frequency temperature coefficient, pushing figure, pulling characteristic, stabilization width, and output power level have to be taken into account. These strongly depend upon the coupling constant β . In the oscillator stabilization by a dielectric resonator, β is adjusted continuously by changing the resonator position for this the distance ' l_y ' between the resonator and the line as shown in Fig. 3.3 has to be selected with great care. A computer program was written to calculate the stabilized oscillator temperature coefficient 'p', pushing figure 'q', stabilization range ' Δa '(SR) with hysteresis, stabilization range ' Δb '(SR) without hysteresis, and maximum frequency deviation ' Δ_{pull} '. The result is plotted against ' Δa ',' Δb ' versus coupling constant ' β ' for various values of ' Q_r ' (resonant circuit Q value) and a resonant frequency of 6GHz. One can choose any other resonant frequency and get the results from the computer program. These results are used in designing any sophisticated microwave system.

3.1.3 Mechanical tuning of a DR mounted on microstrip

In many applications, dielectric resonator is mounted on a microstrip substrate, and the tuning of the resonant frequency is provided by a tuning screw coming

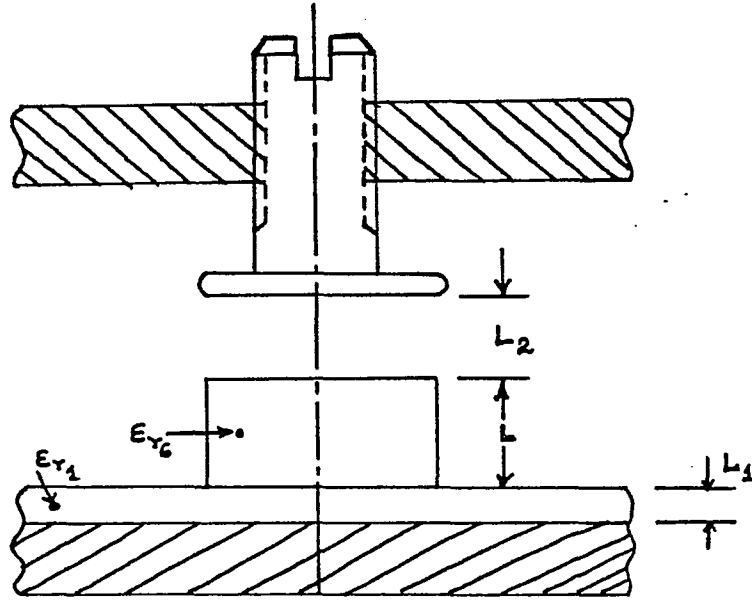


Figure 3.5: Tuning mechanism of a DR mounted on microstrip

from the top cover, this situation is shown in Fig. 3.5. The operation of the tuning mechanism can be explained by the perturbational principle, equation(2.66). When a metal wall of any cavity is moved inward, the change in resonant frequency is proportional to the difference in stored magnetic and electric energies within the displaced volume Δv . If the stored magnetic energy in Δv is larger than the stored electric energy in the volume Δv , then the resonant frequency would increase after the wall has moved inward.

The above resonant system possesses a rotational symmetry. Thus electric field of the mode $TE_{01\delta}$ has only the ϕ - component. This E_ϕ is tangential to the surface of the metal plate at the end of the tuning screw. In the immediate vicinity of the plate, the boundary condition requires that the tangential electric field to be zero. Hence when the screw is lowered the only displaced stored energy is magnetic energy and the resonant frequency has to increase in accordance with equation(2.66). While designing a tuning mechanism, it is of interest to determine the change of frequency as a function of the distance L_2 . Obviously smaller the L_2 ,

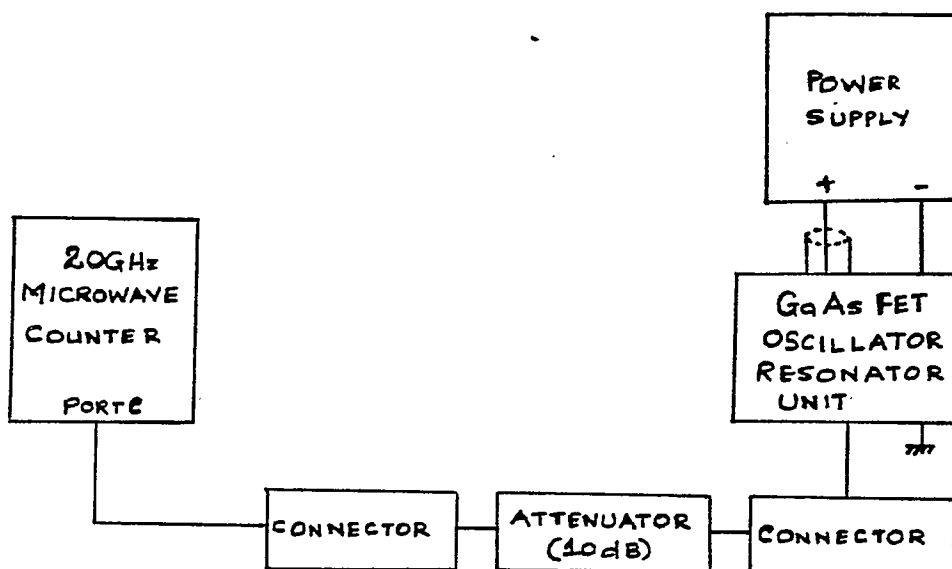


Figure 3.6: Experimental set-up for calculating the oscillation frequency

larger would be the resonant frequency. However bringing the metal surface of the screw closer to the resonator, would produce appreciable surface currents, which in turn reduces the Q factor of the resonator. By knowing how much the overall Q will deteriorate when the frequency is tuned by a given amount, it becomes possible to select materials and their dimensions in such a way that an optimum design is achieved.

An experiment was carried out to measure the oscillation frequency for the sample as shown in Fig. 3.5, the block diagram of the set up is as shown in Fig. 3.6. Length of the tuning screw as measured was 13mm. Number of turns on the mechanical tuning screw was 30. Therefore, pitch of the screw was calculated to be 0.4333mm/turn. The operating voltage of the oscillator was 10Volts and when the current was varied to 85mA, the oscillation frequency was observed to be 10.7GHz on the microwave frequency counter. The power at that frequency was +18.2dBm.

The above measurement was carried out at $L_2=13\text{mm}$. When the tuning screw was turned in to about, $L_2=3.5\text{mm}$ the oscillation frequency was observed to be 10.746GHz . This increase in frequency satisfies the theory as discussed previously. The change in frequency was found to be 46 MHz . If we could know the Q_c due to conductor losses in the two metal plates at a particular value of L_2 , and then by varying L_2 if we could get the Q_c , it is then possible to select the tuning range in which the resonator operates in a satisfactory manner, so that Q_c does not drop below a certain value from its maximum. Usually tuning ranges achieved in practice are between 1% to 5%.

script started on Thu Oct 12 11:54:46 1989

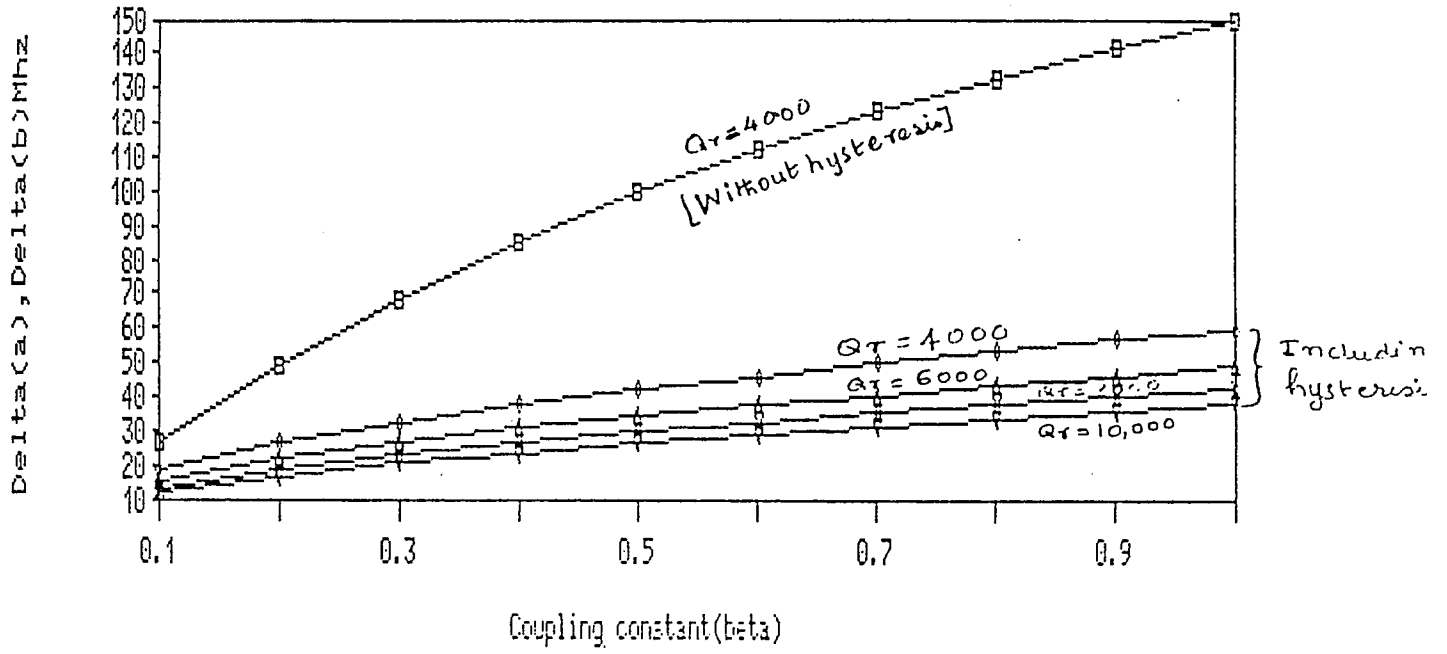
```
cat man.c
#include <stdio.h>
#include <math.h>
main ()
{
    double temp1,temp2,temp3,temp4,temp5,deltaA,deltaB,constant,
        deltafp,deltafo,deltafr,deltat,fr,k,beta,qr,qo,gama,p,q;
    double true=0.0;

    {
        beta = 1;          /*
/*    qo = 10;           */
        qr = 4000;        /*
        temp1 = 3.1;
        temp2 = -100;
        temp4 = 200;
        gama = 0.13;
        temp5 = 0.7;
/*    fr = 6000;       */
        printf("Input the values for beta,qo,qr,fr");
        printf("\n");
        scanf("%f%f%f%f",&beta,&qo,&qr,&fr);
/*    temp1 = deltafr/(deltat*fr); */
/*    temp2 = deltafo/(deltat * fo); */
        temp3 = 1 + beta*qr / ( (1 + beta)*(1 + beta)*qo);
        constant = temp4;
        p = temp1 + temp2/temp3;
        q = temp4/temp3;
        k = temp5 / ( 1 + beta);
        deltafp = gama * fr / ( qr * beta)* 1000;
        deltaA = beta * fr / ( 2 * qo * (1 + beta));
        deltaB = 2 * fr * sqrt ((double)(beta / (qr*qo)));
        printf("The output is\n");
        printf("P=%f ppm/centigrade\n",p);
        printf("Q=%f megahertz/volt\n",q);
        printf("deltaA=%f Mhz\n",deltaA);
        printf("deltaB=%f Mhz\n",deltaB);
        printf("deltafp=%f Khz\n",deltafp);
        printf("k=%f\n", k);
    };
};
```

a.out
Input the values for beta,qo,qr,fr
5 10 4000 6000
The output is
P=1.987515 ppm/centigrade
Q=2.224969 megahertz/volt
deltaA=100.000000 Mhz
deltaB=42.426407 Mhz
deltafp=390.000000 Khz
k=0.466667

script done on Thu Oct 12 11:55:16 1989

$Q_0=10, Q_r=4000, 6000, 8000, 10000, F_r=6000\text{MHz}$



Chapter 4

4.1 Introduction

The effects of the variation of different physical parameters in a simple, shielded dielectric resonator structure are discussed in this chapter. The present study uses an approximate analytical expression for the resonance frequency stability of dielectric resonators. The results are of importance specially in such applications where the dielectric resonators are subjected to varying environmental conditions.

The dielectric resonators are widely used in microwave circuits mainly due to its high Q-value, its low loss characteristics and good temperature stability [11], [12]. Further the advantage of dielectric resonator is that the size of the DR is smaller than the size of an empty resonant cavity at the same frequency as long as the relative dielectric constant of the DR material such as barium tetratitanate ($Ba_2Ti_4O_9$) etc. is much larger than unity. This barium tetratitanate material, usually identified as K-38 was developed with a temperature stable dielectric constant of 38. Generally, the dielectric resonators are placed in conductor shields to reduce the radiation losses and are placed adjacent to a microstrip line. The dielectric resonator then operates like a reaction cavity which reflects the RF energy at the resonant frequency. A typical diagram of such an assembly is shown in Fig. 4.1. The dielectric resonator diameter is 'D' and the height of the dielectric resonator

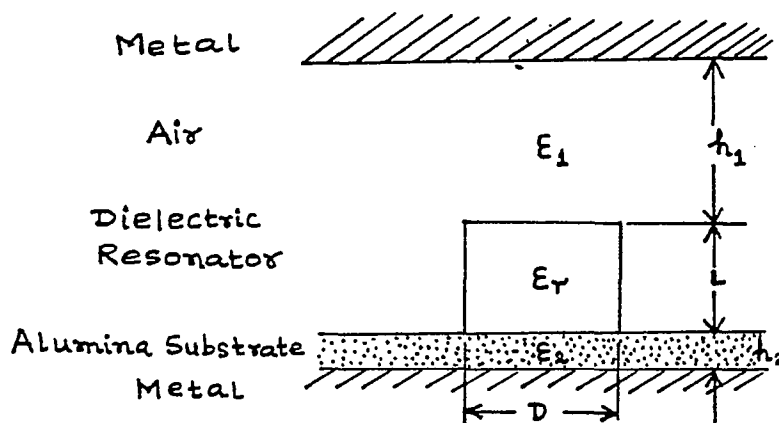


Figure 4.1: DR on a substrate

is 'L'. The relative dielectric constant of the material is considered to be ϵ_r and the same for the substrate is chosen as ϵ_2 . The relative dielectric constant of the dielectric resonator is higher than that of the substrate. The alumina substrate is not convenient to use at the lower end of the microwave spectrum because of its low dielectric constant, also it has high temperature coefficient, in the $120-150 \text{ ppm}/^\circ\text{C}$ range. The surrounding material is either air or some other filling like polyfoam. One of the main limitations of the dielectric resonators is the environmental dependence of the mechanical and electrical properties of the dielectric as the resonant frequency of the system becomes a function of the environmental parameters such as temperature and humidity. The proper selection of the materials and the suitable combination of the dimensions may result in a temperature-compensated system. The other method of reducing the temperature dependence in particular, is by heat sinking with Boron Nitride especially in low power applications. However, one needs to know the type and extent of the variations of these parameters in order to be able to reduce the effects. For example, the effects of the variations of parameters like the dielectric constant ϵ_1 in the region between the dielectric resonator and the top

wall, the diameter of the dielectric resonator, etc. on the frequency of resonance are definitely important for many practical applications of the dielectric resonators especially when these are used as stabilized oscillators [13].

4.1.1 The resonant frequency stability

In the resonant structure shown in Fig. 4.1. 'D' and 'L' are as defined earlier and $\epsilon_1, \epsilon_2, \epsilon_r$ are the dielectric constants of the medium shown. ' h_1 ' is the gap between the dielectric resonator and the top wall and ' h_2 ' is the thickness of the substrate.

The resonant conditions for TE modes [14] [15], [16] are analyzed in details below and are given as,

$$* \xi = \frac{L}{D} \quad (4.1)$$

$$x_\rho = a + b\sqrt{(\epsilon_r - 1)x_o^2 - a\rho_{01}}, a = 0.951\rho_{01}, b = 0.222 \quad (4.2)$$

$$x_z = \sqrt{\epsilon_r x_o^2 - x_\rho^2} \quad (4.3)$$

$$x_i = \sqrt{x_\rho^2 - \epsilon_i x_o^2}, i = 1, 2 \quad (4.4)$$

$$x_\rho^2 + x_z^2 = \epsilon_r x_o^2 \quad (4.5)$$

$$x_\rho^2 - x_1^2 = \epsilon_1 x_o^2 \quad (4.6)$$

$$x_\rho^2 - x_2^2 = \epsilon_2 x_o^2 \quad (4.7)$$

$$x_\rho^2 + x_k^2 = (\epsilon_r - 1)x_o^2 \quad (4.8)$$

$$\frac{x_\rho J_o(x_\rho)}{J_1(x_\rho)} = -\frac{x_k K_o(x_k)}{K_1(x_k)} \quad (4.9)$$

$$\xi = [\tan^{-1}\left(\frac{p_1}{x_1}\right) + \tan^{-1}\left(\frac{p_2}{x_2}\right)]/2x_z \quad (4.10)$$

$$x_o = \frac{\pi D f_o}{c} \quad (4.11)$$

$$p_i = x_i \coth h \left[\frac{2x_i h_i}{D} \right]_{i=1,2} \quad (4.12)$$

where ' f_o ' is the resonant frequency, 'c' the velocity of light, J_n is the n-th order Bessel function of the first kind and K_n is the modified Hankel of the n-th order. The computation of the resonant frequency is done by assuming the eigen value as,

$$K_{\rho_1} a = 2.405 + \frac{Y_o}{2.405 \left[1 + \frac{2.43}{Y_o} + 0.291 Y_o \right]} \quad (4.13)$$

and by solving (4.9) and (4.10) using,

$$x_\rho = 0.951 \rho_{01} + 0.222 \sqrt{(\epsilon_r - 1) x_o^2 - 0.951 \rho_{01}^2} \quad (4.14)$$

where $\rho_{01} = 2.405$ (the first root of the equation $J_o(x) = 0$). This approximation is good for the range $\sqrt{\epsilon_r - 1} x_o < 4$, which holds in practical cases. The equation (4.15) simplifies the job of computation of resonant frequency without utilizing the Bessel functions. By using (4.6),(4.7),(4.8) and (4.11) the resonant frequency stability

$$\frac{\Delta f_o}{f_o} = C_D \frac{\Delta D}{D} + C_L \frac{\Delta L}{L} + C_{h1} \frac{\Delta h1}{h1} + C_{h2} \frac{\Delta h2}{h2} + C_{\epsilon_1} \frac{\Delta \epsilon_1}{\epsilon_1} + C_{\epsilon_2} \frac{\Delta \epsilon_2}{\epsilon_2} + C_{\epsilon_r} \frac{\Delta \epsilon_r}{\epsilon_r} \quad (4.15)$$

Where, the coefficients C_D etc. can be evaluated from the following expressions. Note that ΔA is the small variational change in the value of a general parameter A.

$$C_D = -(1 + M + A_1 \gamma_1 + A_2 \gamma_2) \quad (4.16)$$

$$C_L = \frac{1}{M} \quad (4.17)$$

$$C_{h1} = \frac{A_1 \gamma_1}{M} \quad (4.18)$$

$$C_{h2} = \frac{A_2 \gamma_2}{M} \quad (4.19)$$

$$C_{\epsilon_1} = -\frac{A_1(1-\gamma_1)\Omega_1}{M} \quad (4.20)$$

$$C_{\epsilon_2} = -\frac{A_2(1-\gamma_2)\Omega_2}{M} \quad (4.21)$$

$$C_{\epsilon r} = -\frac{[A_1\theta_1(1-\gamma_1) + A_2\theta_2(1-\gamma_2) - \Gamma_1(1+A_1+A_2)]}{M} \quad (4.22)$$

Where, $M = -\Gamma_2(1+A_1+A_2) + A_1\Delta_1(1-\gamma_1) + A_2\Delta_2(1-\gamma_2)$

$$\Gamma_1 = \frac{\epsilon_r x_o^2}{2x_z^2} \left[1 - \frac{b^2 x_\rho}{x_\rho - a} \right] \quad (4.23)$$

$$\Gamma_2 = \frac{x_o^2}{x_z^2} \left[\epsilon_r - \frac{b^2 x_\rho (\epsilon_r - 1)}{x_\rho - a} \right] \quad (4.24)$$

$$\Delta_i = \frac{x_o^2}{x_i^2} \left[\frac{b^2 x_\rho (\epsilon_r - 1)}{x_\rho - a} - \epsilon_i \right] \quad (4.25)$$

$$\theta_i = \frac{\epsilon_r b^2 x_o^2 x_\rho}{2x_i^2 (x_\rho - a)} \quad (4.26)$$

$$\Omega_i = -\frac{x_o^2 \epsilon_i}{2x_i^2} \quad (4.27)$$

$$\gamma_i = \frac{2h_i c_i}{D} \quad (4.28)$$

$$c_i = \frac{p_i^2 - x_i^2}{p_i} \quad i=1,2 \quad (4.29)$$

here $a = 0.951\rho_{01}$, $b=0.222$.

The practical implementation of equation (4.15) is obvious. From the dimensions of the resonant system and the known properties of materials, one can evaluate the numerical value of each coefficients "C". This value indicates the relative importance of each part used in the system. Then it is possible to select the parts in such a manner that the overall frequency is minimized. When the resonator material is isotropic, we can assume that $\frac{\Delta L}{L} = \frac{\Delta D}{D}$, then

$$C_D \frac{\Delta D}{D} + C_L \frac{\Delta L}{L} = (C_D + C_L) \frac{\Delta L}{L} \quad (4.30)$$

The main factor affecting the resonant frequency stability is the change rate of dimension of the dielectric resonator, and the second factor is the change rate of resonator dielectric constant. For the dielectric resonator terminated with metal on both sides, the equation (4.31)

$$\frac{\Delta f_o}{f_o} = \frac{\Delta L}{L} + \frac{\Delta \epsilon_r}{2\epsilon_r} \quad (4.31)$$

is a good approximation.

The simplest form of temperature effect in microwave resonator is the expansion of the material. It is an experimental fact that most solids expand with increase in temperature. A rod of length L will expand by ΔL when the temperature increases by ΔT . the constant of proportionality is α , the linear coefficient of expansion:

$$\frac{\Delta L}{L} = \alpha \Delta T \quad (4.32)$$

Similarly we have,

$$\frac{\Delta f_o}{f_o} = \tau_f \Delta T \quad (4.33)$$

' τ_f ' is the sensitivity of the resonant frequency with temperature using the linear temperature coefficients we can rewrite equation (4.15) as,

$$\tau_f = C_D \alpha_D + C_L \alpha_L + C_{h1} \alpha_{h1} + C_{h2} \alpha_{h2} + C_{\epsilon 1} \tau_{\epsilon 1} + C_{\epsilon 2} \tau_{\epsilon 2} + C_{\epsilon r} \tau_{\epsilon r} \quad (4.34)$$

Where τ_{ϵ_1} denotes the temperature coefficient of the relative dielectric constant ϵ_1 . Similarly subscript indicate that part of the entire system to which the individual coefficient refers. τ_f is the resulting temperature sensitivity of the entire system, given in $ppm/^\circ C$.

4.1.2 Computation

Based on the equation (4.15), the differential parameters have been varied to simulate the small changes in the environmental conditions and the results are being plotted. The Fig. 4.2 shows the variation of the coefficient C_{ϵ_1} as a function of the distance between the top wall and the dielectric resonator. This simulates the variation in the frequency stability when the enclosure is subjected to variable humidity. The Fig. 4.3 shows the variation of C_D as a function of frequency. The Fig. 4.4 and Fig. 4.5 shows the variation of coefficients C_L and C_{ϵ_r} as a function of ϵ_r . The plots also show the variation with different frequency of operation. These parameters are of importance for the investigations since, in many applications, the dielectric resonators are exposed to different environmental conditions and as such it is important to know the effects of such changes on the frequency stability.

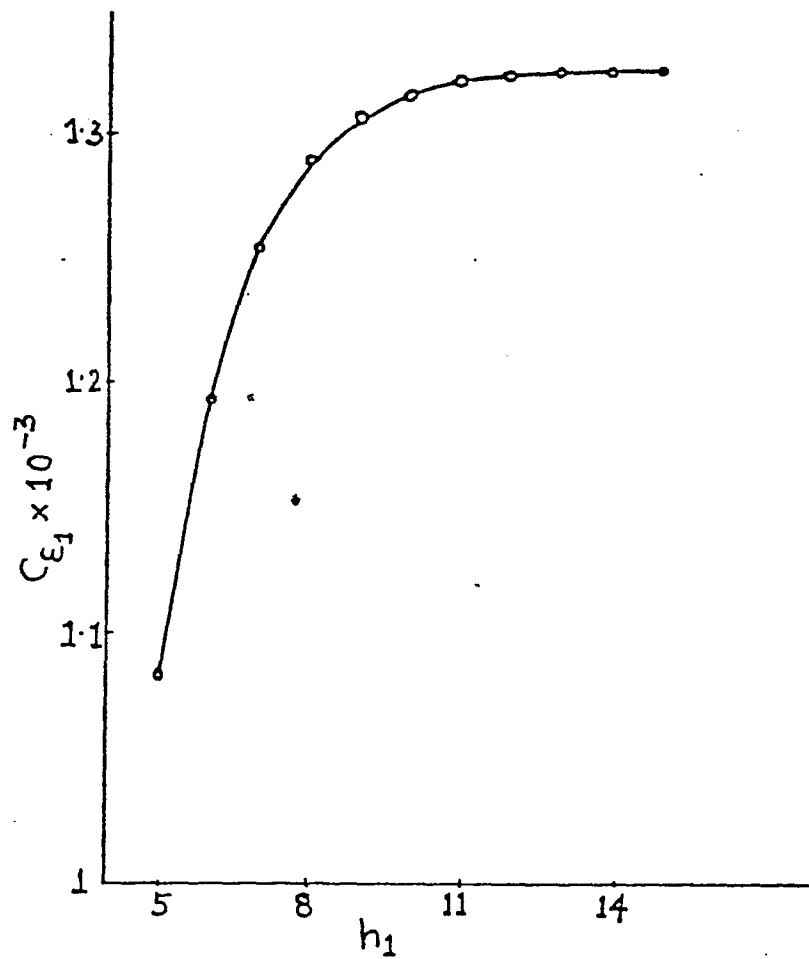


Fig. 4.2.

The Coefficient C_{ϵ_1} as a function of the distance between the DR and the top wall,
 Dia. of DR= 14mm, thickness of substrate= 0.8mm, height of DR= 10mm, $\epsilon_r =$
 30.3, $\epsilon_2 = 2.54$, freq= 4GHz.

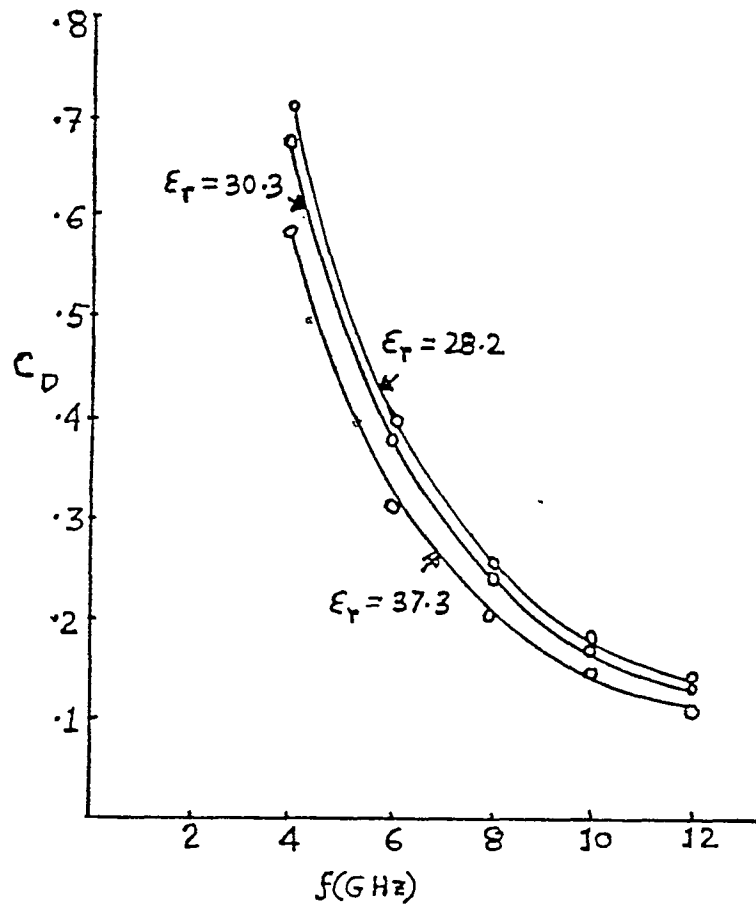


Fig. 4.3.

The Coefficient C_D as a function of frequency for different dielectric materials, thickness of the substrate= 0.8mm, height of DR= 10mm, ϵ_r of substrate= 2.54, h = distance between DR and top wall= 10mm.

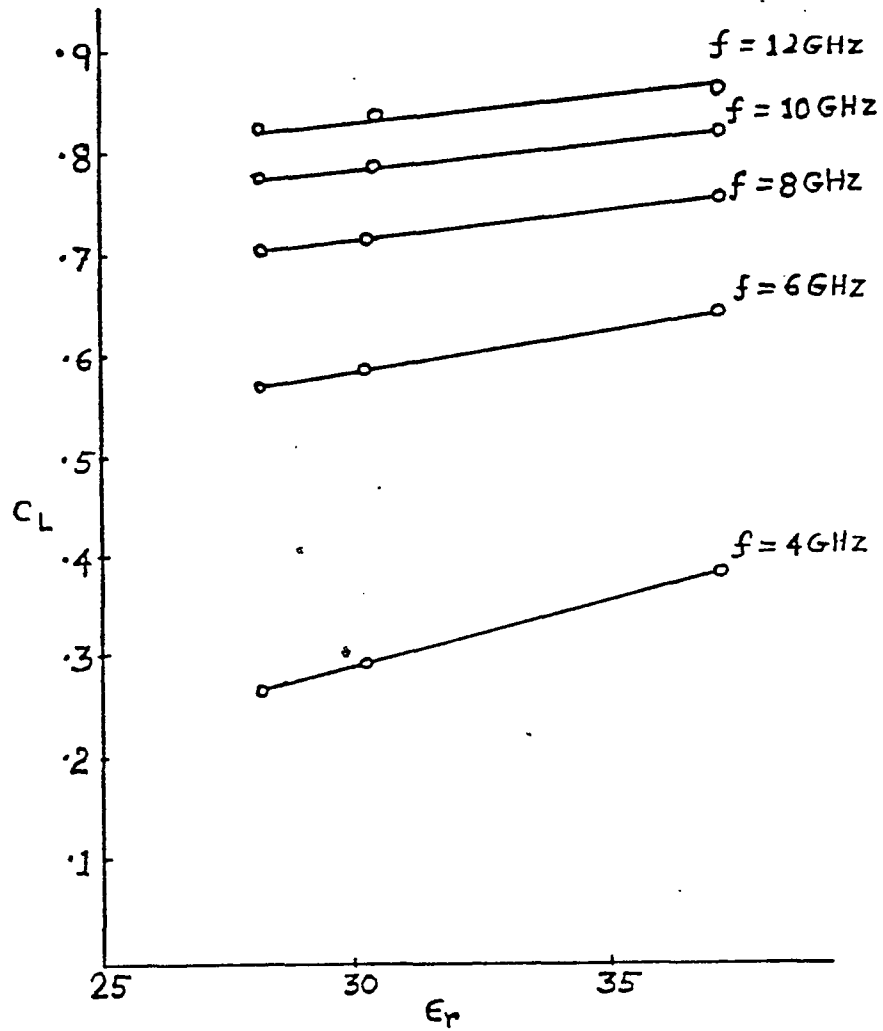


Fig. 4.4.

The Coefficient C_L as a function of ϵ_r at different frequencies, Dia. of DR= 14mm, thickness of substrate= 0.8mm, height of DR= 10mm, ϵ_r of substrate= 2.54, h= 10mm.

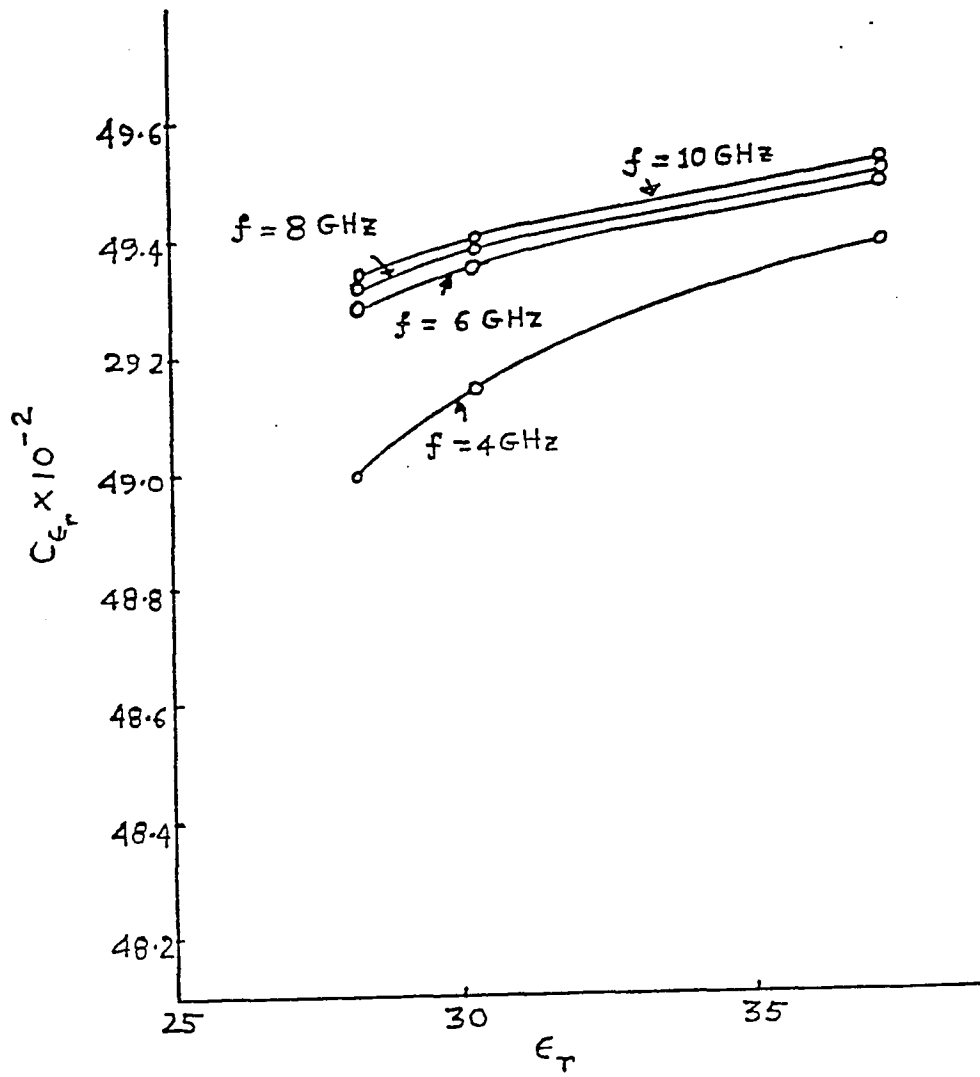


Fig. 4.5.

The Coefficient C_{ϵ_r} as a function of ϵ_r at different frequencies, Dia. of DR= 14mm, thickness of substrate= 0.8mm, height of DR= 10mm, ϵ_r of substrate= 2.54, $h=$ 10mm.

Chapter 5

5.1 Conclusion

The thesis is divided mainly into three parts.

Part 1 - The field distribution in a shielded coupled dielectric resonator has been analysed by using computer models. Both E and H field distribution and also energy distribution have been obtained for different cases (with different dielectric materials, different separation distances between the metal plates etc.). Specially the comparisons have been made with two modes namely 0-th order and 1st order mode. The plots are shown and the comments are made on how the distribution of electric and magnetic energies get affected in all cases that have been investigated.

Part 2 - One important application of dielectric resonator is studied namely GaAs FET oscillator with dielectric resonator used for stabilization. Using a computer modelling technique, one such DR oscillator circuit is investigated in details specially with reference to its pushing figure, stabilization range and pulling characteristics. The experiment has been done to observe the frequency deviation as a function of gate voltage. Also, the experimental data has been obtained on the effect of the resonant frequency by varying the gap width with the help of the tuning screw. The

results are important for any system design using such dielectric resonator stabilized oscillators.

Part 3 - In this last part, the effects of the dielectric resonator characteristics on environmental conditions have been studied and reported. The results will find extensive application in practical cases where dielectric resonators need to be mounted on any outside environment which is subject to a wide variation of temperature and humidity conditions.

```

0 REM          PROGRAM 1    M.R.KAMATH
0 REM Dielectric resonator analysis by perturbational method
0 REM Based on Cohn's model
0 REM
DIM ER(6), NUM(6), DEN(6)
DIM WW(3), DWE(3), DWM(3)
0 PO1=2.40483
0 PO12=PO1*PO1
0 DATA 70,5.25,4.6
00 DATA 1,2.3,1,15
10 LMODE= 0
20 ACC=5
30 PI=3.141593
40 READ ER(6),A,L
50 READ ER(1),L1,ER(2),L2
60 PRINT "INPUT DATA"
70 PRINT "er=";ER(6); "a=";A; "L=";L; "LMODE=";LMODE
80 PRINT "er1=";ER(1); "L1=";L1
90 PRINT "er2=";ER(2); "L2=";L2
00 PRINT "ACCURCY OF SOLVING TRANSC. EQ. : "ACC+1;" DIGITS"
10 FOLD=150*PO1/(PI*A*SQR(ER(6)))
20 FFNEW=FOLD*1.001
30 GOSUB 560
40 DF=FOLD*.1
50 REM****SOLVING TRANSC.EQ*****
60 FFNEW=FOLD+DF
70 FUNCOLD=FUNC
80 GOSUB 560
90 SIGN=FUNC*FUNCOLD
00 FOLD=FFNEW
1 NTRIAL=NTRIAL+1
20 IF SIGN<0 GOTO 350
30 IF NTRIAL>50 THEN GOTO 390
40 GOTO 260
50 DF=-DF*.1
60 COUNT=COUNT+1
70 PRINT "COUNTING....";COUNT
80 IF COUNT<ACC GOTO 260
90 SH1=(X1-XI1)/2
00 SH2=(X2-XI2)/2
10 ETA=120*PI
20 REM*****COMP.AMPL.*****
30 HZ10=COS(TH1)/SH1
40 HR10=-AL1A*HZ10/PO1
50 HRR=BA/PO1
60 HZ20=-COS(TH2)/SH2
70 HR20=-AL2A*HZ20/PO1
80 GOSUB 1550
90 PRINT "WANT TO PLOT THE FIELD? (Y OR N)"
00 INPUT A$
10 IF A$="Y" THEN GOSUB 810
20 PRINT "WANT ENERGY TABLE DISTRI.? (Y OR N)"
30 INPUT A$
40 IF A$="Y" THEN GOSUB 2010
50 END
\ REM*****TRANSC. FUNCTION*****
/ KOA=PI*FFNEW*A/150
30 KOA2=KOA*KOA
90 RADIC=PO12-KOA2*ER(1)
00 AL1A=SQR(RADIC)

```

```

10 RADI=PO12-KOA2*ER(2)
20 AL2A=SQR(RADI)
30 RADA=KOA2*ER(6)-PO12
40 BA=SQR(RADA)
50 AL1L1=AL1A*L1/A
   ) AL2L2=AL2A*L2/A
70 X1=EXP(AL1L1)
80 XI1=1/X1
90 X2=EXP(AL2L2)
00 XI2=1/X2
10 CT1=(X1+XI1)/(X1-XI1)
20 CT2=(X2+XI2)/(X2-XI2)
30 ARG1=AL1A*CT1/BA
40 ARG2=AL2A*CT2/BA
50 TH1=ATN(ARG1)
60 IF TH1<0 THEN PRINT "NEGATIVE LENGTH TH1"
70 TH2=ATN(ARG2)
80 IF TH2<0 THEN PRINT "NEGATIVE LENGTH TH2"
90 FUNC=(TH1+TH2+LMODE*PI)/BA-L/A
00 RETURN
10 REM***COMPT.OF.FIELD DISTRIBBUTION.*****
20 PRINT"HOW MANY POINTS IN EACH REGION? (n1,n,n2)"
30 INPUT N1,N,N2
40 NTOT=N1+N+N2+1
50 DIM ZZ(NTOT),HZ(NTOT),HR(NTOT)
60 REM***REGION1*****
70 DZ=L1/N1
80 Z=-L1
90 FOR I1=1 TO N1
00 AEX1=AL1A*(Z+L1)/A
   ) XP=EXP(AEX1)
   ) XIP=1/XP
30 SHA1=(XP-XIP)/2
40 CHA1=(XP+XIP)/2
50 ZZ(I1)=Z
60 HZ(I1)=HZ10*SHA1
70 HR(I1)=HR10*CHA1
80 Z=Z+DZ
90 NEXT I1
000 REM***REGION INSIDE*****
010 DZ=L/N
020 FOR I=N1+1 TO N1+N
030 ANG=BA*Z/A-TH1
040 ZZ(I)=Z
050 HZ(I)=COS(ANG)
060 HR(I)=HRR*SIN(ANG)
070 Z=Z+DZ
080 NEXT I
090 REM***REGION2*****
100 DZ=L2/N2
110 IF HZ(N1+N)<0 THEN HZ20=-HZ20
120 IF HR(N1+N)<0 THEN HR20=-HR20
130 FOR I2=N1+N+1 TO NTOT
140 AEX2=AL2A*(Z-L2-L)/A
150 SP=EXP(AEX2)
   ) SPI=1/SP
   ) SHA2=(SP-SPI)/2
180 CHA2=(SP+SPI)/2
190 ZZ(I2)=Z
200 HZ(I2)=HZ20*SHA2

```

```

010 HR(I2)=HR20*CHA2
020 Z=Z+DZ
030 NEXT I2
040 REM****PLOTTING.FIELD DISTRI.****
050 CLS
060 KEY OFF
070 SCREEN 1
080 LOCATE 25,1
090 PRINT TIME$+" "+DATE$
100 LINE (0,0)-(319,199),,B
110 VV=99
120 VVV=199
130 HH=319
140 LENGTH=L1+L+L2
150 SCALE=319/LENGTH
160 LH=L1*SCALE
170 LLH=(L1+L)*SCALE
180 LINE (L1H,0)-(LLH,VVV),,B
190 LINE (HH,VV)-(0,VV)
200 FOR I=2 TO NTOT
210 ZL=(ZZ(I)+L1)*SCALE
220 HHL=VV*(1-HZ(I))
230 LINE -(ZL,HHL)
240 NEXT I
250 VAM=.5
260 HHL=VV*(1-VAM*HR(1))
270 PSET (0,HHL)
280 FOR I=2 TO NTOT
290 ZL=(ZZ(I)+L1)*SCALE
300 HHL=VV*(1-VAM*HR(I))
310 LINE -(ZL,HHL),,,&HCCCC
320 NEXT I
330 WAIT 1,0 '(FOR PRINTER), THEN PRESS CTRL BREAK TO GET OUT
340 RETURN
350 REM****PERTURBATIONAL FORMULA****
360 ER(3)=ER(1)
370 ER(4)=1
380 ER(5)=ER(2)
390 KC4A2=KOA2*(ER(6)-ER(4))-PO12
400 KC4A=SQR(KC4A2)
410 HZ102=HZ10*HZ10
420 HZ202=HZ20*HZ20
430 KOB=1/(1+(.4832-.0511/KC4A)/KC4A)
440 IF KC4A<.8 THEN PRINT "BESSEL APPROX. NOT ACCURATE"
450 KOB2=KOB*KOB
460 PRX=KOB2+2*KOB/KC4A-1
470 QRX=1-KOB2
480 SIF1=SIN(TH1*2)
490 SIF2=SIN(TH2*2)
500 THET=(SIF1+SIF2)*.5/(TH1+TH2+LMODE*PI)
510 ARG1=2*AL1L1
520 XH1=EXP(ARG1)
530 XHI1=1/XH1
540 SIG1=(XH1-XHI1)*.25/AL1L1
550 ARG2=2*AL2L2
560 XH2=EXP(ARG2)
570 XHI2=1/XH2
580 SIG2=(XH2-XHI2)*.25/AL2L2
590 A2=A*A
600 WW(1)=ER(1)*HZ102*A2*L1*(SIG1-1)

```

```

10 WW(2)=ER(2)*HZ202*A2*L2*(SIG2-1)
20 WW(3)=ER(6)*A2*L*(1+THET)
30 DWE(1)=ER(3)*HZ102*A2*L1*PRX*(SIG1-1)
40 DWE(2)=ER(4)*A2*L*PRX*(1+THET)
50 DWE(3)=ER(5)*HZ202*A2*L2*PRX*(SIG2-1)
60 DWM(1)=(RADIC/KOA2)*HZ102*A2*L1*PRX*(SIG1+1)
70 DWM(2)=(RADA/KOA2)*A2*L*PRX*(1-THET)
80 DWM(3)=(RADI/KOA2)*HZ202*A2*L2*PRX*(SIG2+1)
90 FOR I=1 TO 3
100 SWW=SWW+WW(I)
110 SDWE=SDWE+DWE(I)
120 SDWM=SDWM+DWM(I)
130 NEXT I
140 PERT=(SDWE-SDWM)*.5/SWW
150 PERFRE=FOLD*(1-PERT)
160 PRINT "COHN'S MODEL"
170 PRINT "FREQ(COHN)=",FOLD,"GHZ"
180 PRINT "PERTURBATIONAL RESULT"
190 PRINT "FREQ(PERT)=",PERFRE,"GHZ"
200 RETURN
210 REM*****ENERGY DISTRIBUTIONAL*****
220 DIM WE(6),WM(6)
230 PRINT "j      eps(j)      we(j)%      wm(j)%
240 PRINT
250 SUME=SWW+SDWE
260 SUMM=SWW+SDWM
270 WE(1)=WW(1)/SUME
280 WE(2)=WW(2)/SUME
290 WE(3)=DWE(1)/SUME
300 WE(4)=DWE(2)/SUME
310 WE(5)=DWE(3)/SUME
320 WE(6)=WW(3)/SUME
330 TEM=(RADIC/KOA2)*(SIG1+1)+(PO12/KOA2)*(SIG1-1)
340 WM(1)=TEM*HZ102*A2*L1/SUMM
350 TEM=(RADA/KOA2)*(1-THET)+(PO12/KOA2)*(1+THET)
360 WM(6)=TEM*L*A2/SUMM
370 TEM=(RADI/KOA2)*(SIG2+1)+(PO12/KOA2)*(SIG2-1)
380 WM(2)=TEM*HZ202*L2*A2/SUMM
390 WM(3)=DWM(1)/SUMM
400 WM(4)=DWM(2)/SUMM
410 WM(5)=DWM(3)/SUMM
420 FOR J=1 TO 6
430 WM(J)=100*WM(J)
440 WE(J)=100*WE(J)
450 PRINT USING "#####.##"; J,ER(J),WE(J),WM(J)
460 NEXT J
470 RETURN

```

```

0 REM          PROGRAM 2   M.R. KAMATH
0 REM          dielectric resonator analysis by variational method
0 REM          based on Simplified Perturbational model
0 REM          q factor computed by the incremental frequency rule
  REM
J DIM ER(6),NUM(6),DEN(6)
0 DIM XX(3),KK(3),ALF(2),FIH(2),LL(2),FCT(3),GCT(3)
0 REM          length should be entered in mm
0 DATA 38,5.25,4.6
00 DATA 1,2.3,1,15
10 LMODE=0
20 READ ER(6),A,L
30 READ ER(1),LL(1),ER(2),LL(2)
40 ER(3)=ER(1)
50 ER(4)=1
60 ER(5)=ER(2)
70 REM
80 REM
90 REM
00 PRINT "input data"
10 PRINT "er=";ER(6);"a=";A;"L=";L;"LMODE=";LMODE
20 PRINT "er1=";ER(1);"L1=";LL(1)
30 PRINT "er2=";ER(2);"L2=";LL(2)
40 PI=3.141593
50 NQ=0
60 REM ***** 2 - DIMENSIONAL SEARCH FOR THE SOLUTION *****
70 REM ***** of the transcendental equation *****
80 XX(2)=2.9
90 IF ER(2)-ER(1)>0 THEN EMAX=ER(2) ELSE EMAX=ER(1)
00 KMIN=XX(2)/SQR(ER(6)-ER(4))
0 KMAX=XX(2)/SQR(EMAX)
20 KK(2)=(9*KMIN+KMAX)/10
30 DXX=.00001
40 DKK=.00001
50 ITER=0
60 PRINT "searching for the eigenvalue..."
70 XX(1)=XX(2)+DXX
80 KK(1)=KK(2)
90 XX(3)=XX(2)
00 KK(3)=KK(2)+DKK
10 FOR ITI=1 TO 3
20 X=XX(ITI)
30 KO=KK(ITI)
40 KO2=KO*KO
50 XIT2=X*X
60 GOSUB 1940
70 RA=KO2*(ER(6)-ER(4))-XIT2
80 IF RA>0 GOTO 550
90 STEPX=STEPX/2
00 STEPK=STEPK/2
10 XX(2)=XX(2)-STEPX
20 KK(2)=KK(2)-STEPK
30 PRINT "step too large. start again with 1/2 smaller step"
40 GOTO 350
50 YY=SQR(RA)
  ) KC4A=YY
/0 GOSUB 2000
80 FCT(ITI)=JOB+YY*KOB/X
90 BA=SQR(KO2*ER(6)-XIT2)
00 FOR JIT=1 TO 2

```

```

10 ALF(JIT)=SQR(XIT2-KO2*ER(JIT))
20 POW=ALF(JIT)*LL(JIT)/A
30 IF POW>8 GOTO 680
40 EP=EXP(POW)
 0 EI=1/EP
60 AGU=(EP+EI)/(EP-EI)
70 GOTO 690
80 AGU=1
90 AGU=AGU*ALF(JIT)/BA
00 FII(JIT)=ATN(AGU)
10 NEXT JIT
20 GCT(ITI)=FII(1)+FII(2)-BA*L/A+LMODE*PI
30 NEXT ITI
40 AL=(FCT(1)-FCT(2))/DXX
50 AU=(GCT(1)-GCT(2))/DKK
60 BL=(FCT(3)-FCT(2))/DXX
70 BU=(GCT(3)-GCT(2))/DKK
80 CL=FCT(2)-AL*XX(2)-BL*KK(2)
90 CU=GCT(2)-AU*XX(2)-BU*KK(2)
00 DENO=AU*BL-AL*BU
10 XNEW=(CL*BU-CU*BL)/DENO
20 KNEW=(CU*AL-CL*AU)/DENO
30 STEPX=XNEW-XX(2)
40 STEPK=KNEW-KK(2)
50 STEP2=STEPX^2+STEPK^2
60 PRINT ITER+1,"koa=",KK(2),"eigx=",XX(2)
70 XX(2)=XNEW
80 KK(2)=KNEW
90 IF STEP2<1E-12 THEN 960
 0 ITER=ITER+1
 0 IF ITER>10 THEN 930
20 GOTO 370
30 PRINT "SOLUTION NOT FOUND AFTER 10 ITERATIONS"
40 GOTO 1870
50 REM IF THE SEARCH IS SUCCESSFUL, RE-EVALUATE THE CONSTANTS
60 KOA=KK(2)
70 FIR=KOA*150/(PI*A)
80 PRINT "Simplified Perturbational model"
90 PRINT "freq(S&P)=",FSP," GHz"
000 EIGX=XX(2)
010 KOA2=KOA*KOA
020 EIG2=EIGX*EIGX
030 RADIC=EIG2-KOA2*ER(1)
040 AL1A=SQR(RADIC)
050 RADI=EIG2-KOA2*ER(2)
060 AL2A=SQR(RADI)
070 RADA=KOA2*ER(6)-EIG2
080 BA=SQR(RADA)
090 AL1L1=AL1A*LL(1)/A
100 AL2L2=AL2A*LL(2)/A
110 IF AL1L1>8 THEN GOTO 1170
120 Z1=EXP(AL1L1)
130 ZI1=1/Z1
140 CT1=(Z1+ZI1)/(Z1-ZI1)
150 SIH1=(Z1-ZI1)*.5
 50 GOTO 1180
170 CT1=1
180 IF AL2L2>8 THEN GOTO 1240
190 Z2=EXP(AL2L2)
200 ZI2=1/Z2

```

```

210 CT2=(Z2+ZI2)/(Z2-ZI2)
220 SIH2=(Z2-ZI2)*.5
230 GOTO 1250
240 CT2=1
 50 ARG1=AL1A*CT1/BA
260 ARG2=AL2A*CT2/BA
270 TH1=ATN(ARG1)
280 TH2=ATN(ARG2)
290 REM *****VARIATIONAL FORMULA*****
300 KC4A2=RADA-KOA2*ER(4)
310 KC4A=SQR(KC4A2)
320 GOSUB 2000
330 X=EIGX
340 GOSUB 1940
350 JOB2=JOB*JOB
360 TRX=JOB2-2*JOB/EIGX+1
370 KOB2=KOB*KOB
380 PRX=KOB2+2*KOB/KC4A-1
390 SIF1=SIN(TH1*2)
400 SIF2=SIN(TH2*2)
410 THET=(SIF1+SIF2)*.5/(TH1+TH2+LMODE*PI)
420 CO12=A*(COS(TH1)^2)/AL1A
430 IF AL1L1>8 THEN 1470
440 SECN=AL1L1/(SIH1*SIH1)
450 PARM1=CT1-SECN
460 GOTO 1480
470 PARM1=1
480 COPAM1=CO12*PARM1
490 CO22=A*(COS(TH2)^2)/AL2A
500 IF AL2L2>8 THEN 1540
510 SECN=AL2L2/(SIH2*SIH2)
520 PARM2=CT2-SECN
530 GOTO 1550
540 PARM2=1
550 COPAM2=CO22*PARM2
560 NUM(1)=ER(1)*COPAM1*TRX
570 NUM(2)=ER(2)*COPAM2*TRX
580 NUM(3)=- (RADIC+KC4A2)*PRX*COPAM1/KOA2
590 NUM(4)=ER(4)*L*(1+THET)*PRX
600 NUM(5)=- (RADI+KC4A2)*PRX*COPAM2/KOA2
610 NUM(6)=ER(6)*L*(1+THET)*TRX
620 DEN(1)=NUM(1)
630 DEN(2)=NUM(2)
640 DEN(3)=ER(3)*PRX*COPAM1
650 DEN(4)=NUM(4)
660 DEN(5)=ER(5)*PRX*COPAM2
670 DEN(6)=NUM(6)
680 DENSUM=0
690 SURVER=-BA*A*(SIF1+SIF2)*PRX/KOA2
700 SURHOR=X*JOB*2*(COPAM1+COPAM2)/KOA2
710 NUMSUM=SURHOR+SURVER
720 FOR J=1 TO 6
730 DENSUM=DENSUM+DEN(J)
740 NUMSUM=NUMSUM+NUM(J)
750 NEXT J
 50 VARKOA=KOA*SQR(NUMSUM/DENSUM)
770 VARFRE=VARKOA*150/(PI*A)
780 PRINT "varitional result"
790 PRINT "freq(var)=",VARFRE," GHz"
800 IF NQ=1 THEN RETURN

```

```

810 PRINT "want the percent error in frequency? (y or n)"
820 INPUT A$
830 IF A$="Y" THEN GOSUB 1880
840 PRINT "want to compute the Q factor? (y or n)"
850 INPUT B$
860 IF B$="y" THEN GOSUB 2060
870 END
880 REM *****percent error *****
890 PRINT "enter the exact frequency in GHz"
900 INPUT EXCFRE
910 PERC=100*(VARFRE/EXCFRE-1)
920 PRINT USING "+##.## _%";PERC
930 RETURN
940 REM ***** function JOB=JO(X)/J1(X) *****
950 XMXO=X-2.4048
960 TEM=(.0282*XMXO-.1177)*XMXO+.2571
970 TEM=(TEM*XMXO-.716)*XMXO+1.4282
980 JOB=TEM*XMXO/(X-3.8317)
990 RETURN
000 REM ***** function KOB=KO(KC4A)/K1(KC4A) *****
010 KI=1/KC4A
020 TEM=(.00445*KI-.02679)*KI+.06539
030 TEM=(TEM*KI-.11226)*KI+.49907
040 KOB=1/(1+TEM*KI)
050 RETURN
060 REM ***** q factor *****
070 NQ=1
075 QD=5000
080 FO=VARFRE
090 PRINT "shield : copper, aluminum, brass, or other? (c,a.b.or o)"
100 INPUT A$
110 IF A$="c" THEN SIGMA=5.8E+07
120 IF A$="a" THEN SIGMA=3.72E+07
130 IF A$="b" THEN SIGMA=1.57E+07
140 IF A$>< "o" GOTO 2180
150 PRINT "enter conductivity in Siemens/meter"
160 INPUT SIGMA
170 IF SIGMA<.1 GOTO 2300
180 SKIN=50/(SQR(FO*SIGMA)*PI)
190 PRINT "skin depth=",1000*SKIN,"microns"
200 LL(1)=LL(1)-SKIN
210 LL(2)=LL(2)-SKIN
220 GOSUB 350
230 DF=VARFRE-FO
240 IF DF/FO<.000001 GOTO 2280
250 Q=FO/DF
260 PRINT "Q(due to shield losses)=",Q
261 QOVER= 1/(1/QD+1/Q)
262 PRINT "Q(OVERALL)=",QOVER
270 RETURN
280 PRINT "insignificant losses in the shield, quit"
290 RETURN
300 PRINT "conductivity too small, quit"
310 RETURN

```

Chapter 6

Bibliography

- [1] S.B. Cohn, "Microwave bandpass filters containing high-Q dielectric resonators," IEEE Trans. Microwave Theory Tech., vol. MTT-16, pp. 218-227, April 1968.
- [2] A.W. Glisson, D. Kajfez, and J. James, "Evaluation of modes in dielectric resonators using a surface integral equation formulation," IEEE Trans. Microwave Theory Tech., vol. MTT-31, pp. 1023-1029, Dec. 1983.
- [3] D. Kajfez, "Basic principles give understanding of dielectric waveguides and resonators," Microwave Syst. News, vol. 13, pp. 152-161, May 1983.
- [4] D. Kajfez and P. Guillon, "Dielectric resonators," Artech House, US, 1986.
- [5] T. Bhattacharjee, "Field distributions in a composite dielectric resonator structure," International Symposium on Recent Advances in Microwave Technology, Beijing, China, Sept. 4-8, 1989.

- [6] T. Bhattacharjee, "Rigorous analysis of coupling in dielectric resonators," IEEE Trans. on Magnetics, vol. 26, No. 2, pp. 735-738, March 1990.
- [7] R.F. Harrington, Time-Harmonic Electromagnetic Fields, New York: MacGraw Hill, 1961.
- [8] T. Bhattacharjee, M.R. Kamath and D. Patel, "Computer aided analysis of Dynamic characteristics of GaAs FET DR oscillator," presented at the conference on Progress in Applied Computational Electromagnetics (ACES), Monterey, CA, March 19-22, 1990.
- [9] K. Shirahata, "Stabilization of solid state microwave oscillator by loading BRF," presented at 1969 European Microwave Conf. (London), Sept. 1969.
- [10] H. Abe et al., "A high power microwave oscillator," IEEE Trans. on Solid-State Circuits Conf. Digest, pp. 164-165, Feb. 1976.
- [11] M. Stiglitz and J.C. Sethares, "Frequency stability in dielectric resonators," Proc. IEEE, vol. 33, pp. 311-312, 1965.
- [12] D.J. Masse et al., "A New Low-loss High-k Temperature compensated dielectric for microwave applications," Proc. IEEE, vol. 59, pp. 1628-1629, 1971.
- [13] T. Bhattacharjee and M.R. Kamath, "Sensitivity of Dielectric Resonators with Environmental conditions," accepted and to be published in International Journal of Electronics (UK).
- [14] T. Itoh and R. Rudokas, "New method for computing resonant frequencies of dielectric resonators," IEEE Trans. Microwave Theory Tech., vol. MTT-25, pp. 52-54, Jan. 1977.

- [15] M.W. Pospieszalski, "Cylindrical dielectric resonators and its applications in TEM line microwave circuits," IEEE Trans. Microwave Theory Tech., vol. MTT-27, pp. 233-238, March 1979.
- [16] Y. Konishi, N. Hoshino and Y. Utsumi, "Resonant frequency of a $TE_{01\delta}^0$ dielectric resonator," IEEE Trans. Microwave Theory Tech., vol. MTT-24, pp. 112-114, Feb. 1976.
- [17] J.K. Plourde and C.L. Ren, "Application of dielectric resonators in microwave components," IEEE Trans. Microwave Theory Tech., vol. MTT-29, pp. 754-769, Aug. 1981.
- [18] A.P.S. Khanna, "Three port S-parameters ease GaAs FET designing," Microwave RF, vol. 24, pp. 81-84, Nov. 1985.
- [19] G. Satoh, "Stabilized microstrip oscillator using a temperature-stable dielectric resonator," IEEE Int. Solid-State Circuits Conf. Digest of Tech. Papers, pp. 184-185, Feb. 1974.